A DEVELOPMENTAL ENGINEERING APPROACH TO BONE REGENERATION

Inaugural dissertation

to

be awarded the degree of Dr. sc. med.
presented at
the Faculty of Medicine
of the University of Basel

by

Dr. med. Celeste Scotti

from Milan, Italy

Approved by the Faculty of Medicine

On application of

Prof. Ivan Martin, PhD

Prof. Dr. med. Marcel Jakob

PD Dr. Andrea Barbero, PhD

Dr. Martin Ehrbar, PhD

Basel, ……..

Prof. Dr. med. Thomas Gasser

Dean

INDEX

ABBREVIATIONS LIST

SSC: Skeletal stem cell

BMSC: Bone marrow stromal cell

ADSC: Adipose-derived stromal cell

HSC: Haematopoietic stem cell

HME: Haematopoietic microenvironment

BM: Bone Marrow

AT: Adipose Tissue

TE: Tissue engineering

DE: Developmental engineering

BTE: Bone tissue engineering

ECM: Extracellular matrix

eECM: engineered ExtraCellular Matrix

CHAPTER 1

INTRODUCTION

INTRODUCTION

Bone tissue is capable of spontaneous self-repair, with no scarring, generating new tissue that is (all but) indistinguishable from surrounding bone. However, in certain circumstances the defect is too large (due to tumour resection, osteomyelitis, atrophic non-unions, peri-prosthetic bone loss), or the underlying physiological state of the patient impairs natural healing (osteoporosis, infection, diabetes, smoking) necessitating intervention. Autologous bone grafting is today the gold standard for bone repair, although the costs of this approach are considerable due to the additional surgical procedures required to harvest the bone material, the consequent donor site morbidity (Silber 2003), and the risk of infection and complications. Additionally, this approach is hampered by the limited amount of donor material available for transplantation which can be prohibitive when dealing with large defects. To resolve these issues, both allograft- and xenograft-based strategies have been proposed, however the risk of rejection in the former and of zoonoses in the latter has reduced their clinical impact. Bone tissue engineering (BTE) is an alternative strategy that has been explored to fill the clinical need for autologous bone transplantation.

Background

Almost half a century has passed since the demonstration that ectopic transplantation of bone marrow and bone fragments leads to the formation of de novo bone tissue which, when transplanted subcutaneously, is later filled with bone marrow (Friedenstein 1966, Tavassoli 1968). Nowadays, the notion that a set of cells present in the bone marrow stroma can be cultured in vitro and can regenerate fully functional bone organs in vivo is well accepted, although the identity and precise molecular characterisation of the cell population responsible is still a matter of study and debate (reviewed in (Bianco 2013, Keating 2012)) and the ex vivo expansion and manipulation of stromal cells derived from various sources

forms the foundation of the majority of current bone tissue engineering attempts to meet the clinical demands for bone regeneration and repair.

Over the last 50 years, the BTE field has made significant advances towards overcoming the limitations of conventional methods which is particularly relevant when an underlying pathology calls for alternatives to the *status quo*. Clinically, several examples of successful application of tissue engineering techniques to bone reconstruction exist within the literature (Quarto 2001, Sandor 2014), however, on the whole, advances in basic science have not translated well into significantly increased clinical application. The reasons are, in part, financial, but additional problems such as low efficiency of differentiation, intra-patient variability in the differentiation potential of ex-vivo cultured cells (Schwartz 1998), as well as the risk of ectopic bone growth (Deutsch 2010), possible transformation (Vilalta 2008) or an incomplete understanding of the underlying pathways which are being manipulated with factors, such as transforming growth factor β (TGF-β) and bone morphogenic proteins (BMPs) (Chapellier 2015, Smith 2008, Siegel 2003), certainly play a role.

Minimal clinical adoption has prompted the exploration and adaptation of alternative methods including the use of stromal cells from non-bone sources (Kern 2006, Evans 2015), most commonly, adipose tissue (Zuk 2002, Murata 2015), but also muscle (Evans 2015); the development of new tissue engineering paradigms in which the focus is shifted from "cells+cytokines" to the engineering and in vitro optimisation of treatments as a means to support in vivo developmental processes by harnessing innate developmental pathways (Lenas 2009A, Lenas 2009B, Scotti 2010, Tonnarelli 2014); and finally, attempts to create "off-the-shelf" products to stimulate the regeneration of bone through adoption of developmental engineering principles (Bourgine 2014, Cunniffe 2015, Gawlitta 2015).

Embryological Development

Bone forming tissues are derived from the mesoderm or a specialized part of the ectoderm named the neuroectoderm(Reichert 2013). Two distinct processes, called intramembranous and endochondral ossification, are executed by the progenitor cells in order to generate bone(Long 2012). During intramembranous ossification, progenitor cells in the connective tissue directly differentiate into osteoblasts and begin secreting osteoid matrix, which calcifies and later becomes lamellar bone. During endochondral ossification (Figure 1), progenitor cells first condensate and, through N-cadherin, upregulate Sox-9 and differentiate into chondrogenic cells, thus forming cartilaginous templates, for the subsequent bone formation(Macjke 2011). The chondrogenic cells further differentiate, becoming the so-called hypertrophic chondrocytes that express characteristic markers such as collagen type X, metalloproteniases (MMPs) and pro-angiogenic factors such as VEGF(Mackie 2011). Mesenchymal stem cells directly adjacent to the hypertrophic matrix ("perichondral cells") form the perichondral bone collar through intramembranous ossification (Riminucci 1998). At the same time, vasculature is attracted towards the central portion and begins to invade the hypertrophic cartilage providing osteoclasts and mesenchymal cells. During this invasion, hypertrophic matrix calcifies and is replaced by woven bone (Mackie 2011, Mackie 2008). From the center, this process continues towards both proximal and distal ends of the bone rudiment. Near both ends, secondary ossification centers appear and undergo the same process. At the aricular surfaces, a thin layer of hyaline cartilage persists and allow for the smooth function of joints. This hyaline cartilage appears similar to the rudimentary cartilage template, but evidence suggests that the mesenchymal progenitors and the process of formation are different (Hyde 2007, Fosang 2011). At the border between diaphysis and epiphysis, a cartilaginous area ("growth plate") persists until adulthood and is responsible for bone lengthening during growth. In fact, endochondral ossification takes place also in adult life in both **skeletal growth** and **repair.**

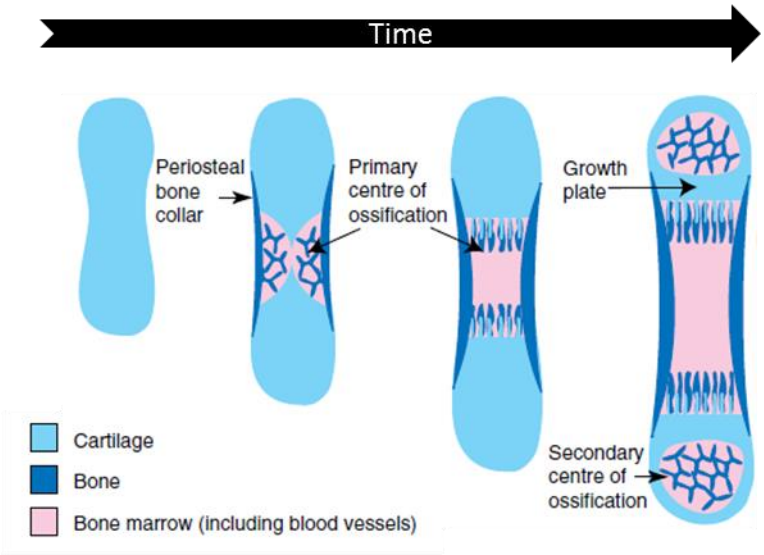

Figure 1: Principle of endochondral ossification. Adapted from Mackie EJ, Tatarczuch L, & Mirams M (2011) The skeleton: a multi-functional complex organ: the growth plate chondrocyte and endochondral ossification. The Journal of endocrinology 211(2):109-121.

Skeletal growth

The growth plate has a well-defined hierarchical structure that reflects the various stages of progenitor cells differentiation (Abad 2002) (Figure 2). Close to the secondary ossification center of the epiphysis there is a zone of resting cartilage, which resembles the hyaline cartilage found in adult joints and contains few chondrocytes. The next zone contains a higher number of cells and is called the proliferative zone. Next to it is the pre-hypertrophic zone, in which the cells begin to oragnize in distinct columns. In the subsequent hypertrophic zone, cells increase in volume and modify their phenotype and the content of the extracellular matrix. In the final zone of remodeling, cells undergo apoptosis and the matrix calcifies, while osteoclasts and vessels invade the zone actively remodeling the matrix, followed by osteoblasts which deposit osteoid matrix.

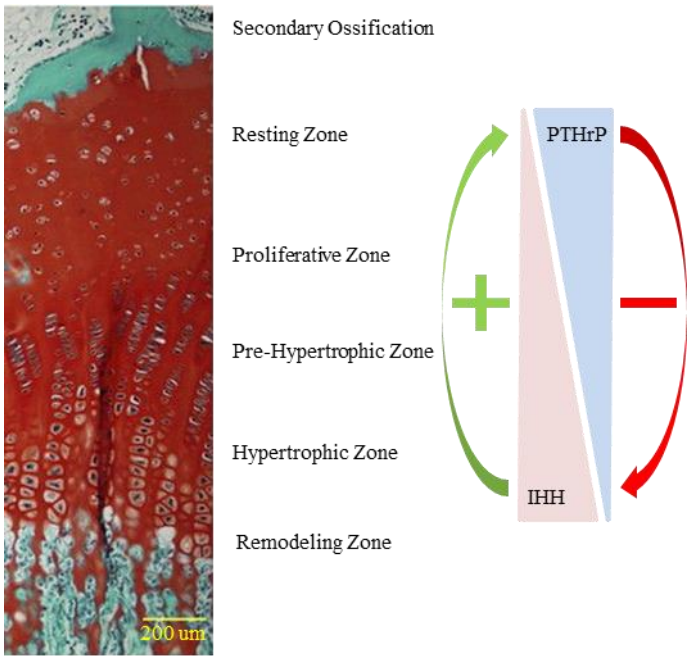

Figure 2: Organization of the growth plate cartilage. Safranin-O staining with fast green counterstaining. Adapted from Kim HK, Stephenson N, Garces A, Aya-ay J, & Bian H (2009) Effects of disruption of epiphyseal vasculature on the proximal femoral growth plate. J Bone Joint Surg Am 91(5):1149-1158.

It is assumed that the proliferating chondrocytes have stem cells features(Abad 2002) as one daughter cell continues proliferating while the other differentiates progressively along the endochondral route. Proliferation is highly regulated by multiple pathways and feedback loops and can be guided by both endocrine and paracrine signals. For example growth hormone (GH) is secreted by the hypophysis and stimulates secretion of insulin-like growth factor 1(IGF-1) by liver cells and pre-hypertrophic chondrocytes, which in turn stimulates proliferating chondrocytes(Abad 2002). Indian hedgehog (IHH) is produced by prehypertrophic chondrocytes and increases proliferation and hypertrophy. On the other hand, parathyroid hormone related peptide (PTHrP) is mainly produced by proliferating chondrocytes and inhibits hypertrophy. IHH can induce expression of PTHrP, whereas PTHrP suppresses IHH expression(Studer 2012). In this way a negative feedback loop is formed (Figure 2), which finely controls the maturation of the growth plate(van Donkelaar 2007). Other signals such as Wingless/Int (Wnt) or bone morphogenic proteins (BMP) can promote chondrocyte proliferation, whereas fibroblast growth factor (FGF) can repress it(Abad 2002).

Any alteration to this fine equilibrium may lead to developmental anomalies. For example, the most frequent disease leading to dwarfism, results from an overactivation of the FGF pathway(Shiang 1994).

The main activity of chondrocytes is secreting extracellular matrix components such as proteoglycans and collagen type II. Other proteins are found in lower concentrations and mainly aid the assembly of the matrix and its interconnections(Abad 2002). Expression of these cartilage-specific matrix components is absolutely dependent on Sox9(Long 2012) and can be stimulated by tumor growth factor beta (TGFb) superfamily members (TGFb-1, BMP-2) and FGF.

Once the chondrocytes become hypertrophic through expression of Runt-related transcription factor 2 (Runx2)(Mackie 2008), they increase production of collagen type X, matrix metalloproteinase 13 (MMP-13), alkaline phosphatase (ALP) and IHH(Studer 2012). Their volume increases up to 10 fold(Bush 2008), though they do not necessarily degrade the ECM to make space(Abad 2002). Thyroxin is the most important systemic regulator of hypertrophy(Shao 2006) and its local effect is most likely transmitted by Wnt signaling(Wang 2007).

The hypertrophic chondrocytes induce matrix mineralization through secretion of matrix vesicles, which contain akaline phosphatase and are able to nucleate hydroxyapatite crystals (Yadav 2011). They are also the master regulator of the endochondral ossification route as they actively communicate with the subsequently invading cells, for example by expressing vascular endothelial growth factor (VEGF) to attract endothelial cells(Ortega 2010), receptor aktivator of NF-kB ligand (RANKL) to attract and differentiate osteoclasts(Boyce 2008), and IHH / Wnt to induce osteoblast differentiation of attracted mesenchymal stem cells(Abad 2002). At the end of hypertrophy, most hypertrophic chondrocytes undergo apoptosis(Long 2012), however, in literature there is a growing body of evidence that few of them transdifferentiate towards osteoblasts and osteocytes(Yang 2014).

The hypertrophic matrix is degraded by apoptotic hypertrophic chondrocytes and osteoclasts (Knowles 2012) through secretion of MMP-13 and MMP-9 respectively (Ortega 2003). Endothelial cells(Abad 2002) or macrophages(Blumer 2008) can aid matrix degradation and may increase MMP-9 expression if MMP-13 is absent(Inada 2004). The degradation of the matrix releases factors which attract additional osteoclasts, endothelial cells and mesenchymal progenitors(Gerber 1999).

When the bone growth finishes during young adulthood, the growth plate closes due to the influence of oestrogens, which deplete the pool of proliferating chondrocytes (Weise 2001).

Skeletal repair

Bone development and repair are tightly linked and are characterized by very similar processes. In addition, the bone is one of the few human tissues that regenerate and not just repair itself with a scar. Being a mechanical-sensitive organ, according to the mechanical and anatomical environment, two distinct processes of fracture healing can occur. If the two stumps are compressed (e.g., by an osteosynthesis device) and no movement occurs, new osteons will directly form at both ends and continue the process of homeostasis detailed above(Bruder 1998). The fracture will thus be bridged by many new osteoid laminae originating by the two bony stumps.

If the fracture is complex, separated by a large gap or subjected to high movement (e.g., dynamically stabilized by an intramedullary nail or just by a cast), a process resembling the embryonic endochondral ossification begins (Martin 1997, Warnke 2004). In the first stage, the fracture gap is filled by blood from the ruptured vessels of the endostium, periosteum and bone itself. The blood clot is rapidly invaded by a wave of inflammatory cells (mainly neutrophils and macrophages)(Warnke 2004) and mesenchymal stem cells. The latter

differentiate to chondrocytes and form a type of disorganized fibrocartilage which represents the soft fracture callus (Figure 3). This tissue has better mechanical properties than the blood clot and is able to temporarly stabilize the fracture(Marcacci 2007). Similarly to embryonic bone development but in a much less organized manner, the fibrocartilage becomes hypertrophic and undergoes endochondral ossification as detailed above. The tissue calcifies, is invaded by vessels and replaced by osteoid matrix. Initially, a woven-bone like structure is fomed to be then replaced by lamellar bone. In particular, the outside shell is substituted by compact bone, whereas the interior of the callus is replaced with bone marrow and trabecular structures (Figure 3). After the callus has ossified, the process of bone homeostasis will reshape it according to the mechanical loads and stresses, until a final shape that can resemble almost perfectly the one before the fracture. Of course, the final shape depends on the previous alignment of the fracture fragments and on the age of the person and may take several years to be fully reached(Bruder 1998). Although usually effective, in several clinical scenarios bone repair is impaired and made impossible determining a high clinical need for bone regeneration strategies.

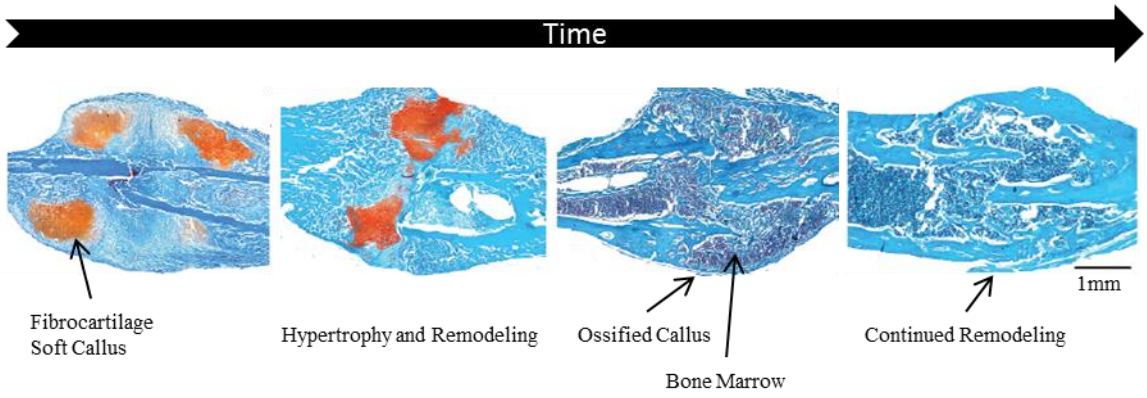

Figure 3: Fracture healing through endochondral ossification, safranin-O and fast green staining. Modified from Ai-Aql ZS, Alagl AS, Graves DT, Gerstenfeld LC, & Einhorn TA (2008) Molecular mechanisms controlling bone formation during fracture healing and distraction osteogenesis. Journal of dental research 87(2):107-118.

The challenge of bone regeneration

Bone has the intrinsic capacity to regenerate without the formation of scar tissue, but will only do so in practice under certain conditions, largely related to (i) the size of the defect, (ii) its location and vicinity to an efficient vascular bed for vascularisation, and (iii) the mechanical stability of this defect. Under suboptimal conditions, complete bone regeneration can not occur properly and a combination of bone and scar tissues will then result in a poor outcome for the patient. In particular, bone loss from trauma, neoplasia, reconstructive surgery and congenital defects remains a major health problem, making the development of effective bone regeneration therapies a primary priority. Existing treatments such as the use of autologous or allogenic bone grafts are successful in many instances. However, complications due to the additional autograft surgery, limited quantity of material available for harvesting, and limited availability of transplant tissue from bone banks remain serious shortcomings. Distraction osteogenesis provides a surgical alternative but requires long healing times. On the other hand, the efficacy of non-viable bone obtained from cadavers and of synthetic materials is still under debate. The combination of osteoconductive substrates with osteoinductive factors (e.g., bone morphogenetic proteins) capable to recruit local osteoprogenitor cells holds a great promise, though optimal combinations, doses and release kinetics for such factors are still far from being identified and implemented in safe and clinically effective products. Therefore, an alternative approach that can improve the outcome of bone defects is highly required.

Bottlenecks in cell-based approaches to bone repair

Osteogenic grafts may be engineered by the combination of suitable scaffolds with viable osteoprogenitor cells. Culture-expanded, bone marrow-derived MSC have been demonstrated to support formation of de novo bone tissue in ectopic and orthotopic animal models, and have been tested in pilot clinical studies for bone repair (Quarto 2001). However,

their use in the routine clinical practice is hampered by a series of technical, scientific and clinical issues, as discussed below.

(i) Inter-donor MSC variability. Despite the advances in identification of putative markers for human MSC (Sacchetti 2008), populations of expanded human MSC are still highly heterogenous and extremely variable in their differentiation potential, when isolated from different donors, even in the same age range. This represents a major bottleneck for the standardization of therapeutic protocols. Indeed, it is generally accepted that only MSC from selected donors are capable of generating bone tissue upon ectopic implantation, and culture conditions allowing reproducible maintenance of MSC osteogenic capacity are yet to be identified.

(ii) Need of a mineralized scaffold substrate. Human MSC have been so far reported to generate bone tissue exclusively through direct osteogenic differentiation, in a manner akin to intramembranous ossification, using a mineralized surface as "priming" substrate (Martin 1997). The need of mineralized scaffolds, as compared to polymeric materials, results in a limited flexibility in the tailoring of the properties required for specific compartments/defect types, especially with regard to mechanical features and degradation rate.

(iii) Cell survival after grafting. Limited MSC survival and function after implantation, especially in the inner core of constructs upscaled in size, is often a limiting factor for the bone repair efficiency. The issue of engraftment can be addressed by accelerating and improving construct vascularization, but no reliable and safe strategy has yet been validated in a clinical setting .

(iv) Complex and costly manufacturing. Ex vivo processing of autologous cells requires dedicated Good Manufacturing Practice (GMP) facilities, with accredited quality management systems. Since these infrastructures are not easily available within the confinement of

hospitals or medical centers, cells and engineered grafts are typically transported to centralized facilities, with obvious logistics-, safety- and cost-related issues.

As a result of these bottlenecks, it is not yet convincing that currently available MSC-based approaches to bone repair can lead to a cost-effective, reproducible and predictable benefit for patients. Therefore, there is a high need of **alternative paradigms** to tackle this challenging clinical scenario.

Develomental Engineering

Initial hopes for the application of tissue engineering to the repair and regeneration of bone have not yet come to fruition. Unfortunately, the unmet clinical need which generated the enthusiasm that surrounded TE in the 1990's (Ingber 2006) persists today (Jakob 2012). Developments, particularly in animal models, have advanced the field, but the resulting clinical impact has been limited.

Traditionally, BTE has focused on tissue replacement through the in vitro/ex vivo generation of implants which effectively mimic the mature tissue as it is found in the adult. This has been achieved through the use of different cells, scaffold materials, and soluble factors to create a mechanical /biochemical profile that is similar to the tissue it is designed to replace (Ingber 2006). Scaffolds give physical strength, durability, malleability and three-dimensional structure, allowing for custom-sized implants with specific mechano-physical characteristics. Different scaffold materials can be combined (Sheehy 2013) or supplemented with growth factors such as BMPs (Deutsch 2010). Various combinations of growth factors are routinely used to guide cell differentiation towards the desired phenotype; however the use of a limited number of factors is a long way from the complexity seen in vivo (Jakob 2012, Sharpe 2005). Bioreactors, using controlled perfusion of media through three-dimensional scaffolds recapitulate, to some degree, mechanical(Haugh 2011, Hoffmann 2015) and

hydrostatic forces (Steward 2012), representing a step towards replicating the tempo-spatial complexity of the in vivo micro-environment, something which may well be impossible to re-create in vitro.

Instead of aiming to phenocopy the adult tissue-state, researchers are drawing on the work of developmental biology, which states that "normal tissue healing in the adult involves progressive remodelling of pre-existing tissue structures" (Ingber 2006) to generate grafts that recapitulate the immature tissue-state. By implanting the precursor-state of a tissue, or "organ germ" (Nakao 2010, Janicki 2010), elements of the implant can interact with natural developmental cues to regulate differentiation and growth, and to provide cues for cell invasion, remodelling, and re-vascularisation in the correct spatio-temporal context. In this manner we might overcome one of the greatest challenges facing TE, i.e. effectively mimicking the complexity of natural developmental processes, thereby leading to formation of an authentic mature tissue.

Recently, Lenas et al. (Lenas 2009A, Lenas 2009B) described a fusion of engineering principles and concepts from developmental biology, which they termed "developmental engineering" (DE). The authors outlined the utility of applying concepts such as path-dependence, robustness, and modularity, to the manufacture of tissue grafts/implants. Robustness, within the context of developmental processes, refers to the ability of a system to function consistently despite external fluctuations. A robust developmental mechanism would therefore be able to cope with a degree of dissimilarity between the native tissue and the implant. A problem encountered when trying to gauge the characteristics necessary for successful stimulation of native repair processes is one of sensitivity; the basic tools and the limited sensitivity of currently applied methods means we are not yet able to predict whether a certain implant will function effectively, leading to much trial and error. However, the modularity of many developmental processes permits ex vivo experimentation to determine optimal conditions and timing for implantation to achieve the best results in vivo (Scotti 2013,

Liebowitz 1995). Additionally, ex vivo experiments can be used to identify markers for the successful completion of multi-stage developmental processes (Hall 2000). In this fashion, the progress of the implant can be monitored, in vivo, through the stages of development, highlighting where problems lie and thus, where refinement is needed. The successful completion of each step of development sets the stage for the next step, providing optimal conditions. This concept, rooted in economics, law (Gerstenfeld 2002) and biology, is called path-dependence and describes a situation where the outcome of one process directly influences the effectiveness of a successive process. Thus, one process acts a check-point for the correct completion of the previous step, and at the same time completion of the previous step sets the stage for the following stages. In the context of bone regeneration, this is exemplified by hypertrophic chondrocytes which act as a natural scaffold for osteogenesis as well as secreting factors which orchestrate the differentiation of osteoblasts from perichondrial cells, as well as the mineralisation and vascularisation of the neo-bone tissue, restoring normoxic conditions required for optimal bone growth and bringing vital materials (Nakao 2007). This concept has experimental support, hypertrophic chondrocytes have been shown to stimulate bone regeneration in vivo, while lesser developed tissues were not as effective in stimulating the formation of bone tissue, likely reflecting the path-dependence of this process (Cunniffe 2015).

Historically, TE has directed the formation of neo-bone through the intramembraneous route relying on the presence of mineralised substrate scaffolds to initiate bone growth through intramembraneous ossification, however more recently numerous studies illustrate the advantages of bone formation through endochondral ossification. As described before, endochondral ossification is the method by which the axial and long bones of the skeleton, (the vast majority of bones) are formed during embryogenesis (Ogawa 2013) and has many features common to bone regeneration after fracture (Sheehy 2014, Jukes 2008) including activation of key signalling pathways such as Indian hedgehog (IHH), parathyroid-related hormone receptor (PTHrP), wingless (wnt), and BMPs (although notably, the post-natal

environment differs from that of the developing embryo (Sheehy 2014)). The process entails the condensation (clustering together through cell surface receptors and adhesion molecules (Kronenberg 2003)) of chondrocytes, which secrete a collagenous (type II) matrix rich in proteoglycans. Under the control of two of the master regulators of bone development, IHH, and PTHrP (see (Ogawa 2003)), chondrocytes at the centre of the proto-bone organ cease to proliferate and become enlarged (hypertrophic), producing large amounts of type X collagen, directing initial mineralisation (Gerstenfeld 2003) and vascularisation through VEGF production, before undergoing apoptosis to leave a cartilage scaffold that will eventually be remodelled into mature bone(Ogawa 2013). This strategy has been exploited for bone regeneration; implantation of hypertrophic human bone marrow derived mesenchymal stromal cells (huBMSCs) in nude mice has been demonstrated to lead to the growth of ectopic bone structures as a result of human cells playing an active role in osteogenesis (Scotti 2010). BMSCs embedded in β-TCP scaffolds were able to generate frank bone in vivo, but chondrogenic priming was necessary for the production of bone containing bone marrow (BM) (Liebowitz 1995), while huBMSCs seeded on collagen type I scaffolds induced towards endochondral ossification formed not only bone organs, but also a fully functional BM which was shown to sustain haematopoiesis in lethally irradiated mice (Scotti 2013). In a previous study cells that were not hypertrophic at the time of implantation failed to generate bone and were resorbed, indicating that the developmental stage is a critical factor in dictating whether the implant will proceed to the next stage (Vortkamp 1997).

There are multiple advantages to implanting chondrogenically primed cells: chondrocytes are more likely to survive the hypoxic in vivo environment (D'Amour 2006), they stimulate vascularization (Gerber 1999), and have been shown to increase bone formation in vivo through BMP production (Jakob 2012). Additionally, by selecting a starting material which most closely matches the in vivo precursor to the tissue of interest, and by guiding those cells though developmental stages using known markers, an intermediate form

of the tissue is generated which "contains all the necessary and sufficient instructive elements for its regeneration" (Martin 2014).

While the adoption of processes which mimic embryogenesis have demonstrated merit (Liebowitz 2015), there are salient physical, biochemical, mechanical, and immunological differences between the developing embryo and a mature tissue microenvironment (Jakob 2012, Sharpe 2005). Accordingly, we must adjust the design of prospective implants to reflect these differences (Tonnarelli 2014). Embryonic development occurs under different immunological and inflammatory settings as well as at a much smaller scale than in the adult, both of these factors must be addressed if embryonic processes are to be harnessed for the successful engineering of bone grafts.

Paracrine signalling gradients which function at the embryonic scale are likely to be inefficient in a much larger graft. Modular implants, comprising many smaller units may be utilised to overcome this hurdle (modular implants – cellular sheets (Yang 2007)) in addition to addressing some of the limitations of mass transfer such as necrosis at the core of the engineered tissue.

The immunological milieu controlling developmental processes and the influx of cells at the embryonic stage of bone growth remains to be fully elucidated. This is likely to be a crucial step if we are to fully harness the potential of developmental engineering, as immune factors are significant mediators of bone healing and re-growth (Sheehy 2014), which can result in retardation of healing, if suppressed (Burd 2003). Interestingly, this last point serves to highlight the differences between developmental processes underway during embryogenesis and those involved in the adult: while inflammation represents one of the main drivers of bone repair, it is absent during normal bone development. In fact, the significance of interleukin 1-β (IL-1β) in the re-vascularisation, mineralisation, and cartilage remodelling activity of huBMSCs has been illustrated and will be described in Chapter 3.

In conclusion, the adoption of a developmental engineering paradigm for the regeneration of bone represents a potential method to mitigate the enormous hurdle presented by largely unknown in vivo complexity. By generating pre-cursor organ germs based on observable in vitro-elucidated markers, and allowing natural cues to orchestrate the development of hypertrophic chondrocyte templates, it is foreseeable that future bone repair strategies will achieve clinical use. However, if we are to effectively utilise this technique, a clearer more complete understanding of the biochemical and mechanical forces at work in both the developing embryo and the adult are required.

Proof-of-principle for the developmental engineering of bone

We previously reported for the first time the capacity of expanded human MSC to generate frank bone tissue through an endochondral route if primed in vitro by appropriate stimuli and ectopically implanted in nude mice (Scotti 2010). This milestone work represents a proof of principle for the "Developmental Engineering" paradigm. As a matter of fact, the process closely recapitulated the temporal and spatial sequence of events typical of limb development, namely (i) cellular condensation and hypertrophic chondrogenesis, (ii) dependency from the activation of Indian Hedgehog (IHH) signalling, (iii) formation of a bony collar through perichondral ossification, (iv) MMP-mediated matrix remodelling, vascularization, and osteoclastic resorption, (v) bone matrix deposition over the resorbed cartilaginous template, and (vi) formation of a complete bone organ, including hematopoietic elements. Importantly, we clarified that successful implementation of the endochondral ossification paradigm critically required a cartilaginous template in a mature stage of hypertrophy, either obtained in vitro or in vivo, whereby cells strongly positive for type X collagen were surrounded by osteoblastic cells expressing abundant bone sialoprotein. However, due to the limited reproducibility of human MSC from different donors, the approach was validated using cells from selected primary cells with kown chondrogenic

potential. Moreover, the paradigm was developed with a small scale, scaffold-free transwell model and required to be scaled-up in size in order to be proposed for a clinically relevant scenario.

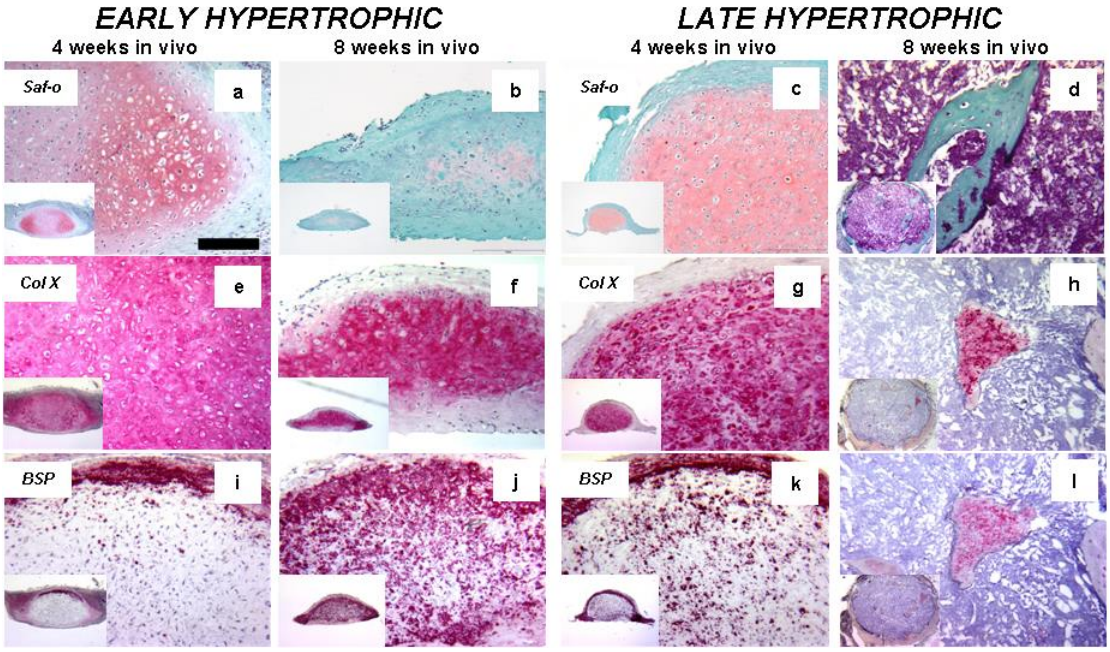

Figure 4. Remodelling of the cartilaginous template after 4 and 8 weeks in vivo. (a, e, i) Four weeks after implantation, early hypertrophic samples had differentiated further towards hypertrophy, displaying larger lacunae, Col X accumulation and initiated BSP deposition in the outer rim. (b, f, j) Eight weeks after implantation, early hypertrophic samples had differentiated even further. This was evidenced by a decrease in GAG accumulation, while Col X was maintained and BSP had also been deposited within the cartilaginous core. (c, g, k) After 4 weeks, late hypertrophic specimens had undergone more intense remodeling, such that GAG and Col X levels were reduced, while BSP had already been deposited within the cartilaginous core. (d, h, l) After 8 weeks, the cartilaginous template was almost completely resorbed: bone structures substituted the GAG positive areas in the central region, while Col X and BSP positive areas were restricted to scattered islands. All the pictures were taken at the same magnification, scale bar = 200μm. Taken from Scotti C, et al. (2010) Recapitulation of endochondral bone formation using human adult mesenchymal stem cells as a paradigm for developmental engineering. Proceedings of the National Academy of Sciences of the United States of America 107(16):7251-7256.

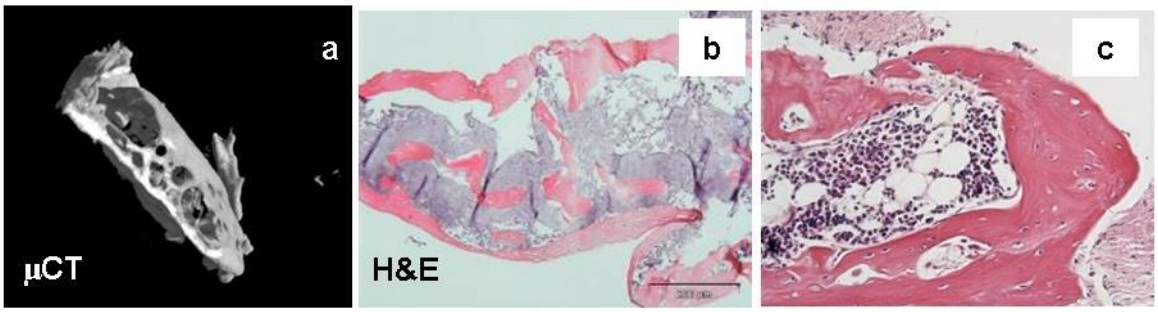

Figure 5. Bone tissue is generated over the cartilaginous template after 8 weeks in vivo. a) Microtomography showing bone trabeculae after 5 weeks of in vitro culture and 8 weeks in subcutaneous pouches of nude mice. b) Histology confirming the bony nature of the stractures highlighted by the microtomography. c) Histology showing hematopoietic elements and adipose tissue within the mature bone, confirming the generation of a complete bone organ. Taken from Scotti C, et al. (2010) Recapitulation of endochondral bone formation using human adult mesenchymal stem cells as a paradigm for developmental engineering. Proceedings of the National Academy of Sciences of the United States of America 107(16):7251-7256.

A crucial achievement of our previous studies was that during in vitro culture and in vivo implantation, expanded human MSC recapitulated the finely orchestrated events occurring during limb development. (Figures 5 and 6). These data demonstrate that human MSC from adult individuals – if appropriately manipulated – maintain the capacity to undergo an endochondral ossification process by closely recapitulating embryonic pathways involved in limb development: this represents an attractive validation of the "Developmental Engineering" paradigm. In principle, according to this feature, the potential of hMSC to achieve hypertrophic differentiation, enter the endochondral route and subsequently determine bone formation could be even further enhanced with the use of agonists of IHH pathway.

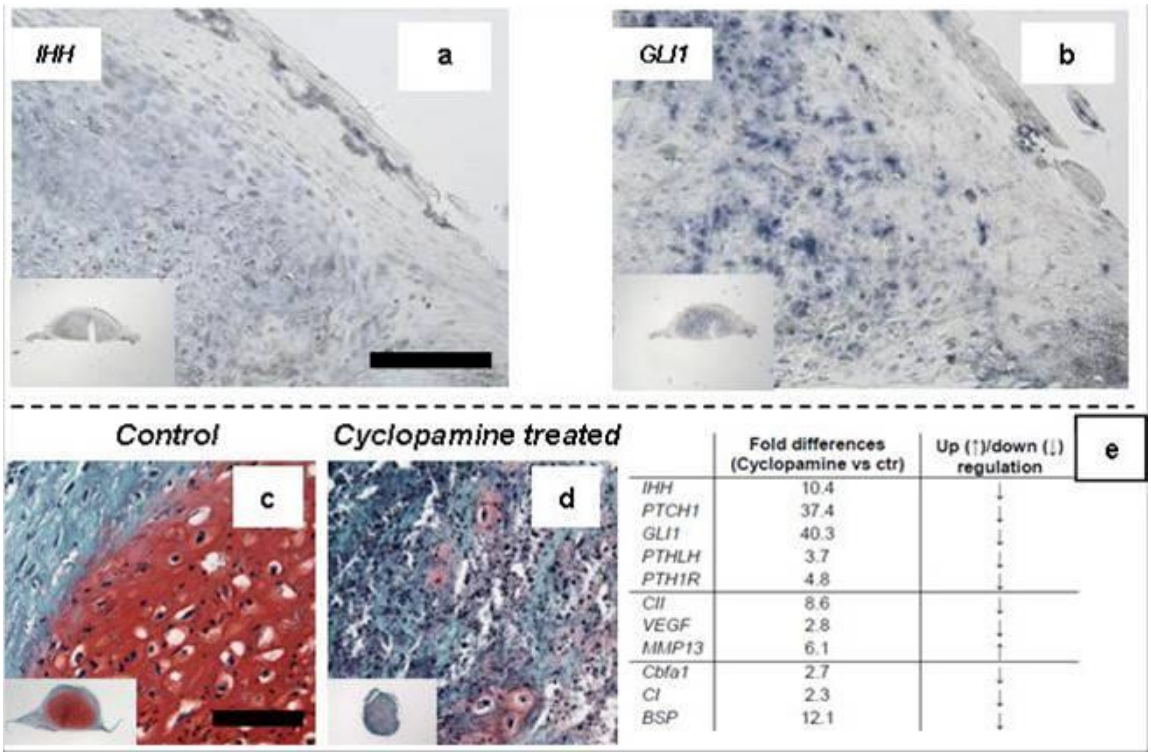

	Fold differences (Cyclopamine vs ctr)	Up (↑)/down (↓) regulation
IHH	10.4	↓
PTCH1	37.4	↓
GLI1	40.3	↓
PTHLH	3.7	↓
PTH1R	4.8	↓
CII	8.6	↓
VEGF	2.8	↓
MMP13	6.1	↑
Cbfa1	2.7	↓
CI	2.3	↓
BSP	12.1	↓

Figure 6. Activation of pathways involved in endochondral ossification (Scotti et al., 2010). a), b) After implantation for 4 weeks, representative genes, assessed by in situ hybridization (IHH, and GLI1 as IHH effect mediator) were expressed. c), d) Functional inhibition of the IHH pathway through administration of cyclopamine blocked the differentiation and maturation of the cartilaginous templates, as assessed by Safranin-O stain. e) mRNA expression of genes involved in IHH signalling (IHH, GLI1, PTCH1), PTH signalling (PTHLH, PTHR1), as well as chondrogenic/hypertrophic genes (Col II, VEGF), and osteogenic genes (Cbfa-1, Col I, BSP) confirmed suppression of the endochondral route by cyclopamine. Taken from Scotti C, et al. (2010) Recapitulation of endochondral bone formation using human adult mesenchymal stem cells as a paradigm for developmental engineering. Proceedings of the National Academy of Sciences of the United States of America 107(16):7251-7256.

The described principles have lead to the development of engineered hypertrophic cartilage as a bone substitute (Scotti 2010), which displays advantageous properties such as resistance to hypoxia (Sheehy 2012, Grimshaw 2000) and gradual vascular invasion(Sheehy 2015). This type of graft has been used in orthotopic models such as calvarial(Kuhn 2014) or femoral segmental defects (van der Stok 2014, Harada 2014) and with strategies as diverse as monolithic constructs (Harada 2014), pellets between 1-3mm in diameter (Bahney 2014) or complex modified structures (Cunniffe 2015). Generation of greater tissue volumes has been proposed using bioreactor systems(Kock 2014, Hoffmann 2015). As a next biomimetic

step, co-cultures of hypertrophic cartilage with endothelial cells have been performed to improve mineralization(Freeman 2015). For clinical applications of engineered hypertrophic cartilage, a remaining drawback is the use of autologous MSC to form the graft. Although necessary to prevent immunologic rejection, autologous MSC use means additional extraction and a significant time-delay. The interdonor variability encountered with MSC (Solchaga 2011) may also lead to unpredictable outcomes. For this reason, there is a high need of bone regeneration strategies characterized by a **standardized bone-forming potential** and a **sustainable cost** for the payers.

Devitalized Extracellular Matrices

The use of allogeneic hypertrophic cartilage of high quality would be possible if immunologic rejection could be prevented. This could be achieved through removal of cells, since matrix constituents are hihgly conserved and may even prevent an adaptive immune response(Bollyky 2009). Indeed, the extracellular matrix itself may hold sufficient cues to instruct cell function and identity(136). Moreover, in the case of hypertrophic cartilage, apoptosis of hypertrophic chondrocytes(Crapo 2011) and the release of matrix bound signals such as VEGF through MMP-mediated matrix degradation are part of the natural developmental and growth processes. Thus devitalization of allogeneic hypertrophic cartilage by chemical or physical means or induction of apoptosis(Bourgine 2013) can be an alternative to the use of patient derived grafts. For these reasons, a devitalized endochondral "engineered extracellular matrix" (eECM) would be an attractive and clinical-compliant strategy to achieve bone regeneration at the most challenging sites.

In fact, from a clinical and commercial standpoint, an eECM with the capacity to induce bone formation would be highly attractive. In particular, it would: (i) avoid autologous cells processing, which is time consuming and costly; (ii) lead to standardized "off the shelf" products; and (iii) by-pass inter-individual variability in the cell differentiation capacity, which severely limits clinical applications of MSC-based approaches, thus making the clinical

translation of this approach more cost-effective, feasible and effective than typical tissue engineering strategies.

General Aim of the Thesis

Briefly, this thesis includes the translational effort towords the development of a clinical "product" from an innovative scientific concept. In other words, upon demonstration of the potential of the developmental engineering paradigm (scotti 2010) for the regeneration of the bone tissue, I aimed at developing a clinically-relevant application of this concept. This strategic goal lead me to (i) the extension of this concept to an upscaled model that allowed showing unprecedented features of engineered "bone organ"; (ii) the application of the paradigm to the process of bone repair, that is tightly linked to bone development; and (iii) the development of an innovative method of devitalization that allows to preserve key factors harbored within the ECM in order to show the potential for an "off-the-shelf" product for bone regeneration.

Specific Aims of the Chapters

The scientific work is presented in the form of three scientific publications.

Chapter 2 Engineering Of A Functional Bone Organ Through Endochondral Ossification

In this chapter, it was hypothesized that human MSC primed through endochondral ossification can engineer a scaled-up ossicle with features of a "bone organ", including physiologically remodeled bone, mature vasculature and a fully functional haematopoietic compartment. This represents the essential backbone on which the subsequent translational works have been based, as well as the prerequisite for the controlled manipulation of HSC niches in physiology and pathology.

Chapter 3 Interleukin-1beta Modulates Endochondral Ossification By Human Adult Bone Marrow Stromal Cells

Inflammatory cytokines present in the milieu of the fracture site are important modulators of bone healing and they are not present during embryonic development. This represents a crucial factor for a successful translation of the developmental engineering paradigm. In this chapter, in order to duplicate some features of the fracture callus, we investigated the effects of interleukin-1β (IL-1β) on the main events of endochondral bone formation by human MSC, namely cell proliferation, differentiation and maturation/remodeling of the resulting hypertrophic cartilage.

Chapter 4 Osteoinductivity Of Engineered Cartilaginous Templates Devitalized By Inducible Apoptosis

A key hurdle that limits translation to the clinic of regenerative therapies is the use of autologous cells. In this chapter, we hypothesized that the preservation of the ECM integrity, serving as a reservoir of multiple growth factors at physiological levels, is a key pre-requisite to recruit and instruct endogenous progenitors to initiate bone regeneration and that this capability can be used to engineer cell-free, off-the-shelf biomaterials to be used for the regeneration of the bone tissue. In particular, we aimed at inducing de novo bone organ formation using cell-free hypertrophic cartilage templates, devitalized by apoptotic induction through retroviral transduction of an inducible Caspase-9 (inducible Death System – iDS). The results reported in this chapter outline a broader paradigm in regenerative medicine, based on the engineering of cell-based but cell-free niches capable to recruit and instruct endogenous cells to the formation of predetermined tissues.

CHAPTER 2

Engineering of a functional bone organ through endochondral ossification

Engineering of a functional bone organ through endochondral ossification

Celeste Scotti[a,1], Elia Piccinini[a,1], Hitoshi Takizawa[b,1], Atanas Todorov[a], Paul Bourgine[a], Adam Papadimitropoulos[a], Andrea Barbero[a], Markus G. Manz[b], and Ivan Martin[a,2]

[a]Departments of Surgery and of Biomedicine, University Hospital Basel, 4056 Basel, Switzerland; and [b]Division of Hematology, University Hospital Zurich, 8091 Zurich, Switzerland

Edited by Robert Langer, Massachusetts Institute of Technology, Cambridge, MA, and approved January 11, 2013 (received for review November 22, 2012)

Embryonic development, lengthening, and repair of most bones proceed by endochondral ossification, namely through formation of a cartilage intermediate. It was previously demonstrated that adult human bone marrow-derived mesenchymal stem/stromal cells (hMSCs) can execute an endochondral program and ectopically generate mature bone. Here we hypothesized that hMSCs pushed through endochondral ossification can engineer a scaled-up ossicle with features of a "bone organ," including physiologically remodeled bone, mature vasculature, and a fully functional hematopoietic compartment. Engineered hypertrophic cartilage required IL-1β to be efficiently remodeled into bone and bone marrow upon subcutaneous implantation. This model allowed distinguishing, by analogy with bone development and repair, an outer, cortical-like perichondral bone, generated mainly by host cells and laid over a premineralized area, and an inner, trabecular-like, endochondral bone, generated mainly by the human cells and formed over the cartilaginous template. Hypertrophic cartilage remodeling was paralleled by ingrowth of blood vessels, displaying sinusoid-like structures and stabilized by pericytic cells. Marrow cavities of the ossicles contained phenotypically defined hematopoietic stem cells and progenitor cells at similar frequencies as native bones, and marrow from ossicles reconstituted multilineage long-term hematopoiesis in lethally irradiated mice. This study, by invoking a "developmental engineering" paradigm, reports the generation by appropriately instructed hMSC of an ectopic "bone organ" with a size, structure, and functionality comparable to native bones. The work thus provides a model useful for fundamental and translational studies of bone morphogenesis and regeneration, as well as for the controlled manipulation of hematopoietic stem cell niches in physiology and pathology.

mesenchymal stem cells | regenerative medicine | stem cell niche | tissue engineering

The term "developmental engineering" has been proposed as an evolution of classic tissue engineering paradigms, consisting of designing regenerative strategies guided by the principles of developmental biology (1). The conceptual transition from the primary target of engineering tissues to that of engineering processes recapitulating the stages of tissue development (e.g., based on self-organization of the cells, activation of specific morphogenetic pathways, and typical spatial and temporal arrangement) has the potential to instruct tissue regeneration to a higher degree of effectiveness and robustness (1). In the context of skeletal tissue biology and repair, this principle has inspired the engineering of hypertrophic cartilage templates as bone substitute materials capable of autonomously progressing through endochondral ossification, the embryonic developmental pathway of long bones and of the axial skeleton (2). The concept was successfully implemented not only using murine embryonic stem cells (ESCs) (3) but also adult human-derived bone marrow (BM) mesenchymal stem/stromal cells (MSCs) (4–6), whose molecular regulation was consistent with the known signaling pathways of fetal bone development (4).

Beyond the potential advantages of adopting a developmental engineering strategy for bone regeneration (4), recapitulation of endochondral ossification could lead to the engineering of a fully functional "bone organ," defined as an osseous matrix with mature vascularization and including the pivotal component of a hematopoietic BM (7). In mouse models it is well established that osteoblastic/osteoprogenitor cells have a crucial role in what has been defined as the hematopoietic stem cell (HSC) niche (8–10). It was also demonstrated, using human cells, that $CD146^+$ skeletal progenitor cells were able to recreate a hematopoietic microenvironment upon ectopic implantation in mice (11). Interestingly, using mouse embryonic limb-derived MSCs it was reported that the endochondral ossification process is required for the formation of an adult HSC niche (12), consistent with the onset of hematopoiesis at the sites of hypertrophic cartilage remodeling in long bones during skeletal growth (2). To the best of our knowledge, despite phenotypical evidence of the presence of putative HSCs within reconstituted ossicles (12–14), engineering of a human cell-induced bone organ hosting fully functional hematopoiesis has not yet been achieved.

We hypothesized that a functional bone organ can be engineered following a developmental engineering approach, which implies proceeding through a cartilage intermediate. A hypertrophic cartilage template would contain all necessary signals to initiate bone tissue formation, vascularization, remodeling, and establishment of a functional BM. To test this hypothesis, we first developed an upscaled model of endochondral ossification, necessary to study spatial patterns of bone tissue formation and to generate sufficient space for BM cells, in a quantity allowing for further analyses. We then used inflammatory regulators to enhance tissue remodeling and HSC homing and demonstrated the functionality of the cells in the ectopically engineered bone organ by transplantation into lethally irradiated mice.

Results

Development of an Upscaled Endochondral Ossification Model. We investigated the possibility of scaling up the size of engineered hypertrophic cartilage tissues while maintaining the previously reported composition and efficiency of ossification (4). Human MSCs were thus seeded into collagen-based scaffolds (8-mm diameter, 2 mm thick), as templates for tissue development. During the last 2 wk, culture medium was further supplemented with IL-1β (50 pg/mL) to accelerate remodeling of a large cartilage mass (15). The resulting constructs resembled most features of the small-scale model, namely a core cartilaginous tissue surrounded

Author contributions: C.S., E.P., H.T., A.B., M.G.M., and I.M. designed research; C.S., E.P., H.T., P.B., and A.B. performed research; C.S., E.P., H.T., A.T., P.B., and A.P. analyzed data; and C.S., E.P., and I.M. wrote the paper.

The authors declare no conflict of interest.

This article is a PNAS Direct Submission.

[1]C.S., E.P., and H.T. contributed equally to this work.

[2]To whom correspondence should be addressed. E-mail: imartin@uhbs.ch.

This article contains supporting information online at www.pnas.org/lookup/suppl/doi:10.1073/pnas.1220108110/-/DCSupplemental.

by a mineralized ring positive for bone sialoprotein (BSP). Furthermore, the construct contained approximately 10-fold greater amounts of DNA, calcium, and glycosaminoglycans (GAG) and maintaining an approximately fourfold larger diameter, both in vitro and in vivo (Fig. S1 *A*–*C*). Likely because of mass transfer limitations in static culture conditions, the construct core included areas devoid of cells and matrix. Successful entering of the endochondral route was mirrored by the marked up-regulation of several key genes compared with postexpanded MSCs, including collagen type 2 ($\sim 10^7$-fold), type 10 ($\sim 10^6$-fold), and BSP ($\sim 10^5$-fold) (Fig. S1*D*). Upon implantation in vivo for up to 12 wk, samples underwent extensive remodeling, with hypertrophic cartilage areas being progressively and almost entirely replaced by BM and bone at increasing densities of mineralization, as assessed by histological and micro-CT analyses (Fig. 1). Additionally, the central construct core was progressively filled with matrix and ultimately remodeled into trabecular-like bone structures.

Contribution of Grafted Cells to the Bone Organ Formation. The bone matrix derived by remodeling of the hypertrophic cartilage template displayed distinct morphological features in different regions. After 5 wk in vivo, denser extracellular matrix (ECM) was deposited in the outer zone, starting from the external ring, and in the central zone, starting from the inner border of hypertrophic cartilage and progressing toward the core, as shown by Masson's trichrome staining (Fig. 2 *A* and *B*). At the end of the remodeling process, after 12 wk in vivo, the outer zone presented typical characteristics of the compact, cortical bone (e.g., elongated osteocytes, flattened bone-lining cells, and lamellar-like structures), whereas the inner zone resembled the cancellous bone (e.g., bigger cells and trabecular structure with higher surface area) (Fig. 2 *C* and *D*). By analogy with embryonic limb development, where cortical bone is formed through direct, intramembranous ossification and cancellous bone is formed through indirect, endochondral ossification, we termed the outer bone "perichondral bone" and the inner bone "endochondral bone." After 5 wk in vivo, human cells, detected by in situ hybridization (ISH) for human Alu repeats, were interspersed in the cartilaginous template with mouse cells (Fig. 2 *A* and *B*). After 12 wk in vivo, human cells were located only in the endochondral bone (Fig. 2*D*) and colocalized with Osterix-expressing cells with osteoblast and osteocytes appearance (Fig. S2 *A* and *B*), whereas the perichondral bone was populated by only mouse cells (Fig. 2*C*). Consistently with the typical fate of late hypertrophic chondrocytes during endochondral ossification, after 5 wk in vitro many human BM-derived mesenchymal stem/stromal cells (hMSCs) expressed the cleaved form of caspase 3 (Fig. S3*A*). However, after 5 wk in vivo most of the cells in the cartilaginous template were caspase 3 negative (Fig. S3*B*) and Osterix positive (Fig. S3*C*), suggesting survival and osteoblastic differentiation of part of the hMSC embedded in the cartilaginous template.

Physiological Response of the Endochondral Ossification Model to IL-1β. Inflammatory signals are known to play a critical role in bone tissue development and repair. Considering that IL-1β and TNF-α, the two master regulators of the inflammatory process during fracture repair, have a common mode of action (16), we investigated in more detail the response of the system to IL-1β, a well-characterized proinflammatory cytokine. Pretreatment of hypertrophic cartilage with IL-1β before implantation resulted after 5 wk in vivo in more abundant accumulation of matrix metallopeptidase 13 (MMP-13) and of DIPEN (the cryptic epitope of aggrecan, typically exposed upon its degradation) (Fig. 3*A*). The enhanced remodeling was paralleled by a higher extent of osteoclast recruitment, as assessed by tartrate-resistant acid phosphatase (TRAP) staining (Fig. 3*B*), a lower amount of Safranin-O–positive residual cartilage, and larger areas of BM (Fig. 3 *C* and *D*). Quantification of cytokines in the supernatants after in vitro culture indicated a statistically significant increase ($P < 0.05$) of stromal cell-derived factor-1 (SDF1), IL-8, macrophage-colony stimulating factor (M-CSF), monocyte chemotactic protein-1 (MCP-1), and MMP-13 in response to IL-1β, substantiating the findings observed in vivo and validating the biological functionality of the system (Fig. S4). Quantification of cytokines retained in the samples after 5 wk of in vitro culture also showed an increase of M-CSF (56-fold), MCP-1 (26-fold), receptor activator of

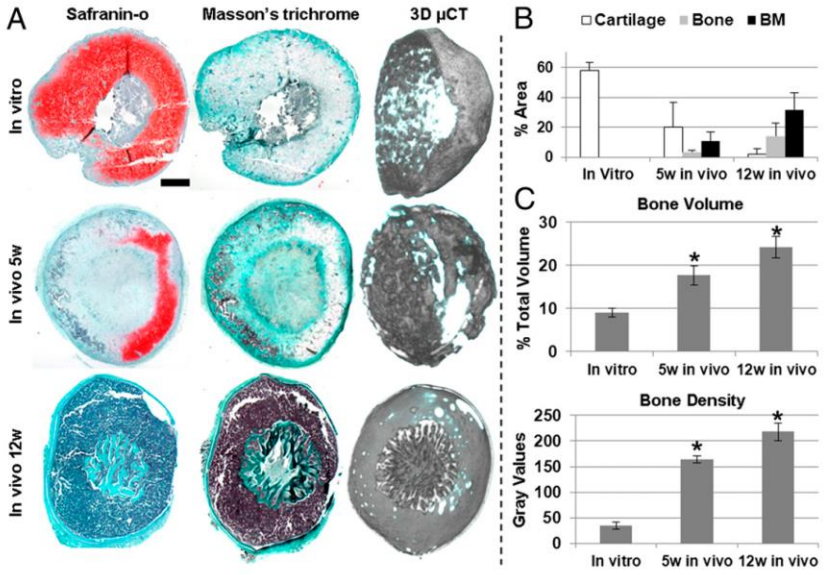

Fig. 1. Characterization of engineered endochondral bone tissue formation. Engineered hypertrophic cartilage templates underwent extensive remodeling in vivo into bone and BM. (*A*) Representative sections (Safranin O and Masson's trichrome) and 3D reconstructed microtomographic images of samples cultured for 5 wk in vitro and implanted ectopically in nude mice for 5 and 12 wk. (Scale bar, 1 mm.) (*B*) Quantitative histomorphometric data ($n = 9$) of cartilage, bone, and BM. (*C*) Quantitative morphometric data ($n = 4$) of mineral volume and density ($P < 0.05$).

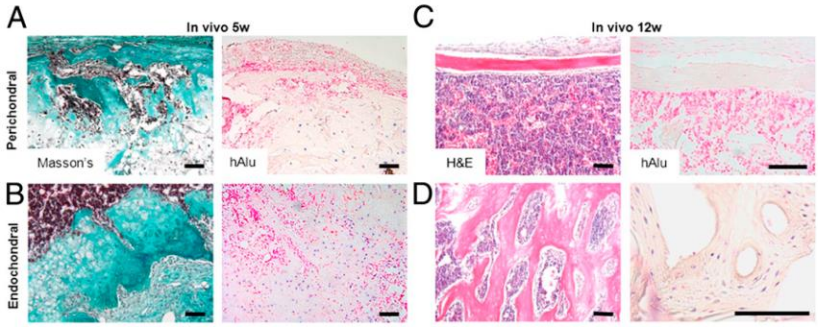

Fig. 2. Perichondral and endochondral bone is formed over the hypertrophic cartilage templates. (*A*) After 5 wk, the outer part of the construct displayed invasion by abundant host-derived cells, deposition of dense ECM, and only few human cells left in the cartilaginous template (*Left*, Masson's trichrome staining; *Right*, ISH for human Alu repeats, highlighting human cells in blue and mouse cells in pink). (*B*) After 5 wk in vivo, in the inner part of the construct denser ECM was deposited over the cartilaginous template where abundant human cells (blue cells) are present. (*C*) After 12 wk in vivo, the outer part of the construct was completely remodeled into cortical-like bone and BM, as shown by H&E staining. Importantly, ISH demonstrates presence of only host-derived cells (pink cells). (*D*) After 12 wk in vivo, trabecular-like bone was formed in the inner construct areas, and human cells could still be located within the mature bone tissue. (Scale bars, 100 μm.)

nuclear factor kappa-B ligand (RANKL) (29-fold), MMP-13 (12-fold), and osteoprotegerin (OPG) (sixfold) compared with untreated controls. In particular, the establishment of an environment prone to remodeling was confirmed by a 4.3-fold increase in the RANKL/OPG ratio (17).

Development of Mature Vascularization. Because angiogenesis is a process critically required in the endochondral ossification route, we next assessed the pattern of vascularization of hypertrophic cartilage upon implantation. After 5 wk in vivo, staining for CD31 indicated that blood vessels had penetrated only the outer part of the constructs, corresponding to the areas positive for collagen type 10, whereas cartilaginous regions not overtly hypertrophic were still avascular (Fig. 4*A* and Fig. S5*A*). Consistent with the physiology of blood vessels maturation (18), mural NG2 proteoglycan $(NG2)^+$ pericytes surrounded the newly formed vascular structures (Fig. 4*B*). At 12 wk the constructs, now consisting predominantly of BM and bone/osteoid tissues positive for collagen type 1 (Fig. 4*C* and Fig. S5*B*), included vessels with a sinusoid-like structure, consistently stabilized by α-smooth muscle actin (α-SMA) (Fig. 4*D*). Collectively, these data indicate a coordinated progression of implant remodeling and vascularization, driven by the onset of hypertrophy and thus consistent with patterns observed in the growth plate and during bone repair through callus formation (2, 16).

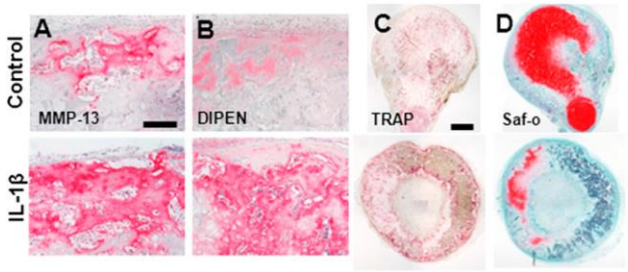

Fig. 3. Effect of IL-1β on endochondral bone formation. (*A*) Increased MMP-13 accumulation is evident after 5 wk in vivo in IL-1β–treated samples. (*B*) This is also paralleled by an enhanced aggrecan remodeling, as demonstrated by increased DIPEN staining. (Scale bar, 200 μm.) (*C*) Increased host-derived osteoclast recruitment is shown by TRAP staining. (Scale bar, 1 mm.) (*D*) Notable reduction in cartilaginous ECM and increase in BM content are demonstrated by the Safranin O staining.

Development of a Functional HSC Niche. We then investigated whether generated ossicles, previously reported to include regions with morphological features of BM foci (4), could induce homing and maintenance of phenotypically and functionally defined HSC (Fig. 5*A*). In vitro-manufactured constructs were implanted into B6.Cg-Foxn1nu/J $CD45.2^+$ mice. After 12 wk, ossicles and femurs from transplanted and untreated mice were recovered, crushed, and analyzed by FACS. Interestingly, frequencies of putative HSC ($LKS^+CD34^-CD135^-CD150^+$), megakaryocyte-erythroid progenitors (MEP: LKS^-CD34^-), and common myeloid /granulocyte-macrophage progenitors (CMP/GMP: LKS^-CD34^+) (19) in constructs displayed a similar distribution as found in femurs from control mice and mice carrying engineered ossicles (Fig. 5 *B* and *C*). The hematopoietic functionality of the recovered ossicle-derived cells was then assessed by transplantation in C57BL/6 $CD45.1^+/CD45.2^+$ lethally irradiated mice in a competitive setting using $CD45.1^+$ support cells. As early as 1 mo after transplantation, peripheral blood contained more than 80% ossicle-derived cells (Fig. 5*D*), consisting predominantly of B cells and myeloid-lineage cells (Fig. 5*E*). Relative frequencies of donor and competitor-derived blood cells displayed a dose-dependent correlation, as assessed by administering different numbers of ossicle-derived cells (Fig. 5*F*). Sequential bleeding at 1, 2, and 3.5 mo after transplantation confirmed the long-term self-renewing capacity of the ossicle-derived HSC, with stable engraftment and multilineage reconstitution (Fig. 5*E*). Relative frequencies of the different lineages were comparable to the control, demonstrating a similar functionality of HSC derived from the native femur or the ectopically engineered ossicles (Fig. 5*E*). Femoral BM of recipient mice, cytofluorimetrically analyzed 3.5 mo after transplantation, demonstrated a consistent contribution of donor-derived $CD45.2^+$ cells within the compartments of phenotypic HSCs (LKS^+CD34^-), multipotent progenitors (LKS^+CD34^+), CMP/GMP (LKS^-CD34^+), and MEP (LKS^-CD34^-) (Fig. 5*F*). Moreover, the efficiency of reconstitution of these pools was similar in the mice transplanted with femur-derived or with different doses of ossicle-derived cells. These data prove the capacity of the engineered hypertrophic cartilage tissues to support and drive the homing and maintenance of functional HSCs.

Discussion

Adherent MSCs isolated from human postnatal BM have long been identified as having the capacity to ectopically generate "miniature ossicles," including bone matrix and hematopoietic tissue architectures and reproducing physiological and pathological processes of skeletal elements (20). The present study reports

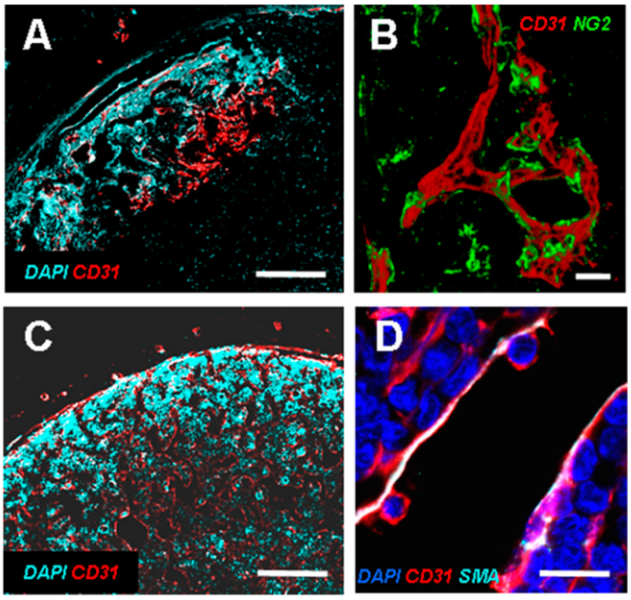

Fig. 4. In vivo vascularization of the implanted hypertrophic cartilage templates. (*A*) After 5 wk only the outer region of the engineered tissue was vascularized, as shown by CD31 staining. (*B*) Vessels were already stabilized by $NG2^+$ pericytes. (Scale bars, 100 μm.) (*C*) After 12 wk tissues were deeply vascularized, and the BM displayed sinusoid-like vascular structures with a partially SMA-positive wall, indicative of mature stabilization (*D*). (Scale bars, 20 μm.)

that adult hMSCs can be further manipulated to ectopically engineer a full-fledged "bone organ," at a size, structure, and degree of biological functionality comparable to that of native bones. The claim regarding the functionality of the implant is based on (*i*) the recapitulation of typical processes of bone tissue development and remodeling, coupled with the formation of a mature vascular network, (*ii*) the physiological response to inflammatory signals, known to regulate resorption, and of the cartilage intermediate, and (*iii*) the establishment of large BM spaces, capable of hosting and sustaining fully functional HSCs.

The bone organ model was engineered by activating hMSCs toward an endochondral ossification route and thus by invoking a "developmental engineering" paradigm. The autonomous, self-organized progression of the processes, recapitulating bone development (4), was critically required (*i*) to promote osteogenesis in the absence of priming by a ceramic-based scaffold, and (*ii*) to induce efficient vascularization in the absence of cocultured endothelial cells. At 12 wk after implantation, these features allowed the formation of bone matrix by active donor cells down to the core of the grafts, namely at approximately 4 mm from the outer edges. The endochondral ossification route thus seems to address the issues of vascularization of the engineered tissue and cell survival, which are considered as key bottlenecks for a coherent clinical exploitation of cell-based bone regeneration strategies (21).

The host origin of the perichondral bone vs. the contribution of human cells in the central endochondral bone could be related to the spatial patterns of composition and vascularization of the cartilaginous template. Formation of the endochondral bone would be driven by the implanted cells, capable of surviving the hypoxic condition of an avascular environment and of switching on the expression of the master osteoblastic transcription factor Osterix (22). Because Osterix expression in the central region was associated with hypertrophic chondrocytes, our findings would argue for the direct contribution of terminally differentiated cartilage cells to endochondral bone formation. Instead, formation of the perichondral bone would be driven by host osteoprogenitor cells, colonizing the construct from the outer surface through the network of ingrowing blood vessels, and primed to intramembranous bone formation by the external mineralized layer, containing BSP. The formation of bone tissue by two distinct processes, namely endochondral and intramembranous, resembles the distinct responses taking place during fracture healing (16). This feature, recognized thanks to the use of a model upscaled in size, suggests the possible use of engineered hypertrophic cartilage as a surrogate of fracture callus, in pathologies where this does not form efficiently (e.g., atrophic nonunions). Moreover, the recruitment of resident cells for bone formation at the implant periphery warrants further investigations on the nature of the delivered instructive signals, which could develop the perspective of engineering decellularized ECMs based on hypertrophic cartilage to induce endogenous regeneration of bone tissue (23).

The use of IL-1β during the last phase of in vitro culture was introduced with the double intent of demonstrating a physiological response of the system to inflammatory signals and accelerating resorption of the large mass of hypertrophic cartilage. In line with the known effect on growth plate and fracture callus cartilage (16), in our model IL-1β induced (*i*) enhanced MMP-13–mediated endogenous ECM preprocessing; (*ii*) enhanced host osteoclast-mediated ECM remodeling by increased M-CSF levels and RANKL/OPG ratios; (*iii*) faster vascularization, despite a minimal reduction in VEGF content (15); and (*iv*) larger regions of BM, possibly because of an increased synthesis of SDF1, IL-8, M-CSF, and MCP-1. Instead, IL-1β did not induce a reduction of bone mass by increased bone resorption (24), because its administration was temporally confined to the phase preceding bone matrix deposition. Further studies are required to validate the functionality of the engineered bone organ in the context of an immunocompetent model at an orthotopic site, where loading and inflammation would further regulate bone development and homeostasis.

The marrow component of the engineered bone organ, occupying the majority of its volume, was demonstrated to include phenotypically and functionally defined HSCs at a comparable frequency to normal bones of the same mice. These unprecedented findings validate the physiological nature of the in vivo-established ossicle and reinforce the evidence of self-organization ability of hMSC-based hypertrophic cartilage templates into functional hematopoietic niches. Interestingly, the increased amount of host-derived BM in response to IL-1β seemed to mirror the enhanced

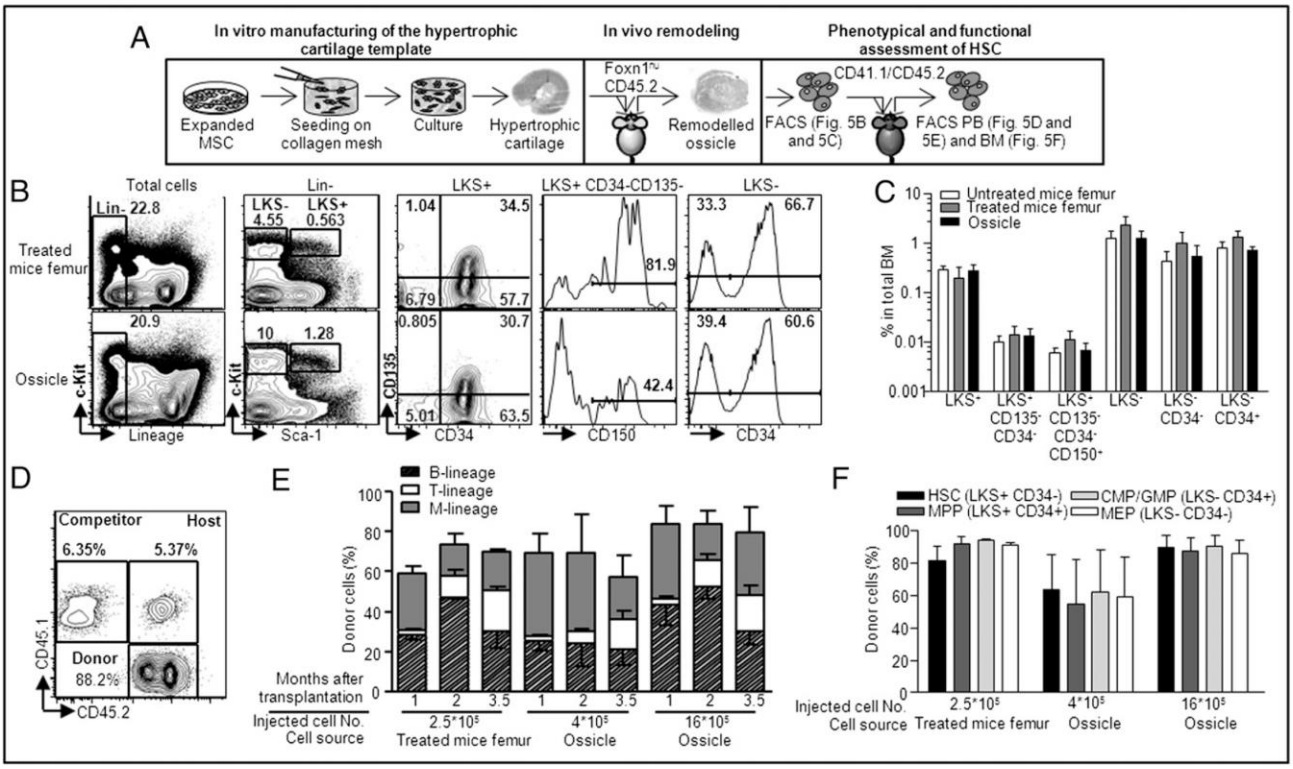

Fig. 5. Homing and maintenance of functional mouse HSCs in the implanted templates. (*A*) In vitro manufacturing and in vivo remodeling. Three months after implantation, cells were harvested from untreated, treated femur, or in vivo-remodeled templates and transplanted into lethally irradiated congenic animals. (*B*) Representative profile of HSCs and progenitors in treated femur or in vivo-remodeled ossicles 3 mo after in vivo implantation (*C*) Summary of cytofluorimetric analysis of BM HSCs and progenitors (n = 3–4). (*D*) Representative profile of peripheral blood analysis. (*E*) Time-course analysis of donor engraftment and lineage distribution in peripheral blood of repopulated recipients (n = 3–5). (*F*) Summary of cytofluorimetric analysis of BM HSCs and progenitors in recipient mice 3.5 mo after transplantation (n = 3–5). Error bars represent SDs of n = 3–4 measurements.

osteoclast recruitment, as recently outlined in the context of HSC niches in a murine model (25). The developed system, although requiring further investigations to specify the mode of establishment (e.g., a direct vs. indirect niche effect of the human cells in triggering homing of the mouse HSC), offers the opportunity to address a variety of critical questions at the interface between HSC biology and regenerative medicine. The model can be exploited to dissect cues that regulate HSC engraftment, by engineering marrow environments with defined and genetically controlled properties (e.g., by knockin/out of specific factors, possibly defined by high-throughput screening systems) (13, 26). In fact, the capacity of the ectopic marrow to attract and retain rare circulating HSCs advocates its function as a "stem cell trap," ultimately providing a tool to investigate the physiological factors and mechanisms underlying the still debated concept of the HSC niche. Furthermore, on the basis of the concept of mutual influences between the BM microenvironment and leukemia cells (27, 28), the possibility of establishing a human origin BM microenvironment in humanized hematopoietic murine models (29–31) has a large relevance to investigate the development and progression of blood cell malignancies. Last but not least, the generation of an extramedullary bone organ, accessible to advanced imaging techniques (e.g., intravital confocal microscopy) (14), opens the perspective to investigate and exploit processes underlying the efficient expansion of HSCs for therapeutic purposes (13).

In conclusion, we have reported an upscaled model based on adult human cells that displays morphological, phenotypic, and functional features of a "bone organ." The system can be used in fundamental investigations of the biology of bone development and of HSC niches, as well as in translational studies related to restoration of bone tissue and of normal hematopoiesis.

Materials and Methods

All human samples were collected with informed consent of the involved individuals, and all mouse experiments were performed in accordance with Swiss law. All studies were approved by the responsible ethics authorities and by the Swiss Federal Veterinary Office. MSCs were expanded for two passages (accounting for an average of 13–15 doubling), to minimize the loss of chondrogenic potential, and characterized by flow cytometry for putative MSC markers, with results consistent with our previous report (4). Cells were then seeded onto type I collagen meshes at a density of 70×10^6 cells/cm^3 and cultured in chondrogenic conditions for 3 wk in a serum-free chondrogenic medium, followed by 2 wk in a serum-free hypertrophic medium (4). Samples were implanted in s.c. pouches of nude mice (four samples per mouse) and retrieved after 5 or 12 wk. The resulting in vitro and in vivo tissues were analyzed histologically, immunohistochemically, biochemically (glycosaminoglycans, DNA, protein content), by real-time RT-PCR, and by microtomography. Tissue development in vivo was evaluated histologically, immunohistochemically, and by microtomography. Total BM cells, obtained from long bones of control or treated mice (CD45.2$^+$) or from the engineered ossicles by crashing/collagenase digestion, were treated with red blood cell lysis buffer and transplanted into lethally (9.5 cGy)-irradiated congenic animals (CD45.1/2$^+$). Blood samples were collected from the transplants and analyzed by flow cytometer after staining with antibodies against CD45.1/2 allotype, B (CD19), T (CD3ε), and myeloid lineage markers (CD11b/Gr-1). The survival and contribution to bone formation by MSC was evaluated with ISH for human Alu sequences. A more complete and detailed description of the methods is included in *SI Materials and Methods*.

ACKNOWLEDGMENTS. We thank Allison Hoch for proofreading the manuscript. The work was partially funded by Swiss National Science Foundation

Grant NMS1725 (to I.M.), by AO Foundation Grant S-11-13P (to A.P.), and by the Promedica Foundation (Chur, Switzerland) and the clinical research focus program "Human Hemato-Lymphatic Diseases" of the University of Zürich (both to M.G.M.).

1. Lenas P, Moos M, Luyten FP (2009) Developmental engineering: A new paradigm for the design and manufacturing of cell-based products. Part I: From three-dimensional cell growth to biomimetics of in vivo development. *Tissue Eng Part B Rev* 15(4):381–394.
2. Kronenberg HM (2003) Developmental regulation of the growth plate. *Nature* 423 (6937):332–336.
3. Jukes JM, et al. (2008) Endochondral bone tissue engineering using embryonic stem cells. *Proc Natl Acad Sci USA* 105(19):6840–6845.
4. Scotti C, et al. (2010) Recapitulation of endochondral bone formation using human adult mesenchymal stem cells as a paradigm for developmental engineering. *Proc Natl Acad Sci USA* 107(16):7251–7256.
5. Janicki P, Kasten P, Kleinschmidt K, Luginbuehl R, Richter W (2010) Chondrogenic pre-induction of human mesenchymal stem cells on beta-TCP: Enhanced bone quality by endochondral heterotopic bone formation. *Acta Biomater* 6(8):3292–3301.
6. Farrell E, et al. (2011) In-vivo generation of bone via endochondral ossification by in-vitro chondrogenic priming of adult human and rat mesenchymal stem cells. *BMC Musculoskelet Disord* 12:31.
7. Wilson A, Trumpp A (2006) Bone-marrow haematopoietic-stem-cell niches. *Nat Rev Immunol* 6(2):93–106.
8. Méndez-Ferrer S, et al. (2010) Mesenchymal and haematopoietic stem cells form a unique bone marrow niche. *Nature* 466(7308):829–834.
9. Calvi LM, et al. (2003) Osteoblastic cells regulate the haematopoietic stem cell niche. *Nature* 425(6960):841–846.
10. Zhang J, et al. (2003) Identification of the haematopoietic stem cell niche and control of the niche size. *Nature* 425(6960):836–841.
11. Sacchetti B, et al. (2007) Self-renewing osteoprogenitors in bone marrow sinusoids can organize a hematopoietic microenvironment. *Cell* 131(2):324–336.
12. Chan CK, et al. (2009) Endochondral ossification is required for haematopoietic stem-cell niche formation. *Nature* 457(7228):490–494.
13. Chen Y, et al. (2012) Human extramedullary bone marrow in mice: A novel in vivo model of genetically controlled hematopoietic microenvironment. *Blood* 119(21):4971–4980.
14. Lee J, et al. (2012) Implantable microenvironments to attract hematopoietic stem/cancer cells. *Proc Natl Acad Sci USA* 109(48):19638–19643.
15. Mumme M, et al. (2012) Interleukin-1β modulates endochondral ossification by human adult bone marrow stromal cells. *Eur Cell Mater* 24:224–236.
16. Gerstenfeld LC, Cullinane DM, Barnes GL, Graves DT, Einhorn TA (2003) Fracture healing as a post-natal developmental process: Molecular, spatial, and temporal aspects of its regulation. *J Cell Biochem* 88(5):873–884.
17. Jurado S, et al. (2010) Effect of IL-1beta, PGE(2), and TGF-beta1 on the expression of OPG and RANKL in normal and osteoporotic primary human osteoblasts. *J Cell Biochem* 110(2):304–310.
18. Carmeliet P, Jain RK (2011) Molecular mechanisms and clinical applications of angiogenesis. *Nature* 473(7347):298–307.
19. Kondo M, et al. (2003) Biology of hematopoietic stem cells and progenitors: Implications for clinical application. *Annu Rev Immunol* 21:759–806.
20. Bianco P, et al. (1998) Reproduction of human fibrous dysplasia of bone in immunocompromised mice by transplanted mosaics of normal and Gsalpha-mutated skeletal progenitor cells. *J Clin Invest* 101(8):1737–1744.
21. Meijer GJ, de Bruijn JD, Koole R, van Blitterswijk CA (2007) Cell-based bone tissue engineering. *PLoS Med* 4(2):e9.
22. Nakashima K, et al. (2002) The novel zinc finger-containing transcription factor osterix is required for osteoblast differentiation and bone formation. *Cell* 108(1):17–29.
23. Sadr N, et al. (2012) Enhancing the biological performance of synthetic polymeric materials by decoration with engineered, decellularized extracellular matrix. *Biomaterials* 33(20):5085–5093.
24. Polzer K, et al. (2010) Interleukin-1 is essential for systemic inflammatory bone loss. *Ann Rheum Dis* 69(1):284–290.
25. Mansour A, et al. (2012) Osteoclasts promote the formation of hematopoietic stem cell niches in the bone marrow. *J Exp Med* 209(3):537–549.
26. Gobaa S, et al. (2011) Artificial niche microarrays for probing single stem cell fate in high throughput. *Nat Methods* 8(11):949–955.
27. Lane SW, Scadden DT, Gilliland DG (2009) The leukemic stem cell niche: Current concepts and therapeutic opportunities. *Blood* 114(6):1150–1157.
28. Mercier FE, Ragu C, Scadden DT (2012) The bone marrow at the crossroads of blood and immunity. *Nat Rev Immunol* 12(1):49–60.
29. Rongvaux A, et al. (2011) Human thrombopoietin knockin mice efficiently support human hematopoiesis in vivo. *Proc Natl Acad Sci USA* 108(6):2378–2383.
30. Strowig T, et al. (2011) Transgenic expression of human signal regulatory protein alpha in Rag2-/-gamma(c)-/- mice improves engraftment of human hematopoietic cells in humanized mice. *Proc Natl Acad Sci USA* 108(32):13218–13223.
31. Willinger T, Rongvaux A, Strowig T, Manz MG, Flavell RA (2011) Improving human hemato-lymphoid-system mice by cytokine knock-in gene replacement. *Trends Immunol* 32(7):321–327.

Supporting Information

Scotti et al. 10.1073/pnas.1220108110

SI Materials and Methods

MSC Isolation, in Vitro Culture, and in Vivo Implantation. Human mesenchymal stem cells (MSCs) were isolated from bone marrow aspirates and processed as previously described (1). MSCs were expanded for two passages (referred to as postexpanded MSC), seeded onto type I collagen meshes (8-mm-diameter, 2-mm-thick disks; Ultrafoam, Davol) at a density of 70×10^6 cells/cm^3 and cultured in chondrogenic conditions for 3 wk in a serum-free chondrogenic medium, followed by 2 wk in a serum-free hypertrophic medium, supplemented with 50 nM thyroxine, 7.0×10^{-3} M β-glycerophosphate, 10^{-8} M dexamethasone, and 2.5×10^{-4} M ascorbic acid and IL-1β (50 pg/mL). Samples were implanted in s.c. pouches of nude mice (four samples per mouse) or nude C57BL/6 and retrieved after 5 or 12 wk.

Real-Time RT-PCR Quantitation of Transcript Levels. Total RNA extraction, cDNA synthesis (2), and real-time RT-PCR (7300 AB; Applied Biosystems) were performed to quantitate expression levels of the following genes of interest: type II or type X collagen, bone sialoprotein, osteocalcin (2), Cbfa-1/Runx2 (primer R GCC TTC AAG GTG GTA GCC C; primer F CGT TAC CCG CCA TGA CAG TA; probe CCA CAG TCC CAT CTG GTA CCT CTC CG), matrix metalloproteinase13 (MMP-13; Applied Biosystems, ref. no. Hs00233992_m1), desert hedgehog homolog (DHH; Applied Biosystems, ref. no. Hs00368306_m1), sonic hedgehog homolog (SHH; Applied Biosystems, ref. no. Hs01123832_m1), Indian hedgehog homolog (IHH; Applied Biosystems, ref. no. Hs01081800_m1), patched homolog 1 (PTCH1; Applied Biosystems, ref. no. Hs00970980_m1), glioma-associated oncogene homolog 1 (GLI1; Applied Biosystems, ref. no. Hs00171790_m1), parathyroid hormone-like hormone (PTHLH; Applied Biosystems, ref. no. Hs00174969_m1), parathyroid hormone 1 receptor (PTH1R; Applied Biosystems, ref. no. Hs00174895_m1), bone morphogenetic protein 2 (BMP2; primer R AAC ACT GTG CGC AGC TTC C; primer F CTC CGG GTT GTT TTC CCA C; probe CCA TGA AGA ATC TTT GGA AGA ACT ACC AGA AAC TG), bone morphogenetic protein 4 (BMP4; Applied Biosystems, ref. no. Hs00181626_m1), and bone morphogenetic protein 7 (BMP7-Applied Biosystems, ref. no. Hs00233476_m1). GAPDH was used as housekeeping, reference gene (primer R ATG GGG AAG GTG AAG GTC G; primer F TAA AAG CAG CCC TGG TGA CC; probe CGC CCA ATA CGA CCA AAT CCG TTG AC).

Histological Staining, Immunohistochemistry, and in Situ Hybridization for Alu Repeats. After in vitro and in vivo cultures, the constructs were fixed in 4% (vol/vol) paraformaldehyde, if necessary decalcified with 7% (vol/vol) EDTA solution (Sigma), and embedded in paraffin. Sections (7 μm thick) were stained with H&E (Baker), Masson's trichrome, Alizarin red, or for tartrate-resistant acid phosphatase (TRAP) activity by means of the leukocyte acid phosphatase kit (Sigma). Immunohistochemical analyses were performed to characterize the extracellular matrix (ECM) over the time using the following antibodies: bone sialoprotein (BSP) (Immundiagnostik), MMP-13 (AbCam), Aggrecan cryptical epitope-MMP-generated C-terminal neoepitope (DIPEN) (MD Biosciences), and cleaved caspase 3 (Cell Signaling Technology). Upon rehydratation in ethanol series, sections were treated according to the manufacturer's instructions. The immunobinding was detected with biotinylated secondary antibodies and using the appropriate Vectastain ABC kits. The red signal was developed with the Fast Red kit (Dako Cytomation) and sections counterstained by hematoxylin. Negative controls were performed during each analysis by omitting the primary antibodies. Chromogenic in situ hybridization (Zytovision kit) to detect human *Alu* repeat sequences was performed following the manufacturer's instructions using nuclear fast red (Sigma) as nuclear counterstaining. Histological and immunohistochemical sections were analyzed using an Olympus BX-61 microscope.

Immunofluorescence Images. After in vivo implantation samples were fixed in 4% (vol/vol) paraformaldehyde (Sigma), decalcified with EDTA (Sigma) solution, embedded in optimal cutting temperature (OCT) compound, and snap frozen in liquid nitrogen. Sections (20 μm thick) were incubated with the primary antibodies against Col X (Abcam), CD31 [platelet endothelial cell adhesion molecule (PECAM-1); BD Pharmingen], Col I (MP Biomedicals), NG2 (Chemicon International), α-smooth muscle actin (α-SMA) (MP Biomedicals), Osterix (Abcam), and cleaved caspase 3 (Cell Signaling Technology). As appropriate, secondary antibodies labeled with Alexa Fluor 647, Alexa Fluor 488, or Alexa Fluor 546 (Invitrogen) were used, and DAPI was used to stain nuclei. Fluorescence images were acquired using a confocal Zeiss LSM 710 microscope.

Microtomography. Microtomography was performed at different time points with in vivo implants. After fixation in formalin and storage in PBS, micro-CT data were acquired using a SkyScan 1174 tabletop scanner with unfiltered X-rays (applied voltage 32 kV; current 800 μA). Transmission images were acquired during a 360° scan rotation with an incremental rotation step size of 0.4°. Reconstruction was made using a modified Feldkamp algorithm at an isotropic voxel size of 6.26 μm. Threshold-based segmentation and 3D measurement analyses (bone mineral density and volume) were performed using the CT-Analyzer program (SkyScan) as previously described (3). 3D rendering of the structures was performed using VGStudio MAX 1.2.1 software (Volume Graphics).

Statistical Analysis. The results of real-time RT-PCR, quantitative microtomography, and protein quantification are presented as mean ± SD ($n = 4$). Statistical analysis was performed using the Wilcoxon rank-sum test. P values of 0.05 or less were considered statistically significant.

Proteins Quantification. During culture, cell supernatants were collected after 3, 8, and 15 d of hypertrophic medium change and analyzed for their content of a panel of growth factors, chemokines, and metalloproteinases, according to the manufacturer's instructions (Procarta Immunoassay Kit; Panomics). Protein levels were also determined in tissue lysates collected from constructs cultured for 5 wk.

Flow Cytometry. Femurs and ossicles were smashed with mortar and pestle and filtered with 70-μm nylon filter (BD Biosciences). Red blood cells were lysed in 150 mM ammonium-chloride, 1 mM Na_2EDTA, and 10 mM potassium-hydrogen-carbonate (Sigma) for 1 min at room temperature, and filtered with 40-μm nylon filter (BD Biosciences). The resultant cells were stained with biotinylated lineage antibodies (CD3ϵ, CD4, CD8α, CD19, CD11b, B220, Gr-1, NK1.1, and Ter119) in FACS buffer [PBS, 2% (vol/vol) FBS (Invitrogen), 2 mM EDTA (Ambion)] and detected with streptavidin pacific blue (Invitrogen). Simultaneously, cells were stained with c-Kit PE-Cy5 (clone 2B8), Sca-1APC-Cy7 (D7), CD135 PE (A2F10), CD34 (RAM34), and CD150 (TC15-

12F12.2) and analyzed on FACS CantoII (BD Biosciences). Hoechst 33343 (Invitrogen) was added to the sample to exclude dead cells from the analysis. All antibodies are from eBiosciences or Biolegend unless specified.

Competitive Whole Bone Marrow Transplantation. Cells isolated from respective tissues of implanted nude C57BL/6 ($CD45.2^+$) were suspended in PBS and injected into 9.5 Gy γ-irradiated C57BL/6 mice ($CD45.1/2^+$) together with 2.5×10^5 competitor cells from congenic mice ($CD45.1^+$) to ensure 100% survival. At different time points after reconstitution, peripheral blood was taken from the transplants and lysed with red cell lysis buffer as mentioned above. Cells were stained with CD45.1 FITC, CD45.2 R-Phycoerythrin (PE), CD3ϵ PE-Cy5, CD19 PE-Cy7, Gr-1 allophycocyanin (APC), and CD11b APC-Cy7, and analyzed on FACS CantoII to determine donor chimerism and lineage repopulation. For bone marrow (BM) analysis, BM cells were harvested from femurs and tibiae of transplants by flushing and red blood cell lysis and subjected to the staining described above and flow cytometric analysis.

1. Braccini A, et al. (2005) Three-dimensional perfusion culture of human bone marrow cells and generation of osteoinductive grafts. *Stem Cells* 23(8):1066–1072.
2. Barbero A, Ploegert S, Heberer M, Martin I (2003) Plasticity of clonal populations of dedifferentiated adult human articular chondrocytes. *Arthritis Rheum* 48(5):1315–1325.
3. Papadimitropoulos A, et al. (2007) Kinetics of in vivo bone deposition by bone marrow stromal cells within a resorbable porous calcium phosphate scaffold: An X-ray computed microtomography study. *Biotechnol Bioeng* 98(1):271–281.

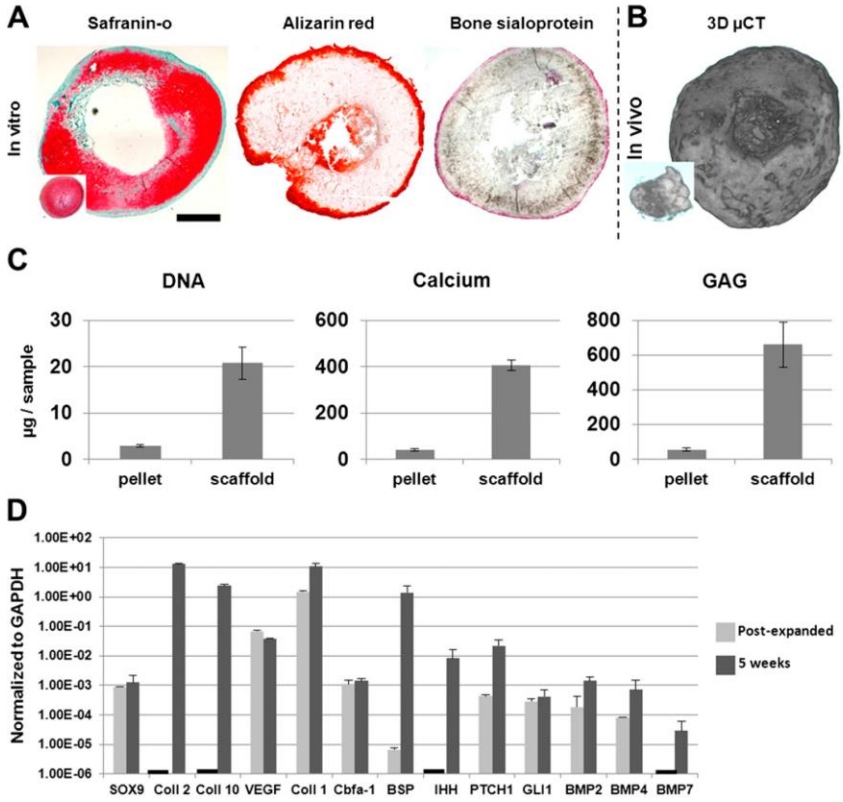

Fig. S1. In vitro characterization and comparison with the previously developed small-scale model. (*A* and *B*) Representative section and microtomographic 3D reconstructed image of samples cultured for 5 wk in vitro and of small-scale sample (*Insets*). (Scale bar, 1 mm.) (*C*) Biochemical characterization of upscaled samples vs. small-scale samples. (*D*) Quantitative real-time RT-PCR demonstrated an up-regulation of chondrogenic (Col 2), hypertrophic (Col 10), osteogenic (Col 1, BSP), Hedgehog pathway (IHH, PATCH1), BMPs (BMP2, BMP4, BMP7) genes compared with postexpanded hMSCs.

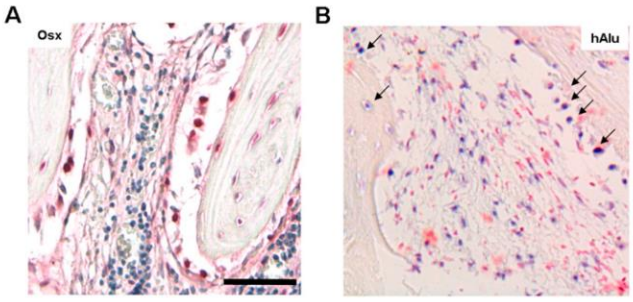

Fig. S2. Human-derived osteoblasts and osteocytes are located in the inner endochondral bone. (*A*) Representative section of samples after 12 wk in vivo immunostained for Osterix. (*B*) in situ hybridization for human Alu repeats showing human cells within the bone trabeculae and outside the bone surface. (Scale bars, 100 μm.)

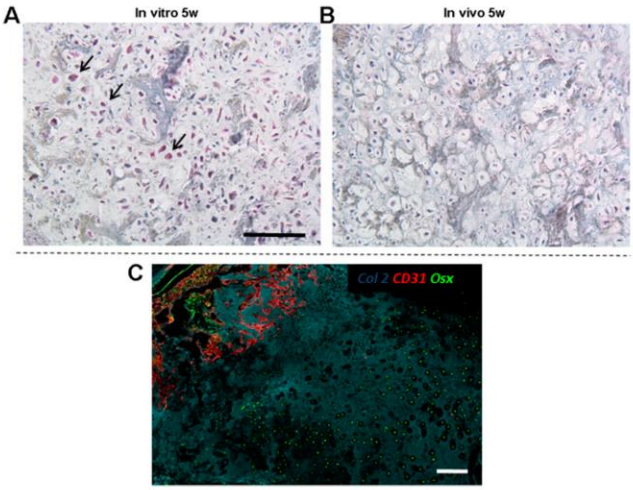

Fig. S3. Survival and Ostrix expression of chondrogenically differentiated human MSCs. (*A* and *B*) Representative section of samples cultured for 5 wk in vitro (*A*) plus 5 wk in vivo (*B*) immunostained for the cleaved caspase 3. (*C*) Osterix expression pattern after 5 wk in vivo: Osterix is mainly expressed in the outer vascularized bone collar and in the inner nonvascularized, cartilaginous tissue. (Scale bars, 100 μm.)

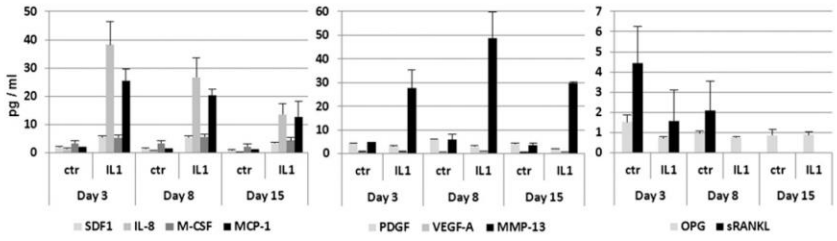

Fig. S4. Protein quantification in supernatants. Concentrations of chemotactic cytokines (SDF1, IL-8, M-CSF, MCP-1), factors involved in hypertrophic cartilage resorption (PDGF, VEGF-1, MMP-13), and factors engaged remodelling (OPG, RANKL). Values are normalized to levels before hypertrophic medium administration (day 0). SDF1, stromal cell-derived factor-1; IL1, interleukin 8; M-CSF, macrophage-colony stimulating factor; MCP-1, monocyte chemotactic protein-1; PDGF, platelet-derived growth factor; VEGF-1, vascular endothelial growth factor A; MMP-13, matrix metalloproteinase 13; RANKL, receptor activator of nuclear factor kappa-B ligand; OPG, osteoprotegerin.

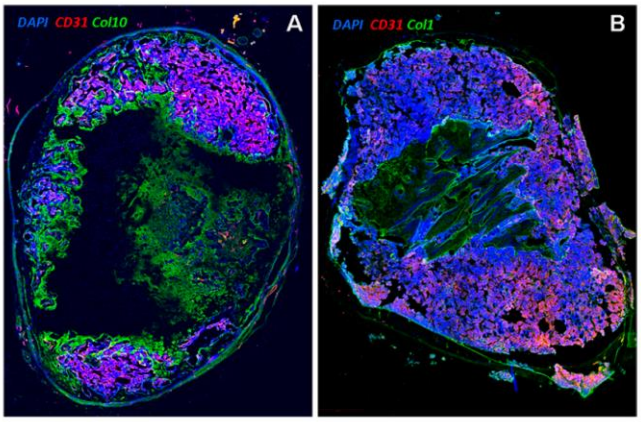

Fig. S5. Vascularization of upscaled hypertrophic cartilage templates in vivo. (*A*) Representative tile-scan of a sample after 5 wk in vivo stained for CD31 and Col10. Vascularization and bone marrow strictly colocalize with the hypertrophic cartilaginous ECM positive for Col10. (*B*) Representative tile-scan of a sample after 12 wk in vivo stained for CD31 and Col1. The whole tissue is now vascularized, and Col1 positive bone and osteoid tissue are located in the inner part of the sample.

CHAPTER 3

Interleukin-1β modulates endochondral ossification by human adult bone marrow stromal cells

European Cells and Materials Vol. 24 2012 (pages 224-236) ISSN 1473-2262

INTERLEUKIN-1β MODULATES ENDOCHONDRAL OSSIFICATION BY HUMAN ADULT BONE MARROW STROMAL CELLS

Marcus Mumme[1,§], Celeste Scotti[1,§], Adam Papadimitropoulos[1], Athanas Todorov[1], Waldemar Hoffmann[1], Chiara Bocelli-Tyndall[1,2], Marcel Jakob[1], David Wendt[1], Ivan Martin[1,*] and Andrea Barbero[1]

[1]Departments of Surgery and of Biomedicine, University Hospital Basel, Hebelstrasse 20, 4031 Basel, Switzerland
[2]Deparment of Rheumatology, University of Basel, Felix Platter Spital, Burgfelderstrasse 101, 4012 Basel, Switzerland

[§]These authors contributed equally to the manuscript

Abstract

Inflammatory cytokines present in the milieu of the fracture site are important modulators of bone healing. Here we investigated the effects of interleukin-1β (IL-1β) on the main events of endochondral bone formation by human bone marrow mesenchymal stromal cells (BM-MSC), namely cell proliferation, differentiation and maturation/remodelling of the resulting hypertrophic cartilage. Low doses of IL-1β (50 pg/mL) enhanced colony-forming units-fibroblastic (CFU-f) and -osteoblastic (CFU-o) number (up to 1.5-fold) and size (1.2-fold) in the absence of further supplements and glycosaminoglycan accumulation (1.4-fold) upon BM-MSC chondrogenic induction. In osteogenically cultured BM-MSC, IL-1β enhanced calcium deposition (62.2-fold) and BMP-2 mRNA expression by differential activation of NF-κB and ERK signalling. IL-1β-treatment of BM-MSC generated cartilage resulted in higher production of MMP-13 (14.0-fold) *in vitro*, mirrored by an increased accumulation of the cryptic cleaved fragment of aggrecan, and more efficient cartilage remodelling/resorption after 5 weeks *in vivo* (i.e., more TRAP positive cells and bone marrow, less cartilaginous areas), resulting in the formation of mature bone and bone marrow after 12 weeks. In conclusion, IL-1β finely modulates early and late events of the endochondral bone formation by BM-MSC. Controlling the inflammatory environment could enhance the success of therapeutic approaches for the treatment of fractures by resident MSC and as well as improve the engineering of implantable tissues.

Keywords: Mesenchymal stem cells; tissue engineering; chondrogenesis; osteogenesis; endochondral ossification.

*Address for correspondence:
Ivan Martin
Institute for Surgical Research and Hospital Management
University Hospital Basel, Hebelstrasse 20,
CH-4031 Basel, Switzerland
Telephone Number: 41-61-265-2384
FAX Number: 41-61-265-3990
E-mail: imartin@uhbs.ch

Introduction

Fracture healing is a finely orchestrated process which recapitulates bone development and typically results in functional tissue regeneration (Gerstenfeld *et al.*, 2003; Behonick *et al.*, 2007; Marsell and Einhorn, 2011). Inflammation plays a crucial role in promoting and directing several aspects of bone regeneration (e.g., vascularisation, cell recruitment, cartilaginous callus production) and involves secretion of tumour necrosis factor-α (TNF-α); interleukin-1 (IL-1), IL-6, IL-11 and IL-18 (Gerstenfeld *et al.*, 2003). Importantly, the typical expression pattern of TNF-α and IL-1, the two master regulators of inflammation in fracture healing, is bimodal, with a peak within the first 24 hours which ends after 7 days, and a second peak after 4 weeks, with some variability, depending of the age of the patient (Cho *et al.*, 2002; Gerstenfeld *et al.*, 2003; Lange *et al.*, 2010). Briefly, the purpose of the first peak is to promote cell recruitment into the haematoma and vascularisation, while the second peak regulates cartilaginous callus remodelling (Cho *et al.*, 2002; Gerstenfeld *et al.*, 2003).

Even though the literature is controversial, numerous clinical studies indicate that the use of nonsteroidal anti-inflammatory drugs (NSAID), frequently used for postoperative pain control, may increase the risk of delayed fracture healing (Giannoudis *et al.*, 2000; Burd *et al.*, 2003; Bhattacharyya *et al.*, 2005). Moreover, several studies in different animal models indicated that a long-acting NSAID therapy is more deleterious than a short-acting NSAID treatment (Krishak *et al.*, 2007; O'Conner *et al.*, 2009; Ochi *et al.*, 2011). Taken together, these results highlight a key role of inflammation in influencing the processes of fracture healing.

Most fractures heal by indirect fracture healing, which consists of a combination of endochondral ossification, leading to formation of a cartilaginous callus, and intramembranous ossification, which results in formation of a periosteal callus. However, the key feature of this process is the remodelling and ossification of the cartilaginous callus (Gerstenfeld *et al.*, 2003). The interaction of a tissue undergoing the endochondral route with inflammatory signals is a crucial process to be investigated. Most *in vitro* studies assessed the effects of inflammatory cytokines on either osteogenic or chondrogenic differentiation capacity of mesenchymal stromal cells (MSC). In particular, IL-1β and TNF-α stimulation has been shown to enhance the extent of mineralisation and expression of osteoblast-related genes during MSC culture in osteogenic medium

(Ding *et al.*, 2009; Hess *et al.*, 2009; Cho *et al.*, 2010), and to inhibit MSC chondrogenesis in a dose-dependent manner (Wehling *et al.*, 2009). However, no study has yet reported on the role of inflammatory cytokines on the different phases of proliferation, differentiation and maturation/remodelling of an endochondral tissue, based on human bone marrow MSC (BM-MSC) *in vitro* or *in vivo*.

With the final goal of identifying specific tissue repair processes regulated by IL-1β during endochondral/perichondral bone formation, we studied the effects of IL-1β on (i) proliferation and commitment of BM-MSC; (ii) osteogenic and chondrogenic differentiation of BM-MSC; (iii) maturation/remodelling of the BM-MSC-generated cartilage tissue during *in vitro* and (iv) *in vivo* endochondral bone formation. Since *in vivo* BM-MSC are typically exposed to a hypoxic environment (Das *et al.*, 2010), the effects of IL-1β during osteogenic and chondrogenic culture were also investigated at different oxygen percentages (19 %, 5 % and 2 %).

Materials and Methods

Cell harvest

Human bone marrow aspirates were harvested from 7 individuals (all male, mean age: 36.7 years, range: 24-49 years) during routine iliac crest bone grafting, in accordance with the rules of the local ethical committee (University Hospital Basel) and after informed consent was obtained.

BM-MSC culture

BM-MSC were isolated from bone marrow aspirates as previously described (Braccini *et al.*, 2005). Nucleated cells were counted after staining with Crystal Violet 0.01 % (Sigma-Aldrich, St. Louis, MO, USA) and seeded in culture dishes at a density of $4.5x10^3$ cells/cm^2 for the clonogenic culture or in culture flasks at a density of $1.7x10^5$ cells/cm^2 for the expansion of BM-MSC.

Clonogenic culture

Cells were cultured for 2 weeks in alpha-MEM (minimal essential medium) (Gibco/Life Technologies, Carlsbad, CA, USA) supplemented with 10 % foetal bovine serum, 1 mM sodium pyruvate, 100 mM HEPES buffer, 100 U/mL penicillin, 100 µg/mL streptomycin, and 0.29 mg/mL L-glutamine (complete medium) with IL-1β (Sigma-Aldrich) (0, 50 or 1000 pg/mL) in the presence or not of 5 ng/mL fibroblast growth factor-2 (FGF-2) in a humidified incubator at 37 °C with 5 % CO_2 with medium changes twice a week.

Expansion of BM-MSC

Cells were cultured for two passages in complete medium supplemented with 5 ng/mL FGF-2 as described earlier (Frank *et al.*, 2002).

Osteogenic differentiation

Osteogenic differentiation was induced in 2D cultures using a defined medium (osteogenic medium) as previously described (Frank *et al.*, 2002). Briefly, BM-MSC were seeded in 6- or 12-well plates at a density of $3x10^3$ cells/cm^2 in alpha-MEM supplemented with 10 % foetal bovine serum (FBS), 10 mM β-glycerophosphate (Sigma-Aldrich), 10 nM dexamethasone (Sigma-Aldrich) and 0.1 mM L-ascorbic acid-2-phosphate (Sigma-Aldrich) and cultured for 2 or 3 weeks, with medium changes twice per week. IL-1β at different concentrations (i.e., 0, 10, 50, 100, 250 and 1000 pg/mL) was added at the beginning of the experiment and at each medium change. Cell layers were cultured for 3 weeks in a humidified incubator at 37 °C with 5 % CO_2 and 19 % oxygen or in a "Sci-tive" Workstation (Ruskinn Technology, Pencoed, South Wales, UK), to maintain constant hypoxic conditions (i.e., 5 % and 2 % oxygen). Medium was changed twice per week.

BM-MSC from three donors were used to study whether inhibition of NF-κB or ERK modulates IL-1β osteogenic responses. BM-MSC were grown for 7 days in 12-well plates with the last three days without FGF-2. Confluent layers were then supplemented with 50 nM pyrrolidine dithiocarbamate (PDTC, NF-κB inhibitor, Sigma-Aldrich) or 10 µM UO126 (MEK/ERK inhibitor, Sigma-Aldrich) (Cho *et al.*, 2010) while in osteogenic medium. After 3 hours IL-1β (50 pg/mL) was added to selected wells and maintained only for the first three days. Cells were then cultured in osteogenic medium (without IL-1β and inhibitors) for an additional 11 days. Control wells were cultured in osteogenic medium without inhibitors and/or IL-1β for the entire 14 days. U0126 was dissolved in dimethyl sulphoxide (DMSO) at a stock concentration of 10 mM. DMSO 1:1000 supplemented to the cells as control was observed not to modulate osteogenic differentiation.

Chondrogenic differentiation

Chondrogenic differentiation was induced in 3D pellet cultures using a defined serum-free medium (chondrogenic medium), as previously described (Jakob *et al.*, 2001). Briefly, BM-MSC were resuspended in Dulbecco's modified Eagle's medium (DMEM) containing 4.5 mg/mL D-glucose, 0.1 mM non-essential amino acids, 1 mM sodium pyruvate, 100 mM HEPES buffer, 100 U/mL penicillin, 100 µg/mL streptomycin, and 0.29 mg/mL L-glutamine supplemented with ITS+1 (10 µg/mL insulin, 5.5 µg/mL transferrin, 5 ng/mL selenium, 0.5 mg/mL bovine serum albumin, 4.7 µg/mL linoleic acid (Sigma-Aldrich), 0.1 mM ascorbic acid 2-phosphate (Sigma-Aldrich), 10 ng/mL TGFβ 1 (R&D Systems, Minneapolis, MN, USA) and 10^{-7} M dexamethasone (Sigma-Aldrich). Aliquots of $4x10^5$ cells/0.5 mL were centrifuged at 1,200 rpm for 5 min in 1.5 mL polypropylene conical tubes (Sarstedt, Numbrecht, Germany) to form spherical pellets. IL-1β at the concentrations described above was added at the beginning of the experiment and at each medium change. Pellets were cultured under different oxygen percentages as previously described.

Endochondral priming in vitro

BM-MSC were cultured in type I collagen meshes (Ultrafoam®, Davol, Warwick, RI, USA) at a density of $40x10^6$ cells/cm^3 in chondrogenic medium. After 3 weeks, cartilaginous tissues were cultured for an

additional 2 weeks in a serum-free hypertrophic medium without TGF-β 1, supplemented with 50 nM thyroxine, 10 mM β-glycerophosphate, 10^{-8} M dexamethasone, and 0.1 mM L-ascorbic acid-2-phosphate (Scotti *et al.*, 2010). Endochondral primed constructs were then analysed or implanted ectopically in nude mice (as described below).

Endochondral bone formation in vivo

Constructs cultured for 5 weeks *in vitro* were implanted subcutaneously in the back of nude mice (CD-1 nu/nu, athymic, 6- to 8-week old females) (4 samples/mouse), following approval by the local veterinary authorities, and retrieved after 5 or 12 weeks. The *in vivo* experiment was performed with BM-MSC from only one human donor, previously selected out of 7 independent preparations based on the capability to generate hypertrophic cartilage *in vitro*.

Analytical methods

CFU-f and CFU-o

After 2 weeks of clonogenic culture, dishes were rinsed with phosphate-buffered saline (PBS) and stained for alkaline phosphatase (AP) using the 104-LL kit (Sigma Diagnostics, St. Louis, MO, USA). The number of AP positive colonies (with more than 32 cells/colony) was counted by three independent investigators to estimate the fraction of colony forming units osteoblastic (CFU-o). The same dishes were then stained with 1 % methylene blue (MB) and the total number of MB positive colonies (AP positive or negative, with more than 32 cells/colony) were counted to estimate CFU-fibroblastic (CFU-f). The diameter of the MB positive colonies was measured using the UTHSCSA ImageTool 3.0 software.

Histological staining, immunohistochemistry and in situ hybridisation (ISH)

Chondrogenic pellets and constructs were fixed in 4 % paraformaldehyde for 24 h at 4 °C, dehydrated in an ethanol series and embedded in paraffin. Sections (5 µm thick) were stained for safranin-O, alcian blue, haematoxylin and eosin (H&E) (J.T. Baker Chemical, Phillipsburg, N.J., USA), alizarin red and Masson's trichrome. Immunohistochemical analyses were performed using primary antibodies against Osterix (Abcam, Cambridge, UK), Osteocalcin (EMD Millipore, Billerica, MA, USA), MMP13 (Abcam) and aggrecan cryptical epitope-DIPEN (MD Biosciences, St Paul, MN, USA) (Scotti *et al.*, 2010). Upon rehydration in a graded ethanol series, sections were digested according to the manufacturer's instructions. The immunobinding was detected with biotinylated secondary antibodies and by Vectastain ABC (Vector Labs, Burlingame, CA, USA) kit. The red signal was developed with Fast red kit (Dako Cytomation; Dako, Glostrup, Denmark), with haematoxylin counterstaining. Negative controls were performed during each analysis by omitting the primary antibodies. Osteogenically cultured layers were washed twice with PBS, fixed for 10 min in 4 % formalin and stained with alizarin red 2 %. Hydroxyapatite deposits in osteogenically cultured layers were stained using the Osteoimage Mineralisation Assay (Lonza, Walkersville, MD, USA), following the manufacturer's instructions. Quantification of safranin O positive areas (21 slides, 10 samples, total 7.35 cm^2) and bone marrow content in Masson's trichrome staining (20 slides, 10 samples, total 7 cm^2) was performed with ImageJ 1.46d (National Institutes of Health, Bethesda, MD, USA) using thresholding and manual selection. ISH for human Alu repeats was performed as previously published (Scotti *et al.*, 2010).

Immunofluorescence images

Samples after *in vivo* culture were fixed in 4 % paraformaldehyde (Sigma-Aldrich), decalcified with EDTA (Sigma-Aldrich) solution, embedded in OCT and snap frozen in liquid nitrogen. Sections (20 µm thick) were incubated with the primary antibodies anti CD31 (PECAM-1; BD Pharmingen, Franklin Lakes, NJ, USA). When needed, a secondary antibody labelled with Alexa Fluo 546 (Invitrogen/Life Technologies, Carlsbad, CA, USA) was chosen and DAPI was used as nuclear staining. Fluorescence images were acquired using a Zeiss (Oberkochen, Germany) LSM-510 confocal microscope. The percentage of area infiltrated by vessels (CD31) was calculated on cross sections of the implant excluding the outer fibrotic capsule (n = 6 per experimental group) with ImageJ 1.46d (National Institutes of Health) using thresholding and manual selection.

Quantification of glycosaminoglycan (GAG) and DNA contents

Chondrogenic pellets and constructs were digested in proteinase K (1 mg/mL proteinase K in 50 mM Tris with 1 mM EDTA, 1 mM iodoacetamide, and 10 mg/mL pepstatin A) for 16 h at 56 °C. The GAG content of the cartilaginous tissues as well as in the supernatant harvested after each media change was determined spectrophotometrically using dimethylmethylene blue, with chondroitin sulphate as standard (Farndale *et al.*, 1986). The DNA content of constructs and cell layers (lysed with 0.01 % sodium dodecyl sulphate, SDS) was measured using the CyQuant cell proliferation assay kit (Molecular Probes, Eugene, OR, USA) and used to normalise the GAG content.

Quantification of calcium

Osteogenically cultured layers and constructs following hypertrophic culture were lysed with 0.5 N HCl. For quantification of calcium deposition, cell layers were harvested and analysed using the RANDOX (Crumlin, Co. Antrim, UK) CA 590 according to the manufacturer's protocol.

Quantification of VEGF and MMP13

VEGF and MMP13 protein levels were determined according to manufacturer in total protein lysates collected from constructs cultured for 5 weeks (Quantikine, human VEGF and human pro-MMP13, R&D Systems).

Quantitative real-time RT-PCR

Total RNA was extracted from cells using TRIzol (Invitrogen/Life Technologies), treated with DNAse and retrotranscribed into cDNA, as previously described (Frank *et al.*, 2002). Real-time reverse transcriptase-polymerase chain reaction (RT-PCR; 7300 Applied Biosystems/Life

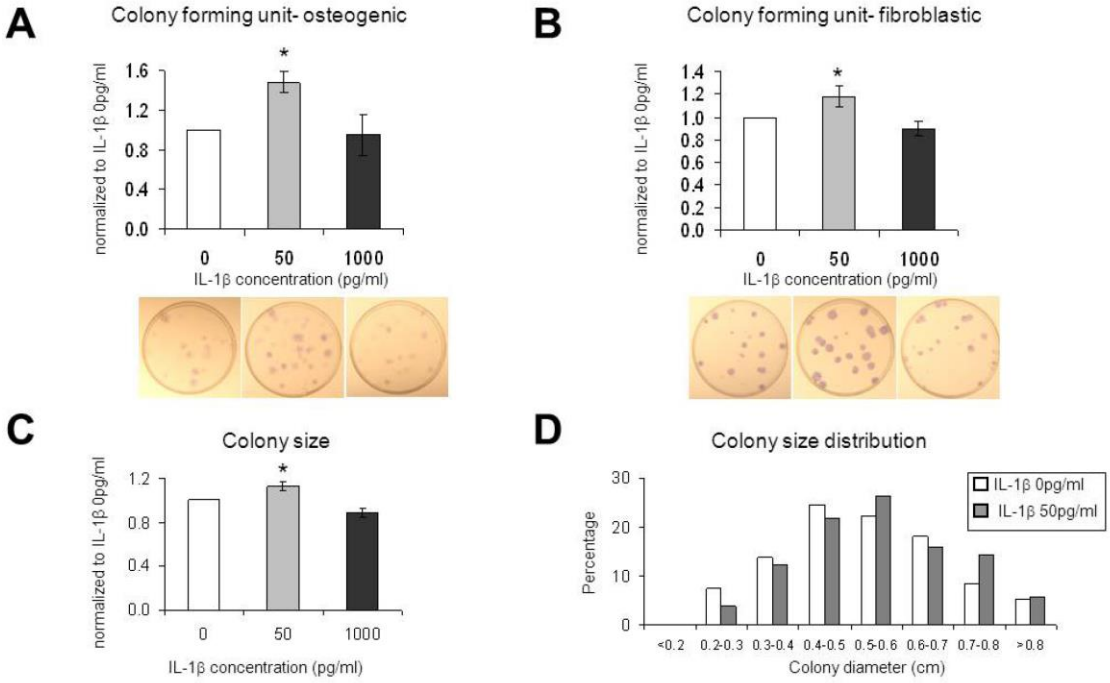

Fig. 1. Effects of IL-1β during clonal culture of human bone marrow stromal cells (BM-MSC). (**A**) Colony forming unit (CFU) -osteoblastic (quantification upper graph, representative colonies stained for alkaline phosphatase, bottom) and (**B**) CFU-fibroblastic (quantification upper graph, representative colonies further stained with methylene blue, bottom). (**C**) Quantification of colony size. $n = 3$ experiments with cells from 3 different donors, 3 plates/donor analysed. Values are mean ± SD, * = $p < 0.05$ from IL-1β 0 pg/mL. (**D**) Colony size distribution of a BM-MSC donor.

Technologies) was performed as previously described (Barbero *et al.*, 2003) to quantify expression levels of mRNA of genes expressed in cartilage (collagen type II), hypertrophic cartilage (collagen type X) in undifferentiated mesenchymal tissues and/or bone (type I collagen, bone sialoprotein, osteocalcin, bone morphogenetic protein (BMP)-2), as well as of genes involved in ECM remodelling, apoptosis and cell proliferation (MMP-13, caspase 3 and Ki-67), using human specific primers and probes. For each sample, the Ct value of each target sequence was subtracted from the Ct value of the reference gene (glyceraldehyde-3-phosphate dehydrogenase, GAPDH), to derive ΔCt. The expression level of each target gene was calculated as $2^{\Delta Ct}$.

Microtomography

Microtomography (μCT) was performed on constructs at different *in vivo* time points, after fixation in formalin and storage in PBS. μCT data were acquired using a SkyScan 1174 table top scanner (SkyScan, Kontich, Belgium) with unfiltered X-rays at an applied voltage of 32 kV and a current of 800 μA. Transmission images were acquired for a 360° scan rotation with an incremental rotation step size of 0.4°. Reconstruction was made with a modified Feldkamp algorithm at an isotropic voxel size of 6.26 μm. Threshold-based segmentation and 3D measurement analyses (bone mineral density and volume) were performed using the CT-Analyser program (SkyScan NV), as previously described (Papadimitropoulos *et al.*, 2007). 3D rendering of the structures was performed using the commercial software VGStudio MAX 1.2.1. (Volume Graphics, Heidelberg, Germany).

Statistical analysis

For each experiment and donor, at least triplicate specimens were assessed and the values presented as mean ± standard deviation of measurements. For the dose response experiments, repeated measures ANOVA was performed using a linear mixed-effects model with a *post-hoc* Dunnett comparison to baseline, corrected for multiple comparisons. This computation was performed with R v. 2.14.2 and the packages "nlme" and "multcomp". Differences between experimental groups were otherwise assessed by two-tailed Wilcoxon tests and considered statistically significant with $p < 0.05$ (Sigma Stat software, SPSS, IBM, Amonk, NY, USA).

Results

Effect of IL-1β on the clonogenicity and proliferation of BM-MSC

We first investigated whether supplementation of IL-1β during the culture of bone marrow cells affected their (i) clonogenicity, (ii) osteogenic commitment in the absence of differentiating factors, and (iii) proliferation. Freshly

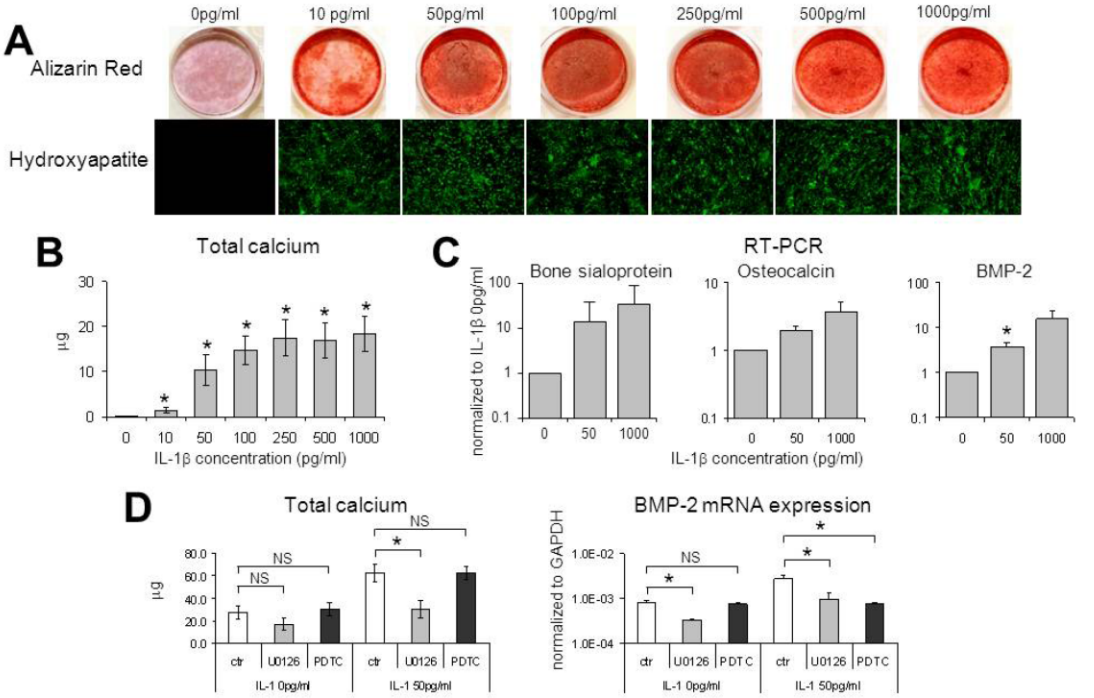

Fig. 2. Effects of IL-1β on the osteogenic differentiation of human bone marrow stromal cells (BM-MSC). (**A**) Representative alizarin red (top) and hydroxyapatite-specific fluorescence (bottom) staining and (**B**) total calcium contents of osteogenically cultured BM-MSC. (**C**) Real time RT-PCR analysis of the expression of bone sialoprotein, osteocalcin and bone morphogenetic protein (BMP)-2, levels are normalised to glyceraldehyde-3-phosphate dehydrogenase (GAPDH) and expressed as fold of difference from those measured in cells not stimulated with IL-1β. $n = 5$ experiments with cells from 5 different donors, 10 specimens analysed. (**D**) Effect of ERK and NF-κB inhibition (through 72 h incubation with 10 µm UO126 and 50 nM pyrrolidine dithiocarbamate (PDTC) respectively) on total calcium accumulation and on BMP-2 mRNA expression (see materials and methods for the description of the experimental design). $n = 3$ experiments with cells from 3 different donors, 6 specimens analysed. Data are mean ± SD. * = $p < 0.05$ from IL-1β 0 pg/mL, NS = no significant differences.

isolated bone marrow nucleated cells were then cultured at clonogenic density without IL-1β or in the presence of 50 pg/mL or 1000 pg/mL of IL-1β. IL-1β at the lowest dose significantly enhanced the fraction of CFU-o and CFU-f (1.5- and 1.2-fold respectively, Fig 1A-B). The average colony size was also increased (by 1.2-fold) following exposure to 50 pg/mL IL-1β (Fig. 1C), indicating an enhanced propensity of the cells to proliferate. By grouping the colony diameters in arbitrary size groups we observed a shift in the distribution upon exposure to 50 pg/mL IL-1β (median value from 0.45 cm to 0.55 cm) (Fig. 1D). The presence of FGF-2 during the clonogenic culture of BM-MSC reduced the IL-1β mediated increases of CFU-o, CFU-f and colony size (data not shown).

Effect of IL-1β on the differentiation of BM-MSC

We then investigated whether IL-1β stimulation enhanced the differentiation capacity of BM-MSC when cultured under chondrogenic or osteogenic conditions. Different doses of IL-1β (0 to 1000 pg/mL) were tested.

Osteogenic differentiation

Following culture of BM-MSC in osteogenic medium, the intensity of staining for calcium and hydroxyapatite deposit strongly increased in presence of IL-1β up to 50 pg/mL and remained almost unchanged at higher doses (Fig 2A). Biochemical analyses confirmed the histological trend: calcium contents increased up to 78-fold by IL-1β 50 pg/mL, higher doses of IL-1β induced a further increase in calcium contents that was not statistically significant (Fig. 2B). RT-PCR analyses indicated that IL-1β at both tested concentrations resulted in the up-regulation of the bone sialoprotein, osteocalcin and BMP-2, however statistically significant differences were observed only in the expression of BMP-2 at the lower dose of IL-1β (Fig. 2C). Interestingly, even a short exposure (3 days) of BM-MSC to 50 pg/mL IL-1β induced a significant increase of calcium deposition and expression of BMP-2 mRNA (Fig. 2D). To understand how IL-1β induces enhanced osteogenic differentiation of BM-MSC, cells were pre-treated with U0126 (an ERK inhibitor) or PDTC (an NF-κB inhibitor), exposed or not with 50 pg/mL IL-1β (3 days) and then induced to osteogenic differentiation. We observed that: (i) U0126 specifically inhibited the IL-1β induced calcium deposition and caused a general down-regulation of BMP-2 expression, (ii) PDTC did not affect calcium deposition but specifically inhibited the IL-1β mediated up-regulation of BMP-2 mRNA (Fig. 2D). No significant

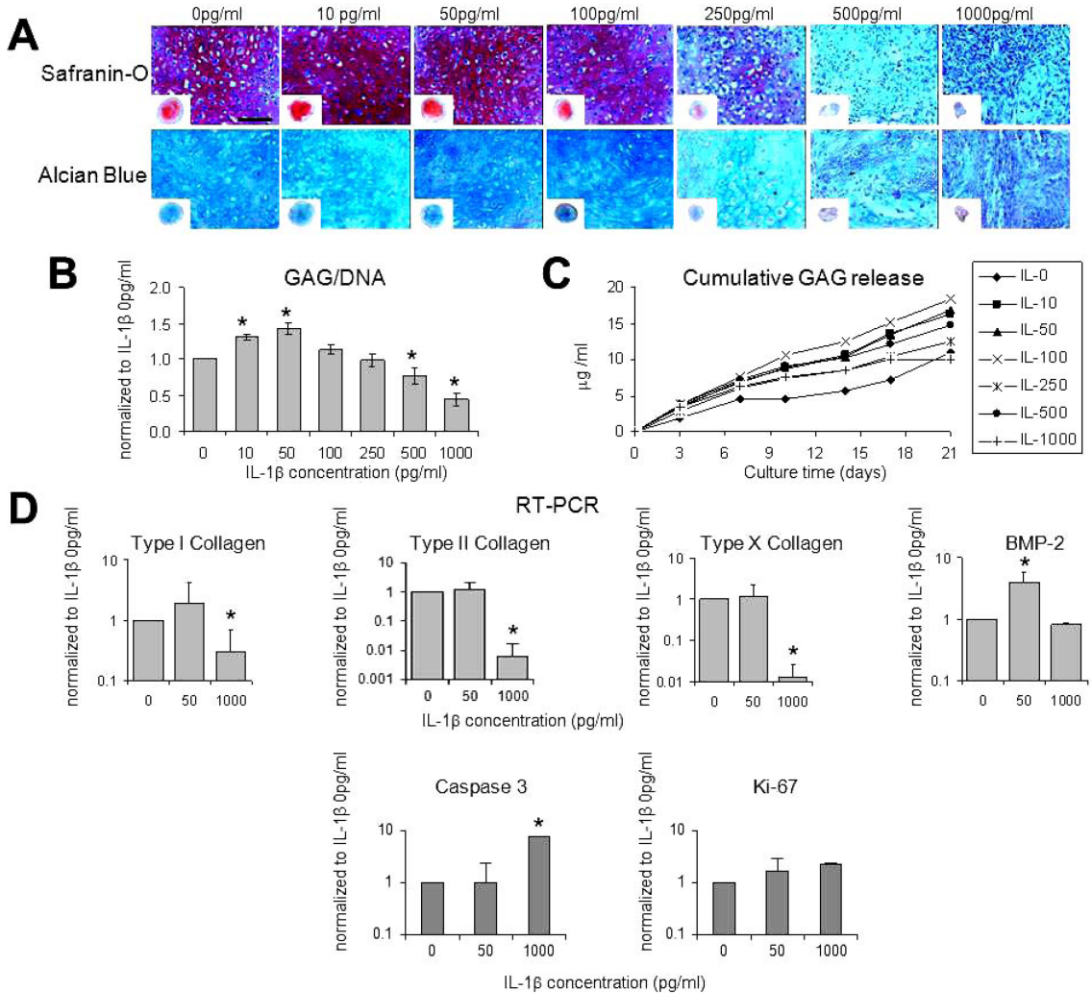

Fig. 3. Effects of IL-1β on the chondrogenic differentiation of human bone marrow stromal cells (BM-MSC). (**A**) Representative safranin-O (top) and Alcian Blue (bottom) staining of chondrogenic pellets. Bar = 50 µm (**B**) Sulphated glycosaminoglycan (GAG) content normalised to the DNA amount of the pellets. Levels are expressed as difference from those measured in cells not stimulated with IL-1β. n = 3 experiments with cells from 3 different donors, 6 specimens analysed. (**C**) GAG released during the chondrogenic culture of a representative BM-MSC donor. (**D**) Real time RT-PCR analysis of the expression of types I, II and X collagen, bone morphogenetic protein (BMP)-2, caspase 3 and Ki67 levels are normalised to glyceraldehyde-3-phosphate dehydrogenase (GAPDH) and expressed as fold of difference from those measured in cells not stimulated with IL-1β. n = 3 experiments with cells from 3 different donors, 6 specimens analysed. Data are mean ± SD. * = $p < 0.05$ from IL-1β 0 pg/mL.

differences in the DNA contents were observed between BM-MSC treated or not with U0126 or PDTC (data not shown), suggesting that the inhibitory effects in calcium deposition and BMP-2 expression of these two compounds were not due to a reduction in cell number/survival.

Collectively these results indicate that IL-1β induced an enhanced mineralisation and expression of BMP-2 by BM-MSC more reproducibly when applied at a low dose. Inhibition of ERK but not of NF-κB counteracted both IL-1β mediated mineralisation increase and BMP-2 upregulation.

Chondrogenic differentiation

MSC were also induced to differentiate in pellet in the absence or presence of IL-1β during the entire culture time. Histological analyses indicated that tissues formed by BM-MSC exposed to low doses of IL-1β (10 and 50 pg/mL) were more intensely stained for cartilage specific matrix than tissues formed in absence of IL-1β, while those exposed to high doses (≥ 250 pg/mL) were less intensely stained (Fig. 3A). Biochemical analyses generally confirmed this trend: GAG contents increased up to 1.4-fold (at the IL-1β dose of 50 pg/mL) and decreased up to 2.3-fold at the highest IL-1β dose (Fig. 3B). DNA

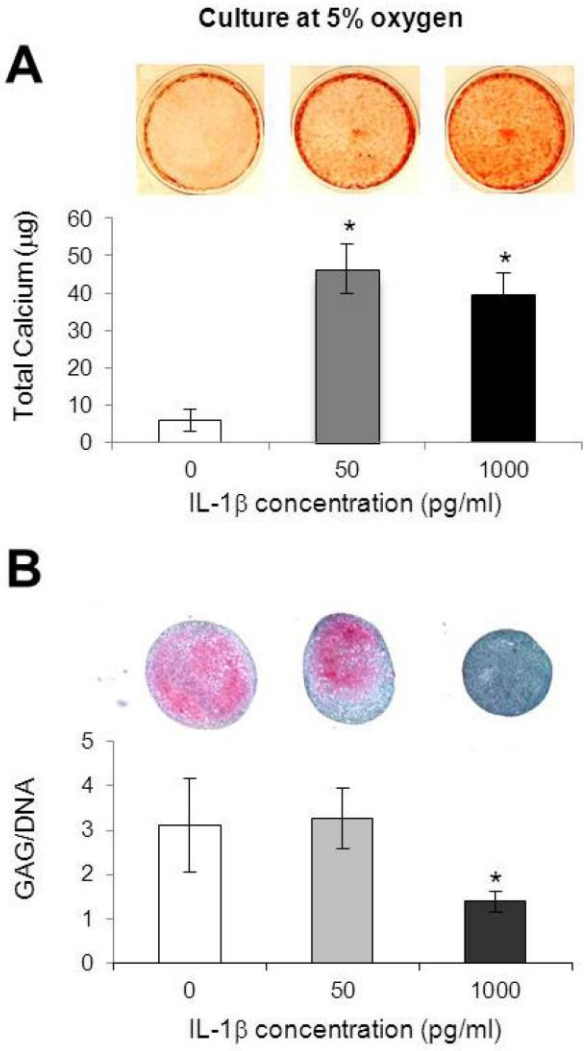

Fig. 4. Effects of IL-1β on the osteogenic and chondrogenic differentiation of human bone marrow stromal cells (BM-MSC) under hypoxic culture. (**A**) Representative alizarin red staining (top) and total calcium contents of osteogenically cultured BM-MSC under 5 % oxygen. (**B**) Representative safranin-O staining (top, scale bar = 500 µm) of and sulphated glycosaminoglycan (GAG) content normalised to the DNA amount of chondrogenic pellets. $n = 3$ experiments with cells from 3 different donors, 6 specimens analysed. Data are mean ± SD. * = $p < 0.05$ from IL-1β 0 pg/mL.

content of pellets gradually decreased with IL-1β, with no statistically significant difference between adjacent groups (data not shown). Biochemical analyses of culture medium harvested at different time of chondrogenic culture indicated that GAG was released to a higher extent by tissues exposed to the lower doses (≥ 100 pg/mL) of IL-1β (Fig. 3C). Cartilaginous tissues generated by BM-MSC not exposed to IL-1β or exposed to low (50 pg/mL) or high (1000 pg/mL) doses of IL-1β were also analysed by RT-PCR. The expression of type I, II and X collagen was not modulated by IL-1β at 50 pg/mL but strongly decreased in samples treated with IL-1β at 1000 pg/mL (3.4-, 170- and 80.1-fold respectively). BMP-2 expression, instead, was enhanced by IL-1β at 50 pg/mL (3.9-fold) but not effected by IL-1β at 1000 pg/mL (Fig. 3D). Interestingly, caspase 3 expression was significantly enhanced by IL-1β at 1000 pg/mL, possibly explaining the loss of DNA and the reduced pellet size, while Ki67 expression was not significantly modulated by IL-1β (Fig. 3D).

Overall these results indicate that low doses of IL-1β during the chondrogenic culture of BM-MSC enhanced the production (accumulation and release) of GAG and the expression of BMP-2 mRNA. Instead high doses of IL-1β reduced extracellular matrix production and chondrogenesis.

Effects of IL-1β under hypoxic culture

BM-MSC were cultured at reduced oxygen percentages (i.e., 5 % and 2 %) under osteogenic and chondrogenic conditions without IL-1β or with 50 pg/mL or 1000 pg/mL IL-1β. At 5 % oxygen, (i) calcium deposition of osteogenically cultured BM-MSC was enhanced following exposure to IL-1β (by 8.0- and 6.8-fold respectively for the concentration 50 pg/mL and 1000 pg/mL) (Fig. 4A), (ii) GAG amounts of pellets was not affected by 50 pg/mL IL-1β but reduced following exposure to 1000 pg/mL IL-1β (by 2.3-fold) (Fig. 4B). At 2 % oxygen, IL-1β (i) enhanced ECM mineralisation (at 50 and 1000 pg/mL) but to lower

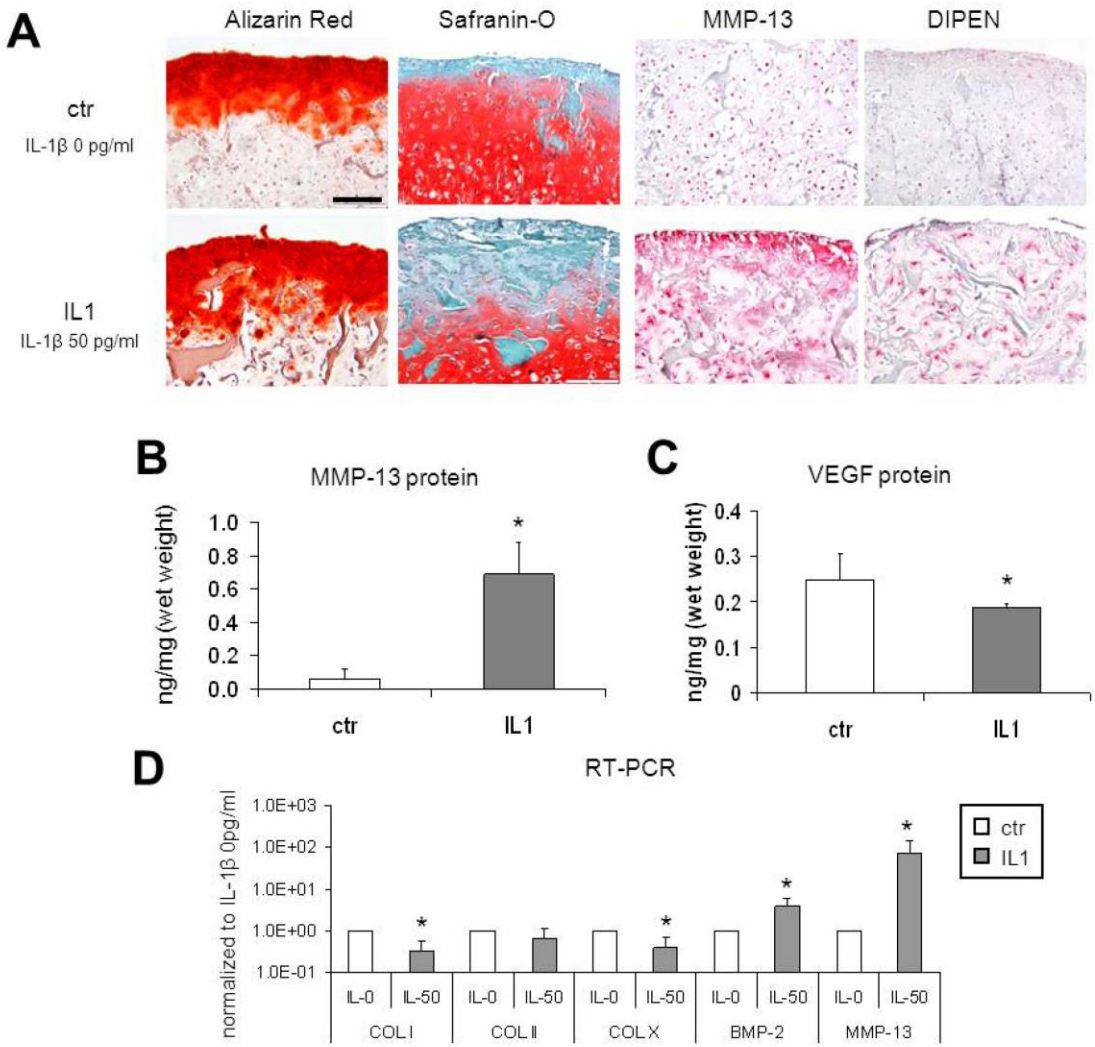

Fig. 5. Effects of IL-1β on *in vitro* formation and remodelling of a newly formed hypertrophic cartilage template by human bone marrow stromal cells (BM-MSC). (**A**) Representative alizarin red, safranin-O, metalloproteinase (MMP)-13 and Aggrecan cryptical epitope (DIPEN) staining of chondrogenic tissues cultured for the last two weeks without or with 50 pg/mL IL-1β. (**B**) MMP-13 protein quantification. (**C**) VEGF protein quantification. (**D**) Real time RT-PCR analysis of the expression of types I, II and X collagens, bone morphogenetic protein (BMP)-2, and MMP-13, levels are normalised to the glyceraldehyde-3-phosphate dehydrogenase (GAPDH) level and expressed as fold of difference from those measured in cells not stimulated with IL-1β. Scale bar = 200 μm; $n = 3$ experiments with cells from 3 different donors, 6 specimens analysed. Data are mean ± SD. * = $p < 0.05$ from IL-1β 0 pg/mL.

extents (data not shown), (ii) reduced GAG accumulation by 24.3 % ($p < 0.05$) at 50 pg/mL and to levels close to the limit of detection at 1000 pg/mL.

Effects of IL-1β on the endochondral bone formation

After demonstrating that IL-1β influenced the capacity of BM-MSC to differentiate towards both the chondrogenic and osteogenic lineage, we investigated the effects of this inflammatory chemokine on the maturation/remodelling of hypertrophic cartilage templates and subsequent endochondral bone formation *in vivo*, using our recently published model (Scotti *et al.*, 2010).

***In vitro* hypertrophic cartilage template formation**

Compared to controls, samples exposed to 50 pg/mL IL-1β contained (i) 38 % more calcium (37.95 ±5.47 μg/mg *vs.* 23.42 ±4.02 μg/mg, $p < 0.05$) resulting in a thicker calcified layer (as evidenced by alizarin red, Fig. 5A), (ii) 12 % less GAG (17.72 ±3.98 μg/mg *vs.* 15.59 ±1.6 μg/mg, $p < 0.05$), (iii) 14-fold higher amounts of MMP-13 protein as demonstrated by ELISA. Immunostaining of the extracellular matrix confirmed increased amount of MMP-13 and higher extent of MMP-mediated activity, as assessed by an increased accumulation of the cryptic cleaved fragment of aggrecan (DIPEN) (Fig 5A). MMP-

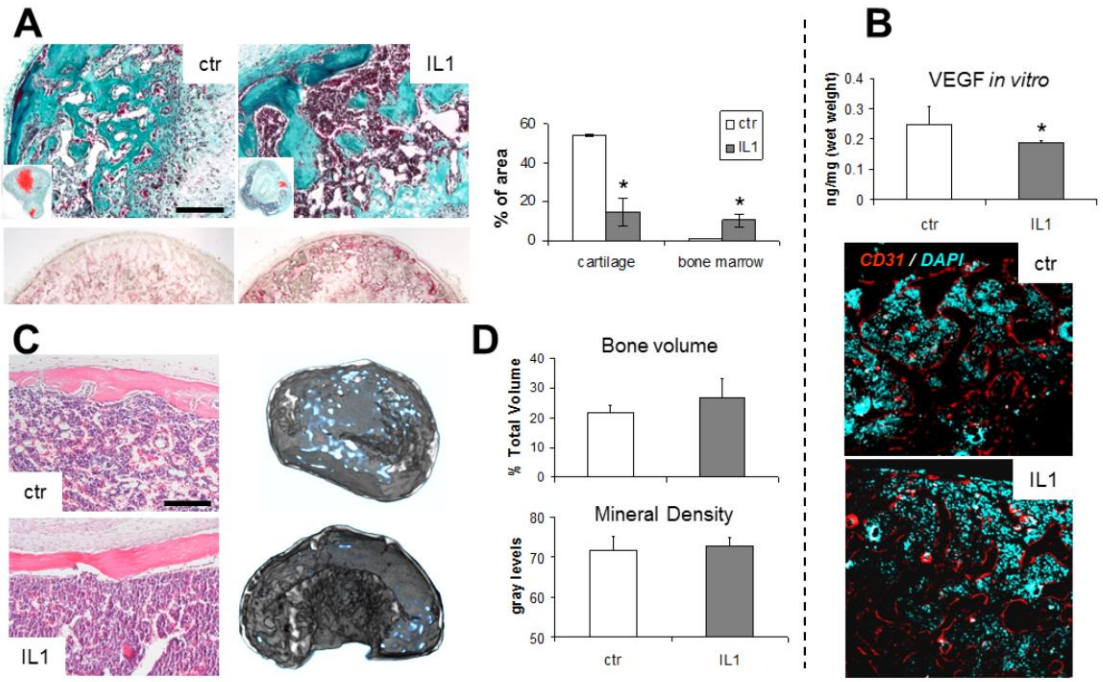

Fig. 6. Effects of IL-1β on the ectopic endochondral bone formation in nude mice of cartilaginous tissues generated with human bone marrow stromal cells (BM-MSC). (**A**) Representative Masson's trichrome and safranin-O (inset) (top) and tartrate-resistant acid phosphatase (TRAP, bottom) stainings and contents of cartilage and bone marrow of tissues harvested after 5 weeks *in vivo*. Scale bar = 200 μm. (**B**) Representative CD31/DAPI staining of constructs after 12 weeks *in vivo*. (**C**) Representative Haematoxylin and Eosin staining (scale bar = 200 μm, left) and 3D reconstructed μCT (right) images of constructs after 12 weeks *in vivo*. (**D**) Quantitative histomorphometric μCT data of constructs after 12 weeks *in vivo*. $n = 2$ experiments with cells from 1 donor, 8 specimens analysed. Data are mean ± SD. * = $p < 0.05$ from IL-1β 0 pg/mL.

13 accumulation within the tissue was also measured and resulted significantly increased in IL-1β treated samples (Fig. 5B). On the contrary, VEGF content was slightly but significantly reduced in IL-1β treated samples (Fig. 5C). Immunostaining for the osteoblastic markers Osterix and osteocalcin increased over time, with no relevant difference between controls and IL-1β treated samples (data not shown). TRAP staining was negative (data not shown). RT-PCR analyses showed that IL-1β treatment did not modify the expression of type II collagen, caused a limited but significant down-regulation of type I collagen (3.2-fold) and type X collagen (2.6-fold), an up-regulation of BMP-2 (3.9-fold) and, in accordance with the biochemical and histological results, a significant and strong up-regulation of MMP-13 mRNA (74.1-fold) (Fig 5D).

Collectively, these results indicated that IL-1β did not enhance the *in vitro* hypertrophic differentiation of BM-MSC but the extent of extracellular matrix calcification and the onset of remodelling of the cartilaginous template at least in part through MMP-13 upregulation.

In vivo tissue development

IL-1β strongly enhanced the remodelling process of the hypertrophic cartilage into bone. In particular, as compared to controls, after 5 weeks *in vivo* IL-1β treated samples showed, (i) reduced safranin-O positive cartilaginous areas (3.6-fold), (ii) larger bone marrow areas (9.1-fold), and (iii) higher density of multinucleated TRAP-positive cells (Fig. 6A). Interestingly, the decrease in VEGF protein within the tissue, measured with ELISA after IL-1β treatment *in vitro*, did not result in an impaired vascularisation *in vivo* (Fig. 6B). As a matter of fact, vessels quantification, performed on CD31-stained sections, showed no difference between controls and IL-1β -treated samples (data not shown).

At the latest *in vivo* time point (12 weeks), both groups could finalise the endochondral process, showing mature bone formation and bone marrow engrafted within the bone trabeculae (Fig. 6C,D). Human cells survived and could be detected within the newly formed bone with ISH for human Alu repeats (data not shown), confirming our previous report (Scotti *et al.*, 2010). Taken together, these data suggest that IL-1β treatment resulted in an accelerated remodelling of the hypertrophic cartilage, ultimately leading to a bone tissue formation similar to that of controls.

Discussion

In this study, we demonstrated that IL-1β modulates the main stages of endochondral/perichondral bone formation of human adult BM-MSC. In particular we reported that

treatment with low dose of IL-1β (50 pg/mL) resulted in: (i) enhanced proliferation and clonogenicity, (ii) enhanced chondrogenic and osteogenic differentiation, (iii) enhanced *in vitro* MMP13-mediated cartilage remodelling and (v) enhanced cartilage resorption (through recruitment of TRAP-positive cells).

In order to achieve an efficient bone fracture healing, tissue repair-competent MSC have first to be recruited to proliferate within an inflammatory milieu. In our clonogenic culture experiment, we have shown that 50 pg/mL IL-1β enhanced the total number of CFU-f and CFU-o as well as the dimension of the resulting colonies. These effects may be partially due to an IL-1β enhanced production of BMP-2. This factor, known to promote mesenchymal progenitor cell proliferation and osteoblastic commitment (Lou *et al.*, 1999; Katagiri *et al.*, 1990) was in fact enhanced in response to inflammatory signals, consistently with previous works (Hess *et al.*, 2009; Cho *et al.*, 2010). In agreement with our findings, Mohanty *et al.* (2010) in their study aimed at assessing changes in the bone marrow during the onset of inflammatory arthritis, observed an increase in CFU-f and CFU-o in the bone marrow of IL1ra-/- *vs.* wild type mice (Mohanty *et al.*, 2010). In contrast, a previous report indicated the inhibitory effects of IL-1β on both the number of BM-MSC derived colonies and colony size (Wang *et al.*, 2002). This discrepancy may be attributed to the modality of IL-1β application (at the time of seeding *vs.* 24 hours after seeding of bone marrow nucleated cells) or the use of different culture medium (DMEM containing 10 % foetal bovine serum *vs.* Iscove's modified Eagle's medium containing 25 % equine serum and hydrocortisone). Indeed, we have also observed in our study that the supplementation of FGF-2 to the culture medium reduced the IL-1β mediated increases of colony numbers and sizes, suggesting the sensitivity of the biological process to accessory signals.

Fracture healing consists of both intramembranous, mainly subperiosteally, and endochondral ossification (Marsell and Einhorn, 2011). We first investigated the effects of IL-1β on the direct osteoblastic differentiation of BM-MSC. Previous studies addressing this issue reported an inhibitory effect of IL-1β as well as of TNF-α on the capacity of *murine* MSC to mineralise the extracellular matrix (Lacey *et al.*, 2009; Lange *et al.*, 2010). The results of our study and of other reports (Hess *et al.*, 2009; Cho *et al.*, 2010), instead, demonstrate that inflammatory cytokines strongly enhanced the mineralisation capacity and the expression of key osteogenic genes by human MSC. Such discrepancy may be due to the inter-species differences in MSC biology (Meisel *et al.*, 2011). Interestingly, we have shown that the IL-1β induced increases of extracellular matrix mineralisation and expression of the osteo-inductive growth factor BMP-2 are caused by the activation of different signalling pathways. While the inhibition of ERK signalling (through the use of U0126) blocked both the IL-1β induced osteogenic responses, the inhibition of NF-κB signalling (through the use of PDTC) blocked significantly only the IL-1β-induced increase of BMP-2 expression. Similarly to our results, Hess *et al.* (2009) showed that a genetic block of the NF-κB pathway inhibits the TNF-α induced increase of BMP-2 expression, but does not block mineralisation of BM-MSC. In order to more extensively elucidate the molecular mechanism of action of IL-1β on this model, further studies on the pathway-associated kinases would be required.

We then investigated the effects of IL-1β on the chondrogenic differentiation of BM-MSC, as the initial stage towards endochondral ossification. In one previous study it was reported that IL-1β decreased proteoglycan synthesis in a dose-dependent manner starting from the lowest dose used (100 pg/mL) (Wehling *et al.*, 2009). Using a broader range of IL-1β concentrations, we instead observed that GAG accumulation by BM-MSC was significantly enhanced at low doses (50 pg/mL), unaffected at intermediate doses (100-250 pg/mL) and significantly reduced at higher doses (≥ 250 pg/mL) of IL-1β. These differences in the IL-1β dose responses can be due to the different type of tissues from which MSC were isolated (bone marrow aspirate from young patients – year range: 24-49 – *vs.* diaphyseal intramedullary reaming of long bone from old patients – year range: 71-78). We recently reported that even a short exposure of 50 pg/mL IL-1β to articular and nasal chondrocytes caused a significant GAG loss (Scotti *et al.*, 2012). However, MSC are less differentiated cells which have osteogenesis as standard differentiation pathway and can more likely respond positively to signals associated with tissue damage, such as inflammation (Caplan and Correa, 2011). Most importantly, this can also be explained by the upregulation of BMP-2, which is crucial for starting the healing process and the formation of the cartilaginous callus (Tsuji *et al.*, 2006). In contrast, chondrocytes are differentiated cells that typically respond to tissue damage with poor regeneration and further damage through MMP-13 upregulation (Goldring *et al.*, 2011).

Since the bone fracture site is a hypoxic environment, we also investigated the effects of IL-1β in BM-MSC cultured at reduced oxygen percentages. We found that IL-1β (50 and 1000 pg/mL) still enhanced ECM mineralisation by BM-MSC osteogenically cultured at oxygen percentages lower than 19 %, a condition known to inhibit osteogenic differentiation of mesenchymal cells (Malladi *et al.*, 2006; D'Ippolito *et al.*, 2006; Hirao *et al.*, 2006; Pattappa *et al.*, 2010; Wang *et al.*, 2011). Instead, IL-1β 50 pg/mL did not alter GAG accumulation at 5 % and slightly reduced it at 2 % oxygen. The latter finding can be due to a more pronounced production of cartilage matrix degradation agents in response to IL-1β under hypoxic conditions. Mathy-Harter *et al.* (2005), in fact, demonstrated that the IL-1β mediated production of nitric oxide by *in vitro* cultured bovine chondrocytes was more pronounced at low (i.e., 1 %) *vs.* atmospheric (i.e., 21 %) oxygen percentages. It is important however to consider that our experimental condition consisting on the culture of BM-MSC under a continuous hypoxic environment does not fully reproduce the variation in oxygen levels during the different stages of fracture healing (Lu *et al.*, 2011).

Endochondral ossification involves differentiation to hypertrophy followed by remodelling of cartilage into bone. We observed that the supplementation of IL-1β during the hypertrophic culture of human BM-

MSC derived chondrogenic tissues did not significantly enhance the expression of type X collagen but markedly increased MMP-13 expression and activity. The absence of an effect on type X collagen is in accordance with a previously published work which compared the effects of IL-1β, TNF-α and macrophage conditioned medium (MCM) on human chondrocytes seeded on a silk scaffold and reported an upregulation of collagen type X only in MCM-treated samples (Sun *et al.*, 2011). It should also be considered that, in our conditions, cell heterogeneity at the different time points may have masked modulation of type X collagen expression. The fact that Welting *et al.* (2011), instead, did find an effect of cycloxygenase-2 (a canonical IL-1β target gene) on hypertrophic differentiation of chondroprogenitors could be due to the use of cells/tissues from animal species other than human. The IL-1β mediated increase in MMP-13 expression and activity is particularly relevant for fracture callus remodelling into bone, since MMP-13 is required for proper resorption of hypertrophic cartilage (Behonick *et al.*, 2007) and subsequent endochondral bone development (Stickens *et al.*, 2004; Kosaki *et al.*, 2007).

As a result of the enhanced *in vitro* extracellular matrix (ECM) pre-processing by MMP-13, we described a faster remodelling of the hypertrophic cartilage, with less cartilaginous ECM and more abundant bone marrow engraftment at the intermediate *in vivo* time point. This last experiment was designed as a proof-of-principle of the *in vivo* effect of *in vitro* pre-treatment of hypertrophic cartilage with IL-1β. Our observation that higher amounts of TRAP-positive cells were present in the IL-1β treated samples reinforces a previous observation on the role of inflammation in chondroclastogenesis and cartilage resorption (Ota *et al.*, 2009). Limitations of this study include: (i) the use of expanded BM-MSC which may not reflect normal behaviour of progenitor cells of the bone marrow; (ii) the *in vitro* nature of the first series of experiments, which again limits its relevance to the normal behaviour of BM-MSC; (iii) the ectopic site of implantation for the *in vivo* experiments which is not the physiological site of bone repair.

The results of this study indicate the concentration-dependent role of IL-1β in regulating the chondrogenic and osteogenic differentiation of human BM-MSC and the remodelling of resulting cartilaginous templates into bone and bone marrow elements. A controlled delivery of IL-1β (e.g., by smart scaffolds) could enhance bone healing by resident MSC as well as improve the engineering of implantable tissues. Further studies are needed to extend the system with the presence of inflammatory cells and other cytokines (Liu *et al.*, 2011), in order to more comprehensively study bone regeneration in an immunocompetent animal model.

Acknowledgements

We are grateful to Dr. Stefan Schären (University-Hospital Basel, Switzerland) for the kind supply of bone marrow samples. We would like to acknowledge the European Union (OPHIS; #FP7-NMP-2009-SMALL-3-246373) and the Swiss National Foundation (NMS1725) for financial support.

References

Barbero A, Ploegert S, Heberer M, Martin I (2003) Plasticity of clonal populations of dedifferentiated adult human articular chondrocytes. Arthritis Rheum **48**: 1315-1325.

Behonick DJ, Xing Z, Lieu S, Buckley JM, Lotz JC, Marcucio RS, Werb Z, Miclau T, Colnot C (2007) Role of matrix metalloproteinase 13 in both endochondral and intramembranous ossification during skeletal regeneration. PLoS One **2**: e1150.

Bhattacharyya T, Levin R, Vrahas MS, Solomon DH (2005) Nonsteroidal antiinflammatory drugs and nonunion of humeral shaft fractures. Arthritis Rheum **53**: 364-347.

Braccini A, Wendt D, Jaquiery C, Jakob M, Heberer M, Kenins L, Wodnar-Filipowicz A, Quarto R, Martin I (2005) Three-dimensional perfusion culture of human bone marrow cells and generation of osteoinductive grafts. Stem Cells **23**: 1066-1072.

Burd TA, Hughes MS, Anglen JO (2003) Heterotopic ossification prophylaxis with indomethacin increases the risk of long-bone nonunion. J Bone Joint Surg Br **85**: 700-705.

Caplan AI, Correa D (2011) The MSC: an injury drugstore. Cell Stem Cell **9**: 11-15.

Cho HH, Shin KK, Kim YJ, Song JS, Kim JM, Bae YC, Kim CD, Jung JS (2010) NF-kappaB activation stimulates osteogenic differentiation of mesenchymal stem cells derived from human adipose tissue by increasing TAZ expression. J Cell Physiol **223**: 168-177.

Cho TJ, Gerstenfeld LC, Einhorn TA (2002) Differential temporal expression of members of the transforming growth factor beta superfamily during murine fracture healing. J Bone Miner Res **17**: 513-520.

Das R, Jahr H, van Osch GJ, Farrell E (2010) The role of hypoxia in bone marrow-derived mesenchymal stem cells: considerations for regenerative medicine approaches. Tissue Eng Part B Rev **16**: 159-168.

Ding J, Ghali O, Lencel P, Broux O, Chauveau C, Devedjian JC, Hardouin P, Magne D (2009) TNF-alpha and IL-1beta inhibit RUNX2 and collagen expression but increase alkaline phosphatase activity and mineralization in human mesenchymal stem cells. Life Sci **84**: 499-504.

D'Ippolito G, Diabira S, Howard GA, Roos BA, Schiller PC (2006) Low oxygen tension inhibits osteogenic differentiation and enhances stemness of human MIAMI cells. Bone **39**: 513-522.

Farndale RW, Buttle DJ, Barrett AJ (1986) Improved quantitation and discrimination of sulphated glycosaminoglycans by use of dimethylmethylene blue. Biochim Biophys Acta **883**: 173-177.

Frank O, Heim M, Jakob M, Barbero A, Schäfer D, Bendik I, Dick W, Heberer M, Martin I (2002) Real-time quantitative RT-PCR analysis of human bone marrow stromal cells during osteogenic differentiation *in vitro*. J Cell Biochem **85** 737-746.

Gerstenfeld LC, Cullinane DM, Barnes GL, Graves DT, Einhorn TA (2003) Fracture healing as a post-natal

developmental process: molecular, spatial, and temporal aspects of its regulation. J Cell Biochem **88**: 873-884.

Giannoudis PV, MacDonald DA, Matthews SJ, Smith RM, Furlong AJ, De Boer P (2000) Nonunion of the femoral diaphysis. The influence of reaming and non-steroidal anti-inflammatory drugs. J Bone Joint Surg Br **82:** 655-658.

Goldring MB, Otero M, Plumb DA, Dragomir C, Favero M, El Hachem K, Hashimoto K, Roach HI, Olivotto E, Borzì RM, Marcu KB (2011) Roles of inflammatory and anabolic cytokines in cartilage metabolism: signals and multiple effectors converge upon MMP-13 regulation in osteoarthritis. Eur Cell Mater **21**: 202-220.

Hess K, Ushmorov A, Fiedler J, Brenner RE, Wirth T (2009) TNFalpha promotes osteogenic differentiation of human mesenchymal stem cells by triggering the NF-kappaB signaling pathway. Bone **45**: 367-376.

Hirao M, Tamai N, Tsumaki N, Yoshikawa H, Myoui A (2006) Oxygen tension regulates chondrocyte differentiation and function during endochondral ossification. J Biol Chem **281**: 31079-31092.

Jakob M, Démarteau O, Schäfer D, Hintermann B, Dick W, Heberer M, Martin I (2001) Specific growth factors during the expansion and redifferentiation of adult human articular chondrocytes enhance chondrogenesis and cartilaginous tissue formation *in vitro*. J Cell Biochem **81**: 368-377.

Katagiri T, Yamaguchi A, Ikeda T, Yoshiki S, Wozney JM, Rosen V, Wang EA, Tanaka H, Omura S, Suda T (1990) The non-osteogenic mouse pluripotent cell line, C3H10T1/2, is induced to differentiate into osteoblastic cells by recombinant human bone morphogenetic protein-2. Biochem Biophys Res Commun **172**: 295-299.

Kosaki N, Takaishi H, Kamekura S, Kimura T, Okada Y, Minqi L, Amizuka N, Chung UI, Nakamura K, Kawaguchi H, Toyama Y, D'Armiento J (2007) Impaired bone fracture healing in matrix metalloproteinase-13 deficient mice. Biochem Biophys Res Commun **354**: 846-851.

Krischak GD, Augat P, Sorg T, Blakytny R, Kinzl L, Claes L, Beck A (2007) Effects of diclofenac on periosteal callus maturation in osteotomy healing in an animal model. Arch Orthop Trauma Surg **127**: 3-9.

Lacey DC, Simmons PJ, Graves SE, Hamilton JA (2009) Proinflammatory cytokines inhibit osteogenic differentiation from stem cells: implications for bone repair during inflammation. Osteoarthritis Cartilage **17**: 735-742.

Lange J, Sapozhnikova A, Lu C, Hu D, Li X, Miclau T 3rd, Marcucio RS (2010) Action of IL-1beta during fracture healing. J Orthop Res **28**: 778-784.

Liu Y, Wang L, Kikuiri T, Akiyama K, Chen C, Xu X, Yang R, Chen W, Wang S, Shi S (2011) Mesenchymal stem cell-based tissue regeneration is governed by recipient T lymphocytes via IFN-γ and TNF-α. Nat Med **17**: 1594-1601.

Lou J, Xu F, Merkel K, Manske P (1999) Gene therapy: adenovirus-mediated human bone morphogenetic protein-2 gene transfer induces mesenchymal progenitor cell proliferation and differentiation *in vitro* and bone formation *in vivo*. J Orthop Res **17**: 43-50.

Lu C, Rollins M, Hou H, Swartz HM, Hopf H, Miclau T, Marcucio RS (2008) Tibial fracture decreases oxygen levels at the site of injury. Iowa Orthop J **28**: 14-21.

Lu C, Saless N, Hu D, Wang X, Xing Z, Hou H, Williams B, Swartz HM, Colnot C, Miclau T, Marcucio RS (2011) Mechanical stability affects angiogenesis during early fracture healing. J Orthop Trauma **25**: 494-499.

Malda J, Klein TJ, Upton Z (2007) The roles of hypoxia in the *in vitro* engineering of tissues. Tissue Eng **13**: 2153-2162.

Malladi P, Xu Y, Chiou M, Giaccia AJ, Longaker MT (2006) Effect of reduced oxygen tension on chondrogenesis and osteogenesis in adipose-derived mesenchymal cells. Am J Physiol Cell Physiol **290**: C1139-1146.

Marsell R, Einhorn TA (2011) The biology of fracture healing. Injury **42**: 551-555.

Martin I, Muraglia A, Campanile G, Cancedda R, Quarto R (1997) Fibroblast growth factor-2 supports *ex vivo* expansion and maintenance of osteogenic precursors from human bone marrow. Endocrinology **138**: 4456-4462.

Mathy-Hartert M, Burton S, Deby-Dupont G, Devel P, Reginster JY, Henrotin Y (2005) Influence of oxygen tension on nitric oxide and prostaglandin E2 synthesis by bovine chondrocytes. Osteoarthritis Cartilage **13**: 74-79.

Meisel R, Brockers S, Heseler K, Degistirici O, Bülle H, Woite C, Stuhlsatz S, Schwippert W, Jäger M, Sorg R, Henschler R, Seissler J, Dilloo D, Däubener W (2011) Human but not murine multipotent mesenchymal stromal cells exhibit broad-spectrum antimicrobial effector function mediated by indoleamine 2,3-dioxygenase. Leukemia **25**: 648-654.

Mohanty ST, Kottam L, Gambardella A, Nicklin MJ, Coulton L, Hughes D, Wilson AG, Croucher PI, Bellantuono I (2010) Alterations in the self-renewal and differentiation ability of bone marrow mesenchymal stem cells in a mouse model of rheumatoid arthritis. Arthritis Res Ther **12**: R149.

Ochi H, Hara Y, Asou Y, Harada Y, Nezu Y, Yogo T, Shinomiya K, Tagawa M (2011) Effects of long-term administration of carprofen on healing of a tibial osteotomy in dogs. Am J Vet Res **72**: 634-641.

O'Connor JP, Capo JT, Tan V, Cottrell JA, Manigrasso MB, Bontempo N, Parsons JR (2009) A comparison of the effects of ibuprofen and rofecoxib on rabbit fibula osteotomy healing. Acta Orthop **80**: 597-605.

Ota N, Takaishi H, Kosaki N, Takito J, Yoda M, Tohmonda T, Kimura T, Okada Y, Yasuda H, Kawaguchi H, Matsumoto M, Chiba K, Ikegami H, Toyama Y (2009) Accelerated cartilage resorption by chondroclasts during bone fracture healing in osteoprotegerin-deficient mice. Endocrinology **150**: 4823-4834.

Papadimitropoulos A, Mastrogiacomo M, Peyrin F, Molinari E, Komlev VS, Rustichelli F, Cancedda R (2007) Kinetics of *in vivo* bone deposition by bone marrow stromal cells within a resorbable porous calcium phosphate scaffold: an X-ray computed microtomography study. Biotechnol Bioeng **98**: 271-281.

Pattappa G, Heywood HK, de Bruijn JD, Lee DA (2011) The metabolism of human mesenchymal stem cells during

proliferation and differentiation. J Cell Physiol **226**: 2562-2570.

Scotti C, Tonnarelli B, Papadimitropoulos A, Scherberich A, Schaeren S, Schauerte A, Lopez-Rios J, Zeller R, Barbero A, Martin I (2010) Recapitulation of endochondral bone formation using human adult mesenchymal stem cells as a paradigm for developmental engineering. Proc Natl Acad Sci U S A **107**: 7251-7256.

Scotti C, Osmokrovic A, Wolf F, Miot S, Peretti GM, Barbero A, Martin I (2012) Response of human engineered cartilage based on articular or nasal chondrocytes to interleukin-1â and low oxygen. Tissue Eng Part A **18**: 362-372

Stickens D, Behonick DJ, Ortega N, Heyer B, Hartenstein B, Yu Y, Fosang AJ, Schorpp-Kistner M, Angel P, Werb Z (2004) Altered endochondral bone development in matrix metalloproteinase 13-deficient mice. Development **131**: 5883-5895.

Sun L, Wang X, Kaplan DL (2011) A 3D cartilage – inflammatory cell culture system for the modeling of human osteoarthritis. Biomaterials **32**: 5581-5589.

Tsuji K, Bandyopadhyay A, Harfe BD, Cox K, Kakar S, Gerstenfeld L, Einhorn T, Tabin CJ, Rosen V (2006) BMP2 activity, although dispensable for bone formation, is required for the initiation of fracture healing. Nat Genet **38**: 1424-1429.

Wang L, Mondal D, La Russa VF, Agrawal KC (2002) Suppression of clonogenic potential of human bone marrow mesenchymal stem cells by HIV type 1: putative role of HIV type 1 tat protein and inflammatory cytokines. AIDS Res Hum Retroviruses **18**: 917-931.

Wang Y, Li J, WangY, Lei L, Jiang C, An S, Zhan Y, Cheng Q, Zhao Z, Wang J, Jiang L (2012) Effects of hypoxia on osteogenic differentiation of rat bone marrow mesenchymal stem cells. Mol Cell Biochem **362**: 25-33.

Wehling N, Palmer GD, Pilapil C, Liu F, Wells JW, Müller PE, Evans CH, Porter RM (2009) Interleukin-1beta and tumor necrosis factor alpha inhibit chondrogenesis by human mesenchymal stem cells through NF-kappaB-dependent pathways. Arthritis Rheum **60**: 801-812.

Welting TJ, Caron MM, Emans PJ, Janssen MP, Sanen K, Coolsen MM, Voss L, Surtel DA, Cremers A, Voncken JW, van Rhijn LW (2011) Inhibition of cyclooxygenase-2 impacts chondrocyte hypertrophic differentiation during endochondral ossification. Eur Cell Mater **22**: 420-436.

Discussion with Reviewers

Reviewer I: Given the large increase in caspase-3, it would be interesting to know whether cell death increases in pellets treated with high IL-1β. Please comment!
Authors: We did not perform specific analyses to assess IL-1β mediated cell death in BM-MSC during pellet cultures. However the reduction in size and DNA contents of pellets cultured with increasing IL-1β concentrations, the necrotic appearance of the pellets treated with the highest doses of IL-1β as well as the large increase in caspase-3 suggest that IL-1β (at high concentration) induces cell death of chondrogenically cultured BM-MSC.

Reviewer I: What can be inferred from this study on the relationship between IL-1β, FGF and ERK signalling in modulating endochondral ossification?
Authors: The current work was not aimed at studying the relationship between IL-1β, FGF and ERK signalling in modulating endochondral ossification. Our results however suggest that FGF-2 and ERK signalling might modulate some BM-MSC responses to IL-1β. We have in fact shown that: (i) FGF-2 counteracted the IL-1β-mediated proliferation of osteoprogenitor cells (ii) inhibition of ERK counteracted both IL-1β mediated mineralisation increase and BMP-2 upregulation. Since both IL-1β and FGF-2 are present at a bone fracture site, future studies will have to be undertaken to investigate the interaction between these two factors in the endochondral differentiation of BM-MSC.

Reviewer II: What is the impact of your findings for translational medicine?
Authors: Local inflammation is known to play a pivotal role in tissue regeneration, whereby absence, excess or disregulation of inflammatory processes may negatively affect bone repair. In accordance with this clinical evidence, our experimental data suggest that low levels of inflammatory cytokines may enhance the process of fracture healing by promoting chondrogenesis and the subsequent phases of callus formation/remodelling. A local control of inflammation might therefore improve the results of bone regeneration strategies.

Reviewer III: How do you think these findings relate to natural phenomena such as, for instance, fracture repair? May this constitute evidence that very low local amounts of IL-1 may have a role in priming chondrogenesis in the callus?
Authors: Local inflammation is known to play a pivotal role in tissue regeneration, whereby absence, excess or disregulation of inflammatory processes may negatively affect bone repair. In accordance with this clinical evidence, our experimental data suggest that low levels of inflammatory cytokines may enhance the process of fracture healing by promoting chondrogenesis and the subsequent phases of callus formation/remodelling. The work is in line with the increasing recognition that controlled management of inflammation is a crucial target towards enhancement of fracture healing. Our study on the one hand prompts for further investigations to better dissect the role of IL-1 and other cytokines in the different phases of bone regeneration, and on the other hand proposes the *in vitro*/ectopic replication of endochondral ossification as a model to address those critical processes.

CHAPTER 4

Osteoinductivity of engineered cartilaginous templates devitalized by inducible apoptosis

Osteoinductivity of engineered cartilaginous templates devitalized by inducible apoptosis

Paul E. Bourgine[a,b], Celeste Scotti[a,b,c], Sebastien Pigeot[a,b], Laurent A. Tchang[a,b], Atanas Todorov[a,b], and Ivan Martin[a,b,1]

[a]Department of Surgery and [b]Department of Biomedicine, University Hospital Basel, University of Basel, 4031 Basel, Switzerland; and [c]IRCCS Istituto Ortopedico Galeazzi, via R. Galeazzi 4, 20161 Milano, Italy

Edited by Robert Langer, Massachusetts Institute of Technology, Cambridge, MA, and approved October 30, 2014 (received for review July 1, 2014)

The role of cell-free extracellular matrix (ECM) in triggering tissue and organ regeneration has gained increased recognition, yet current approaches are predominantly based on the use of ECM from fully developed native tissues at nonhomologous sites. We describe a strategy to generate customized ECM, designed to activate endogenous regenerative programs by recapitulating tissue-specific developmental processes. The paradigm was exemplified in the context of the skeletal system by testing the osteoinductive capacity of engineered and devitalized hypertrophic cartilage, which is the primordial template for the development of most bones. ECM was engineered by inducing chondrogenesis of human mesenchymal stromal cells and devitalized by the implementation of a death-inducible genetic device, leading to cell apoptosis on activation and matrix protein preservation. The resulting hypertrophic cartilage ECM, tested in a stringent ectopic implantation model, efficiently remodeled to form de novo bone tissue of host origin, including mature vasculature and a hematopoietic compartment. Importantly, cartilage ECM could not generate frank bone tissue if devitalized by standard "freeze & thaw" (F&T) cycles, associated with a significant loss of glycosaminoglycans, mineral content, and ECM-bound cytokines critically involved in inflammatory, vascularization, and remodeling processes. These results support the utility of engineered ECM-based devices as off-the-shelf regenerative niches capable of recruiting and instructing resident cells toward the formation of a specific tissue.

developmental engineering | endochondral | osteoinductive | extracellular matrix | hematopoisesis

The clinical gold standard solution to critical bone defects consists of autologous bone transplantation. However, it is associated with severe donor site morbidity, risks for infection, and limited availability of the material (1, 2). Off-the-shelf synthetic or naturally derived bone substitute materials (e.g., ceramics, collagen) allow bypassing of these issues (3) but have reduced regenerative potency, especially in challenging scenarios (e.g., atrophic nonunions, comminuted fractures, large substance loss, compromised environment). Cell-based approaches could introduce a superior biological functionality, but their clinical use remains rather limited (4), predominantly because of their nonpredictable effectiveness combined with their economic, logistic, and interpatient variability issues (5, 6).

Modern approaches to bone tissue engineering aim at triggering regenerative processes by matching the corresponding developmental program and thus recapitulating the embryonic stages of bone tissue development (7). During embryonic development, long bones typically develop by endochondral ossification, a process involving the formation and subsequent remodeling of a hypertrophic cartilage template (8). Following the principles of "developmental engineering," the process of endochondral ossification has been successfully reproduced using embryonic stem cells (9) and human mesenchymal stromal cells (hMSCs) (10–12). A further step was achieved with the upscaling of the graft size, leading not only to the successful formation of large bone tissue but also to the development of a mature organ that includes a fully mature hematopoietic compartment (13).

The increased recognition of the potency of the extracellular matrix (ECM)-derived materials in regenerative processes (14) led us to investigate whether a living cell compartment is strictly required or whether the endochondral route could be initiated by a cell-free ECM, represented by a devitalized hypertrophic template. Addressing this question may lead to a better understanding of the elements regulating the endochondral ossification process and to the generation of cell-based but cell-free off-the-shelf materials capable of instructing host osteoprogenitors toward bone formation. A devitalized approach to endochondral ossification has been envisioned from the beginning of the research in this field (9, 10), as it would bypass the complexity of delivering living cells of possibly autologous origin, but it has never been realized to date.

Existing studies converge on the importance of preserving ECM integrity to elicit the desired regenerative effect (15–17). This implies the use of a devitalization strategy reducing alterations in the composition and architecture of the generated template to mimic both the physiologic regenerative milieu and the 3D structure of the fracture callus. Toward this objective, a devitalization approach has been proposed via the induction of apoptosis (18). In particular, an inducible genetic system (19) can be incorporated into primary hMSCs to specifically induce their apoptosis on exposure to a clinical-grade chemical compound. This strategy offers the possibility to generate hypertrophic cartilage templates that can be subsequently devitalized with, theoretically, minimal changes in the ECM.

Significance

It has been previously reported that hypertrophic cartilage tissues engineered from human mesenchymal stromal cells can efficiently remodel in vivo into bone organs, recapitulating developmental steps of endochondral ossification. We have here demonstrated that the extracellular matrix (ECM) of such engineered cartilage, even in the absence of a living cell component, retains frankly osteoinductive properties. The use of an apoptosis-driven devitalization technique revealed the importance of preserving the ECM integrity and, in particular, the embedded factors to trigger the regenerative process. Although exemplified in a skeletal context, our work outlines the general paradigm of cell-based but cell-free off-the-shelf materials capable of activating endogenous cells toward the formation of specific tissues.

Author contributions: P.E.B., C.S., and I.M. designed research; P.E.B., C.S., S.P., L.A.T., and A.T. performed research; P.E.B. contributed new reagents/analytic tools; P.E.B., C.S., S.P., and A.T. analyzed data; and P.E.B. and I.M. wrote the paper.

The authors declare no conflict of interest.

This article is a PNAS Direct Submission.

[1]To whom correspondence should be addressed. Email: ivan.martin@usb.ch.

This article contains supporting information online at www.pnas.org/lookup/suppl/doi:10.1073/pnas.1411975111/-/DCSupplemental.

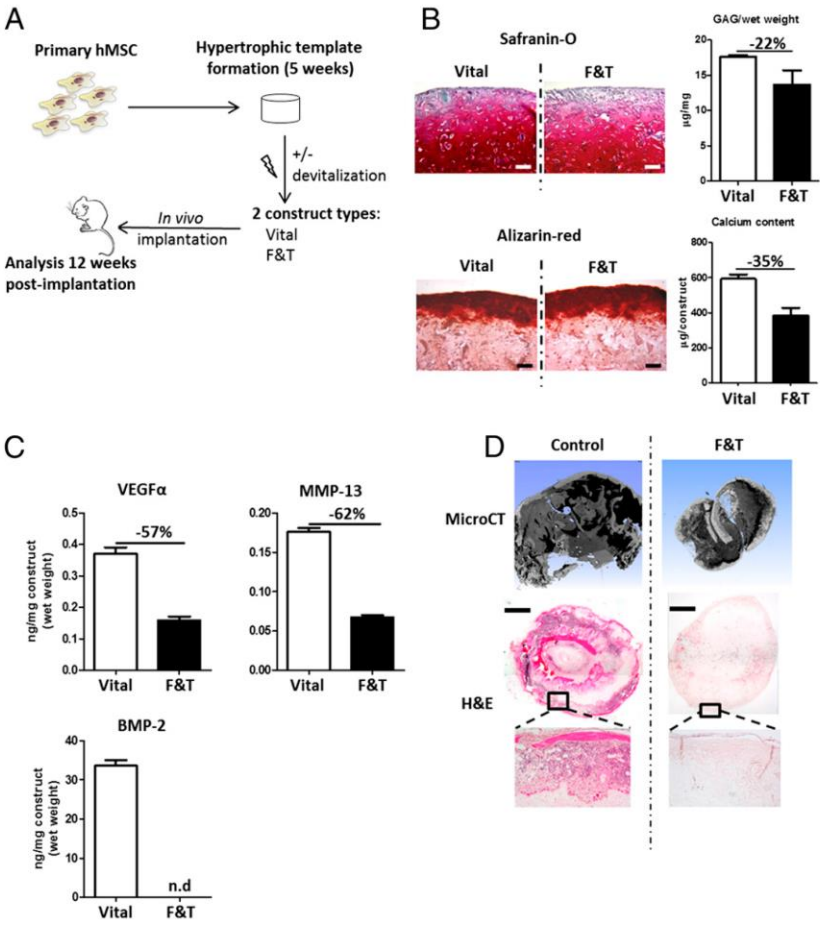

Fig. 1. Assessment of the osteoinductive properties of living (*Vital*) and F&T (*F&T*) devitalized engineered hypertrophic cartilage constructs. (*A*) Experimental scheme for the generation of hypertrophic tissues starting from hMSCs, devitalized and subsequently implanted in nude mice. (*B*) Representative sections of in vitro (5 wk) generated hypertrophic cartilage samples and the effect of the F&T treatment on the GAGs and calcium content ($n = 3$). (Scale bars, 100 µm.) (*C*) Effect of the F&T devitalization on the content of VEGF-α, BMP-2, and MMP-13 protein. (*D*) 3D reconstruction of microtomographic images (MicroCT) and hematoxylin and eosin (H&E) stained representative sections of samples retrieved 12 wk after ectopic implantation in nude mice ($n = 3$). (Scale bars, 1 mm.) Error bars represent SEMs of $n = 3$ measurements.

In this study, we aimed to induce de novo bone organ formation, using cell-free hypertrophic cartilage templates devitalized by apoptotic induction. We hypothesized that the preservation of the ECM integrity, serving as a reservoir of multiple growth factors at physiological levels, is a key prerequisite to recruiting and instructing endogenous progenitors to initiate bone regeneration.

Results

Assessment of the Osteoinductive Properties of Freeze & Thaw Devitalized Constructs. As a first attempt, we tested whether hypertrophic cartilage templates, engineered according to a previously established protocol (13) and devitalized by standard "freeze & thaw" (F&T) treatment, are capable of inducing bone formation (Fig. 1*A*). F&T is a well-established physical devitalization method efficiently leading to cell bursting and limited ECM alteration (20, 21). Primary hMSCs were then seeded at high density on cylindrical collagen meshes (8 mm diameter, 4 mm thickness) and cultured for 3 wk in chondrogenic medium, followed by 2 wk of hypertrophic medium. The resulting grafts successfully displayed the typical pattern of a hypertrophic cartilaginous tissue, consisting of a glycosaminoglycan (GAG)-rich core surrounded by a mineralized ring (*Vital*; Fig. 1*B*). Some constructs were subsequently devitalized, using a recognized method consisting of three F&T cycles followed by a bath in hypertonic solution (*F&T*) (22), leading to the absence of human living cells after implantation (Fig. S1*A*). The *F&T* constructs were still positively stained for GAG and mineral deposits, but quantitative assessments indicated a marked reduction in the wet weight percentage of GAG (−22%) and mineral content (−35%) (Fig. 1*B*). The F&T treatment also reduced the amount of growth factors that are known to play a critical role in hypertrophic cartilage remodeling into bone, including VEGFα (−57%), matrix metalloproteinase 13 (MMP-13; −62%), and bone morphogenetic protein 2 (BMP-2; below detection level; Fig. 1*C*).

On ectopic implantation in nude mice for 12 wk, *Vital* samples were macroscopically colonized by blood cells, in contrast to *F&T* tissues (Fig. S1*B*). *Vital* samples were extensively remodeled, resulting in interconnected mineralized bone trabeculae embedding bone marrow elements (Fig. 1*D*), with minimal cartilage residuals (Fig. S1*B*). In contrast, the retrieved *F&T* samples maintained an outer shell of calcified matrix and abundant remnants of devitalized cartilage, with no evidences of bone or bone marrow formation (Fig. 1*D* and Fig. S1*B*). The failure of *F&T* devitalized hypertrophic constructs to remodel and induce bone formation could be attributed to the absence of living cells within the implanted graft and/or the effect of the devitalization process, leading to a loss of osteoinductive (e.g., BMP-2), angiogenic (e.g., VEGFα), and remodeling (e.g., MMP-13) factors.

Generation of Hypertrophic Constructs Using Death-Inducible hMSCs. To assess whether a better-preserved devitalized hypertrophic ECM can induce endochondral bone formation, we introduced the strategy of devitalization by apoptosis induction (Fig. S2), which was previously proposed to target the living cell fraction with minimal changes in the ECM components (18). Primary hMSCs were thus retrovirally transduced with a death system based on the inducible dimerization of modified caspase 9 (iDS; Fig. S2*A*). To ensure the maximum cell death on induction, the

population was purified on the basis of the expression of the CD19 reporter surface marker (Fig. 2*A*). This allowed for the generation of hMSC-iDS capable of being efficiently induced toward apoptosis in 2D culture (>97%; Fig. 2*B*) by adding the soluble inducer in the culture media. hMSC-iDS could generate hypertrophic cartilage tissues similar to the untransduced cells, as assessed by histological stainings (Fig. 2*C*) and gene expression analysis showing successful induction of chondrogenic and hypertrophic genes (Fig. 2*D*). Hence, the gain of the inducible-apoptosis function did not impair the chondrogenic differentiation and subsequent hypertrophy of hMSC-iDS. Importantly, hMSC-iDS hypertrophic templates continued to express the iDS, as revealed by CD19 immunostaining (Fig. 2*C*), suggesting the possibility of devitalizing the engineered graft by activation of the system.

Devitalization by Apoptosis Induction of Hypertrophic Cartilaginous Templates. Treatment of hypertrophic constructs by *F&T* or apoptosis induction (*Apoptized*) allowed for an effective devitalization, leading to, respectively, 91% and 93% cell killing efficiency, as assessed by flow cytometry measurement of propidium iodide (PI) and annexin V staining (Fig. 3*A*). Conversely, most of the cells from the *Vital* group remained viable (16% of annexin V/PI positivity; Fig. 3*A*). Because the assay measures the apoptosis-driven extracellular translocation of annexin V, the measured cell death is not biased by the reported natural expression of annexin V by chondrocytes (23); in particular, during their mineralization phase (24). Histologic analyses indicated the successful activation of the apoptotic pathway, with clear morphologic evidence of cell and nuclear fragmentation (late stage of apoptosis) throughout *Apoptized* and *F&T* constructs, further confirmed by the presence of cleaved caspase 3 in nucleated cells (Fig. 3*B*). In the *Vital* group, apoptotic cells were mainly found within the hypertrophic outer ring. Luminex-based analysis showed, in *Apoptized* samples, the overall maintenance of factors involved in inflammation [monocyte chemoattractant protein-1 (MCP-1), macrophage colony-stimulating factor (M-CSF), IL-8], angiogenesis (VEGFα), and remodeling [MMP-13, osteoprotegerin (OPG)] processes, with levels similar to those of the *Vital* group. Instead, *F&T* treatment resulted in a severe impairment of ECM composition, with a significant loss in IL-8 (64.9%; $P < 0.0001$), MCP-1 (49.4%; $P = 0.0388$), OPG (37%; $P = 0.0015$), VEGFα (58.7%; $P < 0.0001$), and MMP-13 (32.1%; $P = 0.0307$) compared with the protein content in the *Vital* constructs. Thus, although the two devitalization methods led to a similar killing of the cells, the induction of apoptosis allowed for a better preservation of representative ECM components.

In Vivo Assessment of Hypertrophic Cartilaginous Templates. To assess whether a better-preserved acellular ECM is sufficient to induce vascularization and endochondral bone formation, *Apoptized*, *F&T*, and *Vital* templates were implanted ectopically in immunodeficient mice. On retrieval, samples displayed distinct morphologic patterns. Colonization by host blood cells was evident in *Vital* samples and, to a lower extent, in *Apoptized* ones, whereas *F&T* samples did not display macroscopic evidence of vascularization (Fig. 4*A*). Confocal microscopy confirmed these macroscopic observations, as *Vital* and *Apoptized* samples showed the presence of a mature vasculature characterized by CD31+ vessels stabilized by pericytic cells (NG2 staining; Fig. 4*B* and Fig. S3*A*). In contrast, *F&T* samples were marked by the absence of either cells or blood vessels within the constructs. Collectively, these data indicate the successful recruitment of the host vasculature by *Apoptized*, but not by *F&T* constructs, a prerequisite for the recapitulation of the endochondral ossification route.

Samples were further processed to investigate the presence of bone, cartilage, and bone marrow tissue. Remarkably, *Vital* and *Apoptized* samples, in strong contrast to *F&T* constructs, underwent

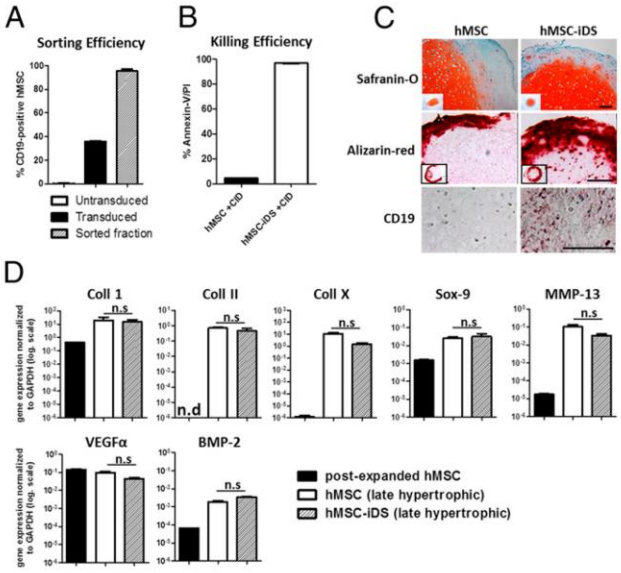

Fig. 2. Generation of hypertrophic constructs using death-inducible hMSCs. (*A*) Flow cytometry measurements of the CD19 (iDS reporter marker) expression by primary hMSC (Untransduced) after iDS retroviral transduction (Transduced) and subsequent enrichment using magnetic beads (Sorted fraction, hMSC-iDS) ($n = 5$). (*B*) Assessment of the efficiency of hMSC-iDS apoptosis induction in 2D culture on overnight exposure to the soluble inducer (+chemical inducer of dimerization) ($n = 4$). (*C*) Histologic sections of in vitro constructs (5 wk) generated by primary untransduced hMSCs and hMSC-iDS displayed a similar hypertrophic cartilage pattern (Safranin-O and Alizarin-red stainings). (Scale bars = 100 μm.) Only the hMSC-iDS expressed the iDS (CD19 immunostaining). (Scale bar = 50 μm.) (*D*) Gene expression analysis of hypertrophic templates generated by hMSCs and hMSC-iDS. Error bars represent SEMs of $n \geq 4$ measurements.

intense remodeling, giving rise after 12 wk to bone structures, including bone marrow spaces (Fig. 5*A*). Interestingly, although cortical external structures were observed in *Vital* and *Apoptized* groups, only *Vital* specimens displayed inner bone trabeculae (Fig. S3 *B* and *C*). The amount of mineralized tissue quantified after segmentation of micro-computerized tomography images was highest in the *Vital* specimens, followed by the *Apoptized* ones (Fig. S3*D*). However, as this technique does not allow discriminating between calcified cartilage and frank bone tissue, more specific quantification of the tissue types in the different groups was carried out, using histological sections. Histomorphometric analysis indicated in *Vital* samples the predominant formation of bone and bone marrow tissues (respectively, 24.9% and 32%), whereas cartilaginous regions were negligible (2%; Fig. 5*B*). *Apoptized* samples displayed a significantly higher bone (14.8%) and bone marrow formation (5.7%) than *F&T* samples (1.5% bone, 0.2% marrow). The latter, in turn, contained the highest percentage of cartilage remnants, confirming the limited efficiency of the remodeling process (Fig. 5*B*).

Ossicles of *Vital* and *Apoptized* constructs were characterized by the presence of osterix and tartrate-resistant-acid-phosphatase-expressing cells, respectively, representing osteoblastic and osteoclastic lineages (Fig. 5*C*). Those cells were predominantly lining the edges of the bone marrow regions, suggesting their involvement in tissue remodeling for marrow colonization. In *Vital* constructs, human cells participated in the bone formation, as assessed by the presence of cells positive for human Alu repeats among nucleated cells (Fig. 5*C*). In contrast, no human cells could be detected within *Apoptized* samples, so the formation of perichondral bone could only be attributed to host osteoprogenitors. *F&T* samples were also

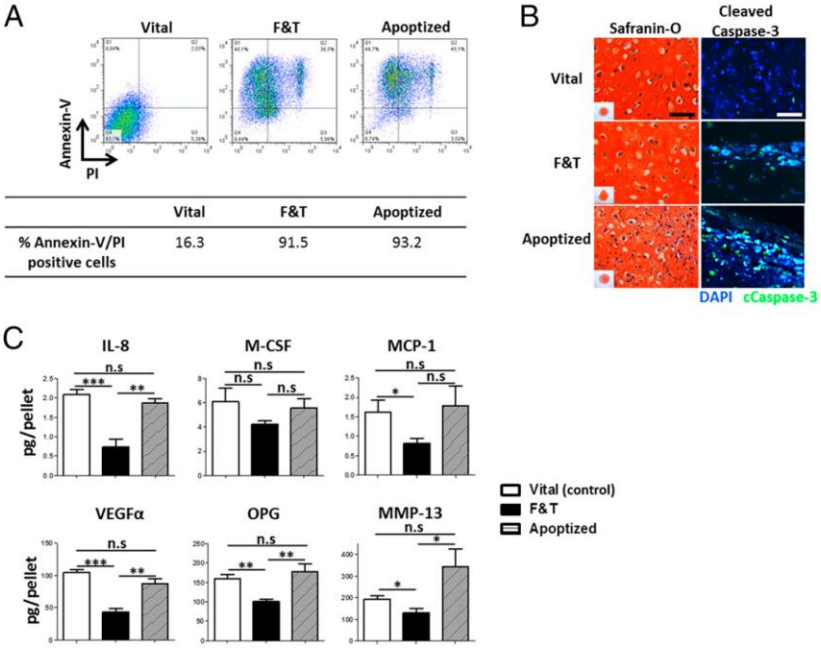

	Vital	F&T	Apoptized
% Annexin-V/PI positive cells	16.3	91.5	93.2

Fig. 3. Devitalization of hypertrophic cartilaginous templates. (*A*) Annexin V/PI flow cytometric analysis of cells retrieved from nondevitalized (*Vital*) or devitalized hypertrophic constructs, based on F&T cycles (F&T) or apoptosis induction (*Apoptized*). Both methods led to efficient tissue devitalization, with a killing efficiency superior to 90%. (*B*) Biochemical (Safranin-O) and immunofluorescence (Cleaved caspase-3) stainings of *Vital* and devitalized constructs. The devitalization processes efficiently induce cell death within the constructs. (Scale bars, 50 μm.) (*C*) Quantitative measurement of ECM proteins loss on devitalization of hypertrophic cartilage. Although the apoptotic method led to a minimal protein loss, the F&T treatment dramatically affected the ECM content. Error bars represent SEMs of $n = 6$ measurements. $*P \leq 0.05$; $**P \leq 0.005$; $***P \leq 0.0005$.

marked by the absence of human cells, but with no evidence of frank bone structures or osteoblastic/osteoclastic cells (Fig. 5*C*).

Discussion

The present study demonstrates the hitherto unreported capacity of devitalized hypertrophic cartilage templates to induce de novo the formation of bone, including a mature vasculature and the presence of a bone marrow compartment, as well as the strict dependency of the regenerative process on the preservation of the ECM matrix and the growth factors and chemokines bound to it. In fact, the formation of heterotopic bone and bone marrow could be achieved only through the implementation of a devitalization strategy minimally affecting ECM integrity.

The deliberate activation of the apoptotic pathway allowed for the preservation of key embedded factors identified as being involved in inflammation (IL-8, MCP-1, M-CSF), vasculature recruitment (VEGFα), and bone remodeling processes (OPG, MMP-13). The initiation of the stage-specific cartilage template remodeling is known to require digestion of the engineered ECM through the identified factors, leading to the attraction of blood vessels via the release of entrapped VEGFα. The ingrowing blood vessels could subsequently deliver osteoblastic, osteoclastic, and hematopoietic precursors, completing cartilage resorption and directing formation of bone and associated stromal sinusoids, and in turn providing the microenvironment for hematopoiesis. Conversely, the use of the F&T as a "crude" devitalization technique led to the dramatic loss of those proteins, resulting in negligible vasculature, host cell recruitment, and tissue remodeling on implantation. These observations provide important information on the nature of the signals to be delivered to initiate endogenous formation of bone tissue and also warrant further investigation to identify the complete set of factors necessary and sufficient to instruct an efficient de novo formation of bone and bone marrow. In particular, our work highlights the paramount role played by the growth factors and chemokines embedded within the MSC-deposited ECM in triggering the tissue regeneration process. The potent biological role of the MSC secretome, appropriately bound to the ECM, is also in line with the recent view of MSCs as an "injury drugstore" and emphasizes the trophic effect of MSCs over their direct participation to the tissue formation (25).

In our study, the induced apoptosis of human hypertrophic chondrocytes is compliant with the physiological apoptosis of hypertrophic chondrocytes occurring during endochondral ossification. However, recent studies indicate that endochondral bone formation necessitates the presence of living hypertrophic chondrocytes, part of which directly contributes to the formation of trabecular structures (13) or the stromal niche for hematopoietic cells (26). As a consequence, despite the use of a cartilage intermediate, bone formation induced by devitalized ECM cannot be defined as being of canonical endochondral origin. Indeed, because the deposited bone tissue was predominantly

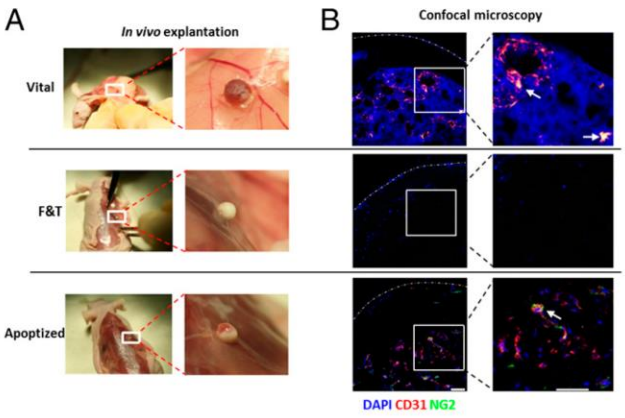

Fig. 4. Vascularization assessment of implanted hypertrophic cartilage tissues. (*A*) Macroscopic view of the samples at the time of explantation. *Vital* and *Apoptized* constructs displayed signs of blood cell colonization, in contrast to *F&T* samples. (*B*) Fluorescence microscopy of representative sections of explanted tissues. *Vital* and *Apoptized* constructs contained sinusoid-like vascular structures, positively stained for CD31 and stabilized by NG2+ pericytes. *F&T* devitalized constructs did not display evidences of vessel formation. (Scale bars, 50 μm.)

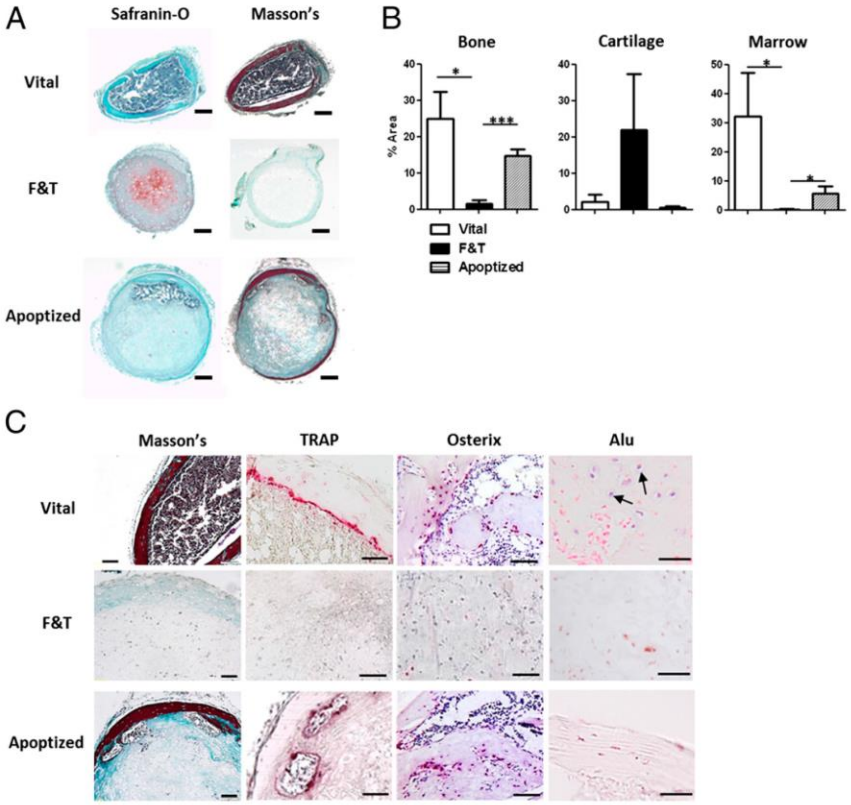

Fig. 5. Endochondral bone formation assessment of implanted hypertrophic cartilage tissues. (*A*) Safranin-O and Masson's Trichrome stainings of constructs retrieved 12 wk after implantation. *Vital* constructs underwent a full remodeling into bone, whereas *F&T* samples resembled an immature collagenous matrix with abundant cartilage remnants. *Apoptized* samples displayed evidence of perichondral bone formation, embedding a hematopoietic compartment. (Scale bars, 200 μm.) (*B*) Histologic quantification of bone, cartilage, and marrow tissue areas in sections of explanted living and devitalized constructs. (*C*) Masson's Trichrome, tartrate-resistant alkaline phosphatase, osterix, and Alu stainings were performed to, respectively, assess the presence of bone tissue, osteoclasts, osteoblasts, and human versus host cells. The presence of host-derived osteoclasts and osteoblasts was detected only in *Vital* and *Apoptized* samples. Human cells were present only in *Vital* constructs (black arrows). (Scale bars, 100 μm.)

perichondral, it could be attributed to the direct ossification of the mineralized cartilage template. A possible strategy to further improve the bone regeneration capacity of *Apoptized* constructs could thus be based on the increase of the surface:volume ratio by manufacturing channeled tissues, as recently described (27), to achieve a higher extent of perichondral bone formation.

Current acellular osteoinductive materials are typically enhanced by the delivery of single growth factors (BMPs). Because of the absence of critical accessory cues and ECM ligands that potentiate their effect, these strategies require supraphysiological doses of the morphogen, raising economic and safety issues (28, 29). Conversely, the osteoinductivity of the devitalized hypertrophic template relies on a mixture of factors accumulated at doses within physiological ranges and presented through a backbone of ECM molecules. Thus, *Apoptized* devitalized hypertrophic cartilage could offer an attractive alternative to currently available off-the-shelf osteoinductive materials, with the potency of cell-based grafts but bypassing both the logistically complex and regulatory costly use of autologous cells and the still-controversial introduction of allogeneic MSCs. As opposed to ECMs derived from native tissues, which are receiving an increased therapeutic interest (30), the present approach offers the opportunity not only to mimic a developmental process to efficiently form bone tissue but also to enrich the engineered templates in targeted proteins. This could be achieved through the overexpression of key identified factors (e.g., BMP-2, VEGFα) during in vitro culture by modified cells, leading to their embedding in the ECM and their preservation by apoptotic induction. The production of "customized" grafts, with an enhanced angiogenic or osteoinductive potency, would be required to target specific classes of patients or compromised environmental conditions at the repair site (e.g., atrophic nonunions requiring extensive vascularization, or simple bone losses requiring only osteoinduction) (31, 32). The ECM-based embedding of different growth factors in a controllable and customizable fashion for specific clinical needs clearly distinguishes the proposed approach from the "smart" ceramic materials, which have been proven to be osteoinductive in large animal models (33).

Obviously, the clinical translation of the proposed system necessitates further development and extensive preclinical studies. In the present work, the apoptosis induction relies on the use of a retroviral vector, leading to the integration of the system in the target cells. Although the approach has been validated for clinical practice (34), the development of alternative nonviral methods capable of efficiently devitalizing hypertrophic cartilaginous templates (e.g., proapoptotic adjuvants) may be preferred. One important issue with clinical implementation of the developed approach is also related to the efficacy in bone formation of *Apoptized* versus *Vital* grafts. At the assessed time, *Apoptized* constructs remained inferior to *Vital* ones, probably because of the lack of donor cells initially contributing to bone formation. Our study thus needs to be extended to a longer time of observation to assess whether this initial difference will be overcome.

The ectopic model used in the present work allows using human cells and investigating the de novo formation of bone tissue independent from osteoconductive events. Therefore, it

represents the most stringent proof of effective osteoinductivity of the devitalized grafts. However, a relevant assessment of the long-term bone-forming capacity of the implanted constructs will require an orthotopic model in immunocompetent animals. This will also allow the study of the regulatory role of osteoprogenitor and inflammatory cells from a bone environment, as well as of mechanical loading parameters.

In conclusion, we demonstrated that engineered hypertrophic cartilaginous matrix, provided a suitable devitalization technique, can deliver the set of factors to induce its remodeling and develop into bone tissue and bone marrow tissue. The findings outline a broader paradigm in regenerative medicine, relying on the engineering of cell-based but cell-free niches capable of recruiting and instructing endogenous cells on the formation of predetermined tissues. The approach can thus be extended to other biological systems to support both innovative translational strategies and fundamental investigations on the role of engineered ECM, decoupled from that of living cells.

Materials and Methods

All human samples were collected with informed consent of the involved individuals, and all mouse experiments were performed in accordance with Swiss law. All studies were approved by the responsible ethics authorities and by the Swiss Federal Veterinary Office.

HMSC-iDS were generated with the use of a retrovirus carrying the inducible death system (iCasp9-ΔCD19) and were purified by magnetic bead sorting based on CD19 expression (35). Cells were expanded for up to four passages (accounting for an average of 15–20 population doubling) to minimize the loss of chondrogenic potential, and were characterized by flow cytometry for putative MSC markers, with results consistent with our previous report (13).

Hypertrophic templates were generated by either the seeding of cells onto type I collagen meshes at a density of 70×10^6 cells/cm^3 (upscaled construct) (13) or using transwell culture seeded at 5×10^5 cells per insert (10). Constructs were cultured in chondrogenic conditions for 3 wk in a serum-free chondrogenic medium, followed by 2 wk in a serum-free hypertrophic medium (13). Samples were devitalized following two different protocols: F&T treatment or apoptosis induction. Samples were implanted in s.c. pouches of nude mice (four samples per mouse) and retrieved after 12 wk. The resulting in vitro and in vivo tissues were analyzed histologically, immunohistochemically, biochemically (glycosaminoglycans, DNA, protein content), by real-time RT-PCR, and by microtomography. Tissue development in vivo was evaluated histologically, immunohistochemically, and by microtomography. The survival and contribution to bone formation by HMSCs was evaluated with in-situ hybridization for human Alu sequences. A more complete and detailed description of the methods is included in *SI Materials and Methods*.

ACKNOWLEDGMENTS. We are grateful to Prof. Stefan Schären for the kind provision of bone marrow aspirates. This work was partially funded by the Swiss National Science Foundation (Grant 310030_133110, to I.M.) and by the Eurostars program (Grant FO132513, to I.M.).

1. Arrington ED, Smith WJ, Chambers HG, Bucknell AL, Davino NA (1996) Complications of iliac crest bone graft harvesting. *Clin Orthop Relat Res* 329:300–309.
2. Boden SD (2000) Biology of lumbar spine fusion and use of bone graft substitutes: Present, future, and next generation. *Tissue Eng* 6(4):383–399.
3. Kolk A, et al. (2012) Current trends and future perspectives of bone substitute materials - from space holders to innovative biomaterials. *J Craniomaxillofac Surg* 40(8): 706–718.
4. Martin I (2014) Engineered tissues as customized organ germs. *Tissue Eng Part A* 20(7-8):1132–1133.
5. Rosset P, Deschaseaux F, Layrolle P (2014) Cell therapy for bone repair. *Orthop Traumatol Surg Res* 100(1, Suppl):S107–S112.
6. Meijer GJ, de Bruijn JD, Koole R, van Blitterswijk CA (2007) Cell-based bone tissue engineering. *PLoS Med* 4(2):e9.
7. Leucht P, Minear S, Ten Berge D, Nusse R, Helms JA (2008) Translating insights from development into regenerative medicine: The function of Wnts in bone biology. *Semin Cell Dev Biol* 19(5):434–443.
8. Kronenberg HM (2003) Developmental regulation of the growth plate. *Nature* 423(6937):332–336.
9. Jukes JM, et al. (2008) Endochondral bone tissue engineering using embryonic stem cells. *Proc Natl Acad Sci USA* 105(19):6840–6845.
10. Scotti C, et al. (2010) Recapitulation of endochondral bone formation using human adult mesenchymal stem cells as a paradigm for developmental engineering. *Proc Natl Acad Sci USA* 107(16):7251–7256.
11. Janicki P, Kasten P, Kleinschmidt K, Luginbuehl R, Richter W (2010) Chondrogenic pre-induction of human mesenchymal stem cells on beta-TCP: Enhanced bone quality by endochondral heterotopic bone formation. *Acta Biomater* 6(8):3292–3301.
12. Farrell E, et al. (2011) In-vivo generation of bone via endochondral ossification by in-vitro chondrogenic priming of adult human and rat mesenchymal stem cells. *BMC Musculoskelet Disord* 12:31.
13. Scotti C, et al. (2013) Engineering of a functional bone organ through endochondral ossification. *Proc Natl Acad Sci USA* 110(10):3997–4002.
14. Benders KE, et al. (2013) Extracellular matrix scaffolds for cartilage and bone regeneration. *Trends Biotechnol* 31(3):169–176.
15. Badylak SF (2007) The extracellular matrix as a biologic scaffold material. *Biomaterials* 28(25):3587–3593.
16. Song JJ, Ott HC (2011) Organ engineering based on decellularized matrix scaffolds. *Trends Mol Med* 17(8):424–432.
17. Crapo PM, Gilbert TW, Badylak SF (2011) An overview of tissue and whole organ decellularization processes. *Biomaterials* 32(12):3233–3243.
18. Bourgine PE, Pippenger BE, Todorov A, Jr, Tchang L, Martin I (2013) Tissue decellularization by activation of programmed cell death. *Biomaterials* 34(26):6099–6108.
19. Tey SK, Dotti G, Rooney CM, Heslop HE, Brenner MK (2007) Inducible caspase 9 suicide gene to improve the safety of allodepleted T cells after haploidentical stem cell transplantation. *Biol Blood Marrow Transplant* 13(8):913–924.
20. Burk J, et al. (2014) Freeze-thaw cycles enhance decellularization of large tendons. *Tissue Eng Part C Methods* 20(4):276–284.
21. Lu H, Hoshiba T, Kawazoe N, Chen G (2012) Comparison of decellularization techniques for preparation of extracellular matrix scaffolds derived from three-dimensional cell culture. *J Biomed Mater Res A* 100(9):2507–2516.
22. Sadr N, et al. (2012) Enhancing the biological performance of synthetic polymeric materials by decoration with engineered, decellularized extracellular matrix. *Biomaterials* 33(20):5085–5093.
23. Lucic D, Mollenhauer J, Kilpatrick KE, Cole AA (2003) N-telopeptide of type II collagen interacts with annexin V on human chondrocytes. *Connect Tissue Res* 44(5):225–239.
24. Kirsch T, et al. (1997) Annexin V-mediated calcium flux across membranes is dependent on the lipid composition: Implications for cartilage mineralization. *Biochemistry* 36(11):3359–3367.
25. Caplan AI, Correa D (2011) The MSC: An injury drugstore. *Cell Stem Cell* 9(1):11–15.
26. Serafini M, et al. (2014) Establishment of bone marrow and hematopoietic niches in vivo by reversion of chondrocyte differentiation of human bone marrow stromal cells. *Stem Cell Res (Amst)* 12(3):659–672.
27. Sheehy EJ, Vinardell T, Toner ME, Buckley CT, Kelly DJ (2014) Altering the architecture of tissue engineered hypertrophic cartilaginous grafts facilitates vascularisation and accelerates mineralisation. *PLoS ONE* 9(3):e90716.
28. Garrison KR, et al. (2010) Bone morphogenetic protein (BMP) for fracture healing in adults. *Cochrane Database Syst Rev* 6:CD006950.
29. Woo EJ (2013) Adverse events after recombinant human BMP2 in nonspinal orthopaedic procedures. *Clin Orthop Relat Res* 471(5):1707–1711.
30. Sicari BM, et al. (2014) An acellular biologic scaffold promotes skeletal muscle formation in mice and humans with volumetric muscle loss. *Sci Transl Med* 6(234): 234ra58.
31. Garcia P, et al. (2012) Temporal and spatial vascularization patterns of unions and nonunions: Role of vascular endothelial growth factor and bone morphogenetic proteins. *J Bone Joint Surg Am* 94(1):49–58.
32. Grayson WL, et al. (2010) Engineering anatomically shaped human bone grafts. *Proc Natl Acad Sci USA* 107(8):3299–3304.
33. Yuan H, et al. (2010) Osteoinductive ceramics as a synthetic alternative to autologous bone grafting. *Proc Natl Acad Sci USA* 107(31):13614–13619.
34. Zhou X, et al. (2014) Long-term outcome after haploidentical stem cell transplant and infusion of T cells expressing the inducible caspase 9 safety transgene. *Blood* 123(25): 3895–3905.
35. Bourgine P, et al. (2014) Combination of immortalization and inducible death strategies to generate a human mesenchymal stromal cell line with controlled survival. *Stem Cell Res (Amst)* 12(2):584–598.

Supporting Information

Bourgine et al. 10.1073/pnas.1411975111

SI Materials and Methods

hMSC Isolation, Transduction, in Vitro Culture, and in Vivo Implantation. hMSCs were isolated from bone marrow aspirates and processed as previously described (1). Briefly, marrow aspirates (20 mL volume) were harvested from healthy donors (seven males and one female, 23–49 y old) during routine orthopedic procedures involving exposure of the iliac crest. A bone marrow biopsy needle was inserted through the cortical bone, and the aspirate was immediately transferred into plastic tubes containing 15,000 IU heparin. For hMSC-iDS generation, cells were plated at 6,000 cells/cm^2 in 60-mm dishes the day preceding the transduction. hMSCs were transduced by incubation with retroviral vector (iCasp9-ΔCD19) supernatants supplemented with 8 μg/μL polybrene (Sigma Aldrich) for 5 min at 37 °C and centrifuged at 1,100 × *g* for 30 min at room temperature in the dishes, followed by fresh medium replacement (1). Cells were expanded for up to four passages and seeded onto type I collagen meshes (disks 8 mm in diameter, 2 mm thick; Ultrafoam, Davol) at a density of 70 × 106 cells/cm^3 to generate upscale constructs. Alternatively, smaller hypertrophic templates were generated by seeding in transwell culture at 5 × 10^5 cells per insert cells. Constructs were cultured in chondrogenic conditions for 3 wk in a serum-free chondrogenic medium (2), followed by 2 wk in a serum-free hypertrophic medium, supplemented with 50 nM thyroxine, 7 mM β-glycerophosphate, 10 nM dexamethasone, and 0.25 mM ascorbic acid and IL-1β (50 pg/mL). Samples were implanted in s.c. pouches of nude mice (four samples per mouse) and retrieved after 12 wk.

Real-Time RT-PCR Quantitation of Transcript Levels. Total RNA extraction, cDNA synthesis, and real-time RT-PCR (7300 AB; Applied Biosystems) were performed to quantitate expression levels of the following genes of interest: type I (Coll I; Applied Biosystems, ref. no. Hs00164004_m1), type II (Coll II; Applied Biosystems, ref. no. Hs01060345_m1), or type X collagen (2); Sox-9 (Applied Biosystems, ref. no. Hs00165814_m1); MMP-13 (Applied Biosystems, ref. no. Hs00233992_m1); VEGFα (Applied Biosystems, ref. no. Hs00900055_m1); and BMP2 (Applied Biosystems, ref. no. Hs00154192_m1). GAPDH was used as reference gene to normalize gene expression values (Applied Biosystems, ref. no. Hs02758991_g1).

Histological Stainings, Immunohistochemistry, and in Situ Hybridization for Alu Repeats. After in vitro and in vivo cultures, constructs were fixed in 4% (vol/vol) paraformaldehyde; if necessary, decalcified with 7% (vol/vol) EDTA solution (Sigma); and embedded in paraffin. Sections (5 μm thick) were stained with H&E (Baker), Masson's trichrome, or Alizarin red or for tartrate-resistant acid phosphatase activity by means of the leukocyte acid phosphatase kit (Sigma, ref. no. 387A-1KT). Immunohistochemical analyses were performed to characterize the ECM using the following antibodies: CD19 (AbCam, ref. no. 31947). On rehydratation in ethanol series, sections were treated according to the manufacturer's instructions. The immunobinding was detected with biotinylated secondary antibodies and using the appropriate Vectastain ABC kits. The red signal was developed with the Fast Red kit (Dako Cytomation), and sections were counterstained by hematoxylin. Negative controls were performed during each analysis by omitting the primary antibodies. Chromogenic in situ hybridization (Zytovision kit) to detect human Alu repeat sequences was performed following the manufacturer's instructions, using nuclear fast red (Sigma) as nuclear counterstaining. Histological and immunohistochemical sections were analyzed using an Olympus BX-61 microscope.

Immunofluorescence Images. After in vivo explantation, samples were fixed in 4% (vol/vol) paraformaldehyde (Sigma), decalcified with EDTA (Sigma) solution, embedded in optimal cutting temperature compound, and snap frozen in liquid nitrogen. Sections (20 μm thick) were incubated with the primary antibodies against CD31 (platelet endothelial cell adhesion molecule 1; BD Pharmingen), NG2 (Chemicon International), and α-smooth muscle actin. As appropriate, secondary antibodies labeled with Alexa Fluor 647, Alexa Fluor 488, or Alexa Fluor 546 (Invitrogen) were used, and DAPI was used to stain nuclei. Fluorescence images were acquired using a confocal Zeiss LSM 710 microscope.

Microtomography. Microtomography was performed with in vivo implants. After fixation in formalin and storage in PBS, microcomputerized tomography data were acquired using a Phoenix nanotom m scanner (General Electric) with 0.5 mm aluminum filtered X-rays (applied voltage, 70 kV; current, 260 μA). Transmission images were acquired during a 360° scan rotation with an incremental rotation step size of 0.25°. Reconstruction was made using a modified Feldkamp algorithm at an isotropic voxel size of 2.5 μm. Threshold-based segmentation and 3D measurement analyses (bone mineral density and volume) were performed using the ImageJ software (ImageJ; National Institutes of Health) with the BoneJ (4) and 3D Shape (5) extensions. 3D rendering of the structures was performed using VGStudio MAX 2.2 software (Volume Graphics).

Statistical Analysis. The results of real-time RT-PCR, protein, and tissue quantification are presented as mean ± SEM. Statistical analysis was performed using the unpaired *t* test. *P* values of 0.05 or less were considered statistically significant.

Proteins Quantification. Protein levels were determined in devitalized (F&T and apoptized) and nondevitalized (living) tissue lysates collected from constructs cultured for 5 wk in vitro. Samples were analyzed for their content of a panel of growth factors, chemokines, and metalloproteinases, according to the manufacturer's instructions (Procarta Immunoassay Kit; Panomics).

1. Bourgine P, et al. (2014) Combination of immortalization and inducible death strategies to generate a human mesenchymal stromal cell line with controlled survival. *Stem Cell Res (Amst)* 12(2):584–598.
2. Scotti C, et al. (2010) Recapitulation of endochondral bone formation using human adult mesenchymal stem cells as a paradigm for developmental engineering. *Proc Natl Acad Sci USA* 107(16):7251–7256.
3. Barbero A, Ploegert S, Heberer M, Martin I (2003) Plasticity of clonal populations of dedifferentiated adult human articular chondrocytes. *Arthritis Rheum* 48(5):1315–1325.
4. Doube M, et al. (2010) BoneJ: Free and extensible bone image analysis in ImageJ. *Bone* 47(6):1076–1079.
5. Sheets KG, et al. (2013) Microglial ramification and redistribution concomitant with the attenuation of choroidal neovascularization by neuroprotectin D1. *Mol Vis* 19:1747–1759.

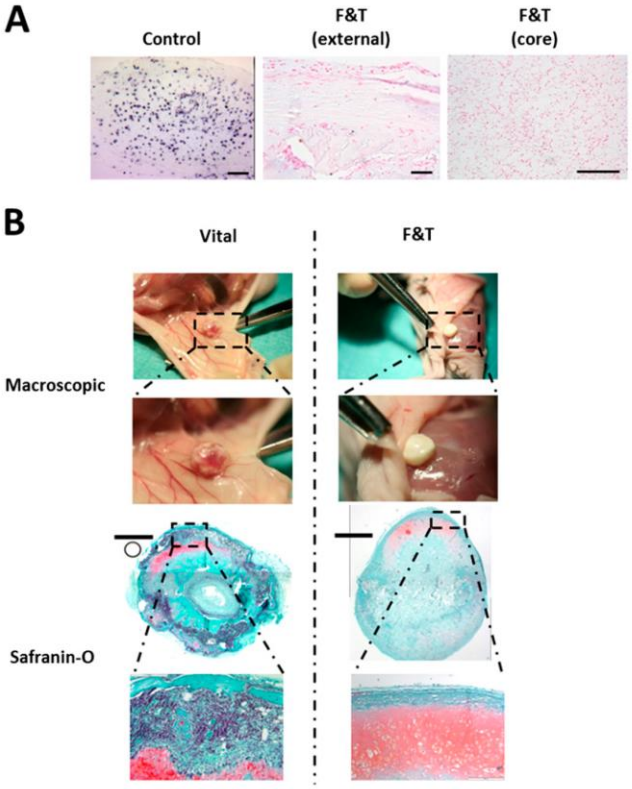

Fig. S1. (*A*) In situ hybridization for Alu repeats. No human cells could be detected in F&T devitalized ossicles 5 wk after in vivo implantation, as demonstrated by the absence of blue positively stained cells in both the external and core part of the ossicle. Purple stained cells (hematoxylin) corresponded to host cell invasion. The control sample consists of an in vitro-generated hypertrophic cartilage template, nondevitalized. (Scale bar, 100 μm.) (*B*) Explantation of non-devitalized (Vital) and F&T devitalized (F&T) ossicles 12 wk after ectopic implantation in nude mice. The Vital ossicles underwent an intense remodeling, giving rise to a mature bone organ with evidence of perichondral and trabecular bone and of a hematopoietic compartment (Safranin-O staining). Conversely, the F&T devitalized ossicles did not showed macroscopic evidences of remodeling and blood cell colonization, as confirmed by histological analysis revealing the absence of bone and bone marrow throughout the samples (Safranin-O). (Scale bar, 1 mm.)

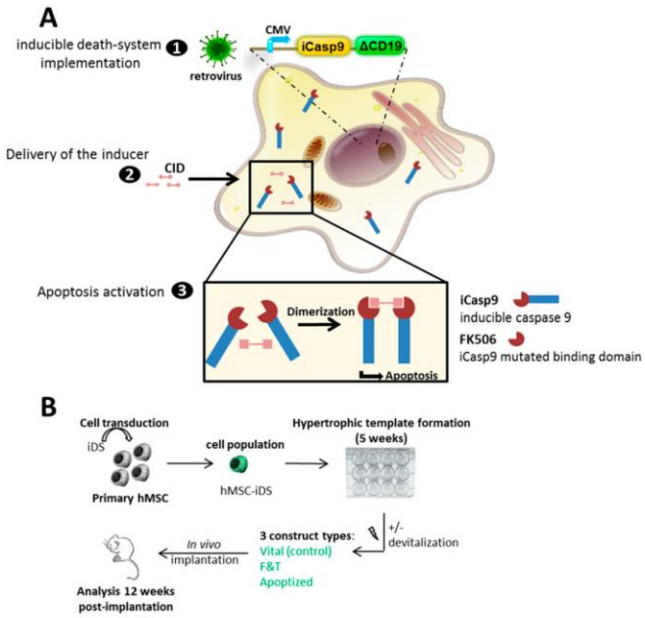

Fig. S2. (*A*) Mode of action of the iDS. The iDS is implemented in the genome of the target cells by the use of a retrovirus (1). Successfully transuded cells constitutively expressed a modified caspase 9 (iCasp9) displaying a mutated binding domain (FK506). The truncated CD19 is used as reporter marker. The delivery of the chemical inducer of dimerization (2) results in the dimerization of the iCasp9 by specific binding. The iCasp9 dimerization leads to the activation of the intrinsic apoptosis pathway (3). (*B*) Experimental set-up to assess the osteoinductive potential of devitalized hypertrophic templates. hMSC-iDS were generated by retroviral transduction. Hypertrophic templates were generated by 5 wk of culture (3 wk chondrogenesis + 2 wk hypertrophy) in the transwell system. Obtained constructs were either nondevitalized (Vital) or devitalized by F&T or apoptosis induction and were subsequently implanted ectopically in nude mice. After 12 wk, samples were retrieved for analysis.

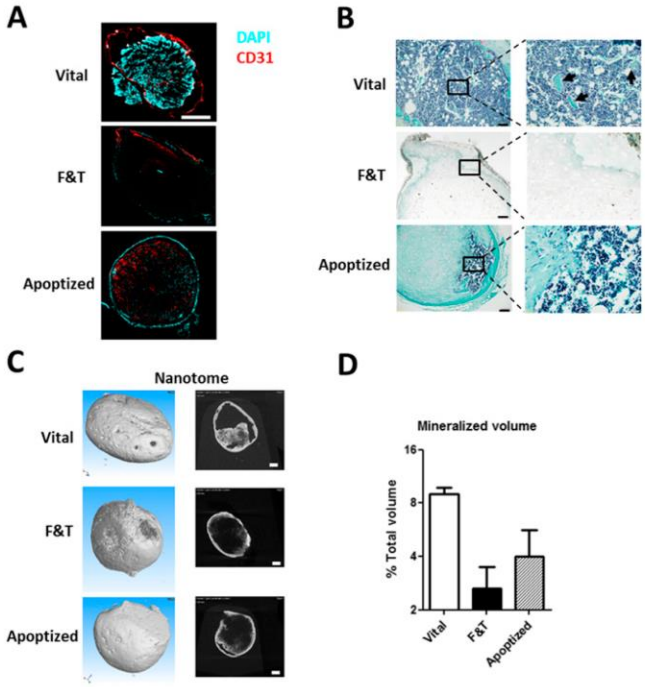

Fig. S3. (*A*) Fluorescence microscopy (DAPI, CD31) of hypertrophic templates retrieved 12 wk after ectopic implantation. F&T samples were characterized by the absence of vessel perfusion and host cell colonization. Apoptized samples were shown to be perfused by vessels although to a lower extent than the Vital constructs. (Scale bar, 0.5 mm.) (*B*) Masson's Trichrome staining revealing the presence of trabecular structure (arrow) only in Vital samples. Despite the presence of perichondral bone and bone marrow, no trabecular bone was found in Apoptized samples. F&T constructs did not show any evidence of frank bone structures. (Scale bar, 0.5 mm.) (*C*) 3D reconstructed microtomographic images of samples cultured for 5 wk in vitro and implanted ectopically in nude mice for 12 wk. (Scale bar, 0.35 mm.) (*D*) Microcomputed tomographic quantification of the mineralized volume in Vital, F&T, and Apoptized samples retrieved 12 wk after in vivo implantation. The measured volume includes both bone and calcified cartilage tissues.

CHAPTER 5

DISCUSSION and CONCLUSIONS

DISCUSSION

In this thesis, three papers are discussed. In the first, we upscaled the previously developed model in order to generate a bone organ that allowed us to better describe the tissue remodeling and the interplay between bone and haematopoietic cells. In the second, we further improved the model by making it more similar to bone repair, by adding a pro-inflammatory cytokine (IL-1β) to the system and evaluating its effect of the bone remodeling and haematopoietic cells processes. In the third, we worked towards developing an eECM by retroviral transduction of an inducible Capsase-9 of human BMSCs. In these three consecutive works, we highlighted the potential for the endochondral route to be translated into clinical practice and progressively streamlined our model by making it more similar to bone repair and more clinically compliant. Further in vitro and in vivo studies are currently ongoing in order to fully elucidate the potential of this strategy.

With the objective of bone repair in a manner which recalls natural healing processes, both cell-based and cell-free methods have been utilised, both have advantages, but currently cell-based therapeutic strategies are the *status quo* in pre-clinical science. This usually comprises BMSCs which have been extracted and either re-injected intra-operatively or cultured ex vivo for several passages to generate many more cells which are then re-injected in their current state, or, more commonly, seeded on a three-dimensional scaffold material. Cell-based strategies, most often utilising BMSCs, have been shown to be more successful at stimulating bone healing than cell-free approaches, resulting in greater mineralisation, ossification, and increased angiogenic potential (Cunniffe 2015, Gawlitta 2015, Kon 2000). These results are supported by data showing cell-based techniques to be clinically advantageous (Liebergall 2013, Dallari 2007). This has obvious implications for the choice of cell source, since a cell containing detectable genetic, epigenetic, proteomic modifications which are optimal for a particular developmental path is not only more likely to produce a higher quality final product, but is also likely to contain additional characteristics which the

limited and basic range of tests at our disposal cannot gauge. That said, ADSCs, which had low intrinsic bone-forming potential and produced no neo-bone in their un-induced state, when chondrogenically primed deposited a proteoglycan-rich cartilaginous matrix and were able to generate a similar amount of bone as non-induced BMSCs (Brocher 2013). This suggests that by re-routing ADSCs through endochondral ossification, a precursor state is created that favours bone formation. It is noteworthy that despite the successful re-routing of ADSCs, uninduced BMSCs achieved better final results, perhaps reflecting intrinsic factors that predispose them to bone formation (Shao 2013).

However, the downsides to autologous cell-based therapy are significant, and can be prohibitive in some cases. The rarity of BMSCs can be limiting to the point of rendering cell extraction unfeasible (especially in the elderly and the ill) and too few Colony Forming Unit - fibroblast (CFU-f) within a BM extract will fail to generate neo-bone tissue (Braccini 2005). Even in healthy individuals, cell extraction requires an additional procedure which carries added morbidity. Eliminating the need for extra surgery is a strong motivation behind intra-operative techniques which, while avoiding the time-expensive and laborious GMP handling of cells in the laboratory, are also limited by the number of BMSCs available for re-injection.

Cell-free technologies have been proposed as an alternative to sidestep many of the barriers associated with cell-based techniques for bone-specific and other areas of tissue engineering. A product which is available "off-the-shelf" following decellularisation and sterilisation, has obvious practical advantages from a surgical perspective, such as the reduction of intra-patient variability, and would allow the selection and preparation of the implant prior to surgery. Additionally, the implant can be re/cellularised with autologous BMSCs prior to use if sufficient BMSCs are available (Gawlitta 2015). Also, a sterile acellular product would be amenable to storage and thus easily transported to areas of need, such as impoverished nations where the resources for preserving cell-based products might be

lacking. All of these reasons would act to increase the clinical up-take and motivated our research in this direction.

Many recent studies have attempted to mimic the inherent complexity of the biological microenvironment, in terms of architecture and biochemical constituents, through the use of decellularised extracellular matrix (ECM) from a variety of animal sources, both human (Badylak 2012) and non-human (Irvine 2011). The latter option presents the possibility of benefiting from existing slaughter processes to access a large volume of material for decellularisation. The risk of zoonoses, especially prion diseses, can be reduced by sourcing animals from prion-free island populations (Lun 2010). The use of cell lines derived from either human or non-human animals to produce a functional eECM presents the possibility of standardisation, reducing donor-to-donor variability.

The concept of using eECM as bone substitutes could represent a significant innovation and breakthrough in the field of bone regeneration. The prospective of generating standardized off-the self-products with customizable properties to provide a consistently effective solution for several clinical scenarios render this approach highly attractive from both clinical and commercial standpoints. The unavoidable increased complexity of eECM as compared to native- or synthetic- derived ECM substitutes could be compensated by their superior biological performance and customization potential that allow not only to support but to actively drive tissue repair. However, the successful implementation of this approach requires deep understanding of the complex events of the bone healing process that can be driven and finely coordinated by the bioactivity of “smart” materials derived from eECM approach. In this context, multidisciplinary efforts have led to the establishment of methods to provide robust biomimetic protocols inspired from biological processes occurring during embryonic tissue development and further revised in the context of adult bone tissue repair, taking into consideration immune and mechanical aspects. The multitude of parameters involved in this approach may also require the use of miniaturized high-throughput devices

(e.g. microfluidic devices) followed by combinatorial analyses in order to define the minimal set of necessary eECM signals which are required for predictable instruction of bone regeneration.

Prospectively, established conditions for the generation of customized eECM can be translated to suitable bioreactor devices to address the challenges of engineered graft production by providing both a more sustainable manufacturing process and a more clinically-compliant procedure. Indeed by using a bioreactor-based approach one could possibly streamline the processes of ECM production and its decellularization within the same device, reducing thus complexity and cost in the manufacturing. Moreover, the reproducible behavior of the cell-lines together with the monitor capabilities of bioreactor technologies may facilitate the establishment of the relevant cell culture parameters and release criteria, predicting ultimately grafts quality. Obviously, GMP-compliant concepts related to the manufacturing devices and processes need to be introduced to conform to regulatory guidelines for the production of engineered grafts for clinical use.

With regard to bone engineering, the works presented in this thesis and others that have been published by other groups suggest that the endochondral route is a promising template. Previously, hypertrophic chondrocytes derived from human BMSCs were shown to be remodelled and replaced by frank bone tissue, including a functional haematopoietic compartment (Scotti 2010). Accordingly, decellularised hypertrophic cartilage has been used as a template to stimulate the regeneration of bone material through endochondral pathways, promoting the invasion and proliferation of host cells – although in the case of Cunniffe et al. (Cunniffe 2015) the implant was not 100% decellularised and was implanted in a nude mouse model. As shown in the third paper discussed in this thesis (Chapter 4), we proposed to induce apoptosis by retroviral transduction of an inducible Caspase-9 of hypertrophic chondrocytes, in order to decellularise ECM and, therefore, generate an eECM for bone regeneration. Importantly, this was shown to be superior to a standard freeze-thaw protocol for the

regeneration of bone. In our work, post-apoptotic cartilage and implants containing live BMSCs, but not non-hypertrophic cartilage, underwent extensive remodelling and after 12 weeks in vivo tested positive for the presence of a BM space, although implants containing live cells outperformed the "apoptosed" tissue. Elsewhere, non-hypertrophic cartilage was shown to be inferior to hypertrophic constructs in a mouse femoral defect model, where only the latter were successful in bridging the defect (Cunniffe 2015).

To date, the use of cell-free techniques has yet to demonstrate equivalence to cell-containing preparations. Developments in the methods used for decellularisation will undoubtedly result in more effective materials, due to greater retention of ECM-associated molecules with simultaneous removal of cellular material, as it happens with the method we proposed, to yield bone-engineering products with off-the-shelf convenience, as well as low-maintenance storage, and increased customisation.

CONCLUSIONS

Intrinsic bone repair mechanisms are highly effective, but in certain cases external intervention is required. In some instances, BTE has been shown to provide clinical relief, but improvement in BTE technologies are required to allow its application to greater numbers of patients, particularly those to whom traditional bone grafting procedures are unfeasible.

BMSCs form bone and BM in vivo which is essential if creation of the HME is required. This is a striking difference compared to typical tissue engineering methods resembling intramembranous ossification. However, the factors (genetic, epigenetic, proteomic, etc.) responsible for the pre-destination of BMSC to form functional bone and BM are unknown. Likely a fraction of these factors driving BMSC to form bone containing BM will also regulate additional steps in skeletal development and remodelling allowing cells to correctly react to autocrine and paracrine developmental signals.

Regardless of cell source, currently live cell-based implants tend to be superior to cell-free, and decellularised alternatives at regenerating bone tissue. Recent advances in decellularisation protocols are bringing the performance of decellulariced and devitalised tissues to ever greater levels, approaching that of vital implants, with the added value of storage, transportation and the possibility of allogenic or xenogenic-derived grafts to circumgate the difficulties in obtaining autologous cells for bone regeneration and repair.

Recent strategies in bone repair and regeneration have sought to embrace a developmental engineering approach, following as closely as possible the natural processes of bone development through the remodelling of hypertrophic cartilage templates via endochondral ossification. Our work represents one of the first efforts aimed at translating the scientifically fascinating but clinically challenging paradigm of developmental engineering to the regeneration of the bone tissue. In particular, we provided the first proof that human adult MSCs can undergo the full endochondral route and generate a bone organ, triggering the development of a new strategy in bone regeneration. The three papers presented in this thesis are tightly connected in the effort of streamlining the implementation

of the endochondral route to the clinic. Of course, further improvements and simplifications are required to really make this happen.

In the Introduction, I outlined bottlenecks that limit the translation to the clinic of experimental bone regeneration strategies. In the following, I discuss how the proposed strategy address these issues and can be used to overcome current hurdles.

(i) **Inter-donor MSC variability**. This remains a relevant issue in all MSC-based regenerative therapies. However, this can be overcome by providing a decellularized hypertrophic cartilage eECM, to be then re-cellularized *in situ*. In fact, the manufacturing of such an eECM can be obtained with allogeneic MSC, previously tested as per endochondral potential, and subsequently decellularized (e.g., as shown in Chapter 4) to minimize eECM immunogenicity.

(ii) **Need of a mineralized scaffold substrate.** This issue has been totally overcome by the endochondral approach to bone regeneration. In fact, being based on the chondrogenic differentiation of MSCs, a mineralized substrate is not strictly needed by this approach. Of course, some degree of mineralization may help in order to improve bone formation but it is not mandatory with this strategy, allowing for the use of more flexible ECM, hydrogel or polymer material.

(iii) **Cell survival after grafting**. In our work we showed that bone formation can be achived independelty from cell survival, with a decellularized eECm approach. In addition, we showed the role of both cell survival and cell apoptosis following implantation. This reflects the dual role of hypertrophic chondrocyte that can either participate to bone formation at some extent or massively die through apoptosis and leave the ECM to be colonized by skeletal progenitor cells and hematopoietic cells. This is also confirmed by the fact that, although being able to generate bone tissue with hematopoietic compartments, a fully decellularized ECM can be remodeled into a bone organ at a lesser extent than vital tissues.

(iv) **Complex and costly manufacturing**. We are currently addressing this issue by developing bioreactor-based culture of hypertrophic cartilage templates. Bioreactor culture allows out-scaling and automating the production of tissues, making it more affordable, controlled and reproducible.

In an effort to further streamline bone regeneration strategies, future research will be aimed at dissecting the intricate interplay between the ECM and cells, in order to identify potential molecular targets and allow for the development of biologics capable to trigger the execution of the endochondral ossification route. For example, as growth factors and cytokines harbored within the ECM can trigger the process, one could speculate that even only the secretome of hypertrophic chondrocytes may be enough to do so. And that, also, a combination of such a secretome with a scaffold providing structural stability can be a more efficient solution compared to an eECM. In addition, a biologic or a small molecule characterized by a high safety (e.g., compared to BMPs) and a very specific mode of action could be even more feasible to be manufactured and commercialized, from a pharmacologic standpoint. However, as mentioned above, considering the challenging mechanical demands to the bone tissue, a combination approach including a scaffold biomaterial (being either an ECM or a synthetic biomaterial) will always be required.

By combining all the abovementioned concepts, we can envision a large scale production of hypertrophic cartilage tissue, in an automated, highly controlled bioreactor manufacturing system, using engineered human cells (e.g., MSCs or iPS) with high endochondral potential and capable to undergo apoptosis upon induction. This will allow the generation of a series of cost-effective custom eECMs to be used for tissue regeneration at the most challenging sites.

REFERENCES

1. Abad V, et al. (2002) The role of the resting zone in growth plate chondrogenesis. Endocrinology 143(5):1851-1857.

2. Ai-Aql ZS, Alagl AS, Graves DT, Gerstenfeld LC, & Einhorn TA (2008) Molecular mechanisms controlling bone formation during fracture healing and distraction osteogenesis. Journal of dental research 87(2):107-118.
3. Badylak SF, Weiss DJ, Caplan A, Macchiarini P. Engineered whole organs and complex tissues. Lancet. 2012;379:943–52.
4. Bahney CS, et al. (2014) Stem cell-derived endochondral cartilage stimulates bone healing by tissue transformation. Journal of bone and mineral research : the official journal of the American Society for Bone and Mineral Research 29(5):1269-1282.
5. Bianco P, Cao X, Frenette PS, Mao JJ, Robey PG, Simmons PJ, et al. The meaning, the sense and the significance: translating the science of mesenchymal stem cells into medicine. Nat Med. 2013;19:35–42.
6. Blumer MJ, Longato S, & Fritsch H (2008) Localization of tartrate-resistant acid phosphatase (TRAP), membrane type-1 matrix metalloproteinases (MT1-MMP) and macrophages during early endochondral bone formation. Journal of anatomy 213(4):431-441.
7. Bollyky PL, et al. (2009) Intact extracellular matrix and the maintenance of immune tolerance: high molecular weight hyaluronan promotes persistence of induced CD4+CD25+ regulatory T cells. Journal of leukocyte biology 86(3):567-572.
8. Bourgine P, Scotti C, Pigeot S, Tchang L, Todorov A, Martin I. Osteoinductivity of engineered cartilaginous templates devitalized by inducible apoptosis. Proceedings of the National Academy of Sciences. 2014;111:17426–31.
9. Bourgine PE, Pippenger BE, Todorov A, Jr., Tchang L, & Martin I (2013) Tissue decellularization by activation of programmed cell death. Biomaterials 34(26):6099-6108.
10. Boyce BF & Xing L (2008) Functions of RANKL/RANK/OPG in bone modeling and remodeling. Archives of biochemistry and biophysics 473(2):139-146.
11. Braccini A, Wendt D, Jaquiery C, Jakob M, Heberer M, Kenins L, et al. Three-dimensional perfusion culture of human bone marrow cells and generation of osteoinductive grafts. Stem Cells. 2005;23:1066–72.
12. Bridges JB & Pritchard JJ (1958) Bone and cartilage induction in the rabbit. Journal of anatomy 92(1):28-38.
13. Brocher J, Janicki P, Voltz P, Seebach E, Neumann E, Mueller-Ladner U, et al. Inferior ectopic bone formation of mesenchymal stromal cells from adipose tissue compared to bone marrow: rescue by chondrogenic pre-induction. Stem Cell Res. 2013;11:1393–406.
14. Bruder SP, Kraus KH, Goldberg VM, Kadiyala S. The effect of implants loaded with autologous mesenchymal stem cells on the healing of canine segmental bone defects. J Bone Joint Surg Am. 1998;80:985–96.
15. Burd TA, Hughes MS, Anglen JO. Heterotopic ossification prophylaxis with indomethacin increases the risk of long-bone nonunion. J Bone Joint Surg Br. 2003;85:700–5.
16. Bush PG, Parisinos CA, & Hall AC (2008) The osmotic sensitivity of rat growth plate chondrocytes in situ; clarifying the mechanisms of hypertrophy. J Cell Physiol 214(3):621-629.
17. Chapellier M, Bachelard-Cascales E, Schmidt X, Clément F, Treilleux I, Delay E, et al. Disequilibrium of BMP2 levels in the breast stem cell niche launches epithelial

transformation by overamplifying BMPR1B cell response. Stem Cell Reports. 2015;4:239–54.
18. Crapo PM, Gilbert TW, & Badylak SF (2011) An overview of tissue and whole organ decellularization processes. Biomaterials 32(12):3233-3243.
19. Cunniffe G, Vinardell T, Murphy M, Thompson E, Matsiko A, O'Brien F, et al. Porous decellularized tissue engineered hypertrophic cartilage as a scaffold for large bone defect healing. Acta Biomaterialia. 2015;
20. D'Amour KA, Bang AG, Eliazer S, Kelly OG, Agulnick AD, Smart NG, et al. Production of pancreatic hormone-expressing endocrine cells from human embryonic stem cells. Nat Biotechnol. 2006;24:1392–401.
21. Dallari D, Savarino L, Stagni C, Cenni E, Cenacchi A, Fornasari PM, et al. Enhanced tibial osteotomy healing with use of bone grafts supplemented with platelet gel or platelet gel and bone marrow stromal cells. J Bone Joint Surg Am. 2007;89:2413–20.
22. Deckers MM, et al. (2002) Dissociation of angiogenesis and osteoclastogenesis during endochondral bone formation in neonatal mice. Journal of bone and mineral research : the official journal of the American Society for Bone and Mineral Research 17(6):998-1007.
23. Deutsch H. High-dose bone morphogenetic protein–induced ectopic abdomen bone growth. The Spine Journal. 2010;
24. Ding J, Ghali O, Lencel P, Broux O, Chauveau C, Devedjian JC, et al. TNF-alpha and IL-1beta inhibit RUNX2 and collagen expression but increase alkaline phosphatase activity and mineralization in human mesenchymal stem cells. Life Sci. 2009;84:499–504.
25. Evans CH. Native, living tissues as cell seeded scaffolds. Ann Biomed Eng. 2015;43:787–95.
26. Fosang AJ & Beier F (2011) Emerging Frontiers in cartilage and chondrocyte biology. Best practice & research. Clinical rheumatology 25(6):751-766.
27. Franklin ME, Treviño JM, Portillo G, Vela I, Glass JL, González JJ. The use of porcine small intestinal submucosa as a prosthetic material for laparoscopic hernia repair in infected and potentially contaminated fields: long-term follow-up. Surg Endosc. 2008;22:1941–6.
28. Freeman FE, Haugh MG, & McNamara LM (2015) An in vitro bone tissue regeneration strategy combining chondrogenic and vascular priming enhances the mineralization potential of mesenchymal stem cells in vitro while also allowing for vessel formation. Tissue engineering. Part A 21(7-8):1320-1332.
29. Friedenstein AJ, Piatetzky-Shapiro II, Petrakova KV. Osteogenesis in transplants of bone marrow cells. J Embryol Exp Morphol. 1966;16:381–90.
30. Frost HM (1987) Bone "mass" and the "mechanostat": a proposal. The Anatomical record 219(1):1-9.
31. Gawlitta D, Benders KE, Visser J, van der Sar AS, Kempen DH, Theyse LF, et al. Decellularized cartilage-derived matrix as substrate for endochondral bone regeneration. Tissue Eng Part A. 2015;21:694–703.
32. Gerber HP, et al. (1999) VEGF couples hypertrophic cartilage remodeling, ossification and angiogenesis during endochondral bone formation. Nature medicine 5(6):623-628.

33. Gerber HP, Vu TH, Ryan AM, Kowalski J, Werb Z, Ferrara N. VEGF couples hypertrophic cartilage remodeling, ossification and angiogenesis during endochondral bone formation. Nat Med. 1999;5:623–8.
34. Gerstenfeld LC, Cruceta J, Shea CM, Sampath K, Barnes GL, Einhorn TA. Chondrocytes provide morphogenic signals that selectively induce osteogenic differentiation of mesenchymal stem cells. J Bone Miner Res. 2002;17:221–30.
35. Gerstenfeld LC, Cullinane DM, Barnes GL, Graves DT, Einhorn TA. Fracture healing as a post-natal developmental process: molecular, spatial, and temporal aspects of its regulation. J Cell Biochem. 2003;88:873–84.
36. Grimshaw MJ & Mason RM (2000) Bovine articular chondrocyte function in vitro depends upon oxygen tension. Osteoarthritis and cartilage / OARS, Osteoarthritis Research Society 8(5):386-392.
37. Hall BK, Miyake T. All for one and one for all: condensations and the initiation of skeletal development. Bioessays. 2000;22:138–47.
38. Harada N, et al. (2014) Bone regeneration in a massive rat femur defect through endochondral ossification achieved with chondrogenically differentiated MSCs in a degradable scaffold. Biomaterials 35(27):7800-7810.
39. Haugh MG, Meyer EG, Thorpe SD, Vinardell T, Duffy GP, Kelly DJ. Temporal and spatial changes in cartilage-matrix-specific gene expression in mesenchymal stem cells in response to dynamic compression. Tissue Eng Part A. 2011;17:3085–93.
40. Hernigou P, Mathieu G, Poignard A, Manicom O, Beaujean F, Rouard H. Percutaneous autologous bone-marrow grafting for nonunions. Surgical technique. J Bone Joint Surg Am. 2006;88 Suppl 1 Pt 2:322–7.
41. Hessle L, et al. (2002) Tissue-nonspecific alkaline phosphatase and plasma cell membrane glycoprotein-1 are central antagonistic regulators of bone mineralization. Proceedings of the National Academy of Sciences of the United States of America 99(14):9445-9449.
42. Hoffmann W, Feliciano S, Martin I, de Wild M, Wendt D. Novel Perfused Compression Bioreactor System as an in vitro Model to Investigate Fracture Healing. Frontiers in Bioengineering and Biotechnology. 2015;3.
43. Hyde G, Dover S, Aszodi A, Wallis GA, & Boot-Handford RP (2007) Lineage tracing using matrilin-1 gene expression reveals that articular chondrocytes exist as the joint interzone forms. Developmental biology 304(2):825-833.
44. Inada M, et al. (2004) Critical roles for collagenase-3 (Mmp13) in development of growth plate cartilage and in endochondral ossification. Proceedings of the National Academy of Sciences of the United States of America 101(49):17192-17197.
45. Ingber DE, Mow VC, Butler D, Niklason L, Huard J, Mao J, et al. Tissue engineering and developmental biology: going biomimetic. Tissue Eng. 2006;12:3265–83.
46. Irvine S, Cayzer J, Todd E, Lun S, Floden E, Negron L, et al. Quantification of in vitro and in vivo angiogenesis stimulated by ovine forestomach matrix biomaterial. Biomaterials. 2011;32:6351–61.
47. Jakob M, Saxer F, Scotti C, Schreiner S, Studer P, Scherberich A, et al. Perspective on the evolution of cell-based bone tissue engineering strategies. Eur Surg Res. 2012;49:1–7.
48. Janicki P, Kasten P, Kleinschmidt K, Luginbuehl R, Richter W. Chondrogenic pre-induction of human mesenchymal stem cells on beta-TCP: enhanced bone quality by endochondral heterotopic bone formation. Acta biomaterialia. 2010;6:3292–301.

49. Jukes J, Both S, Leusink A, Sterk L, van Blitterswijk C, de Boer J. Endochondral bone tissue engineering using embryonic stem cells. Proceedings of the National Academy of Sciences. 2008;
50. Keane T, Swinehart I, Badylak S. Methods of tissue decellularization used for preparation of biologic scaffolds and in vivo relevance. Methods. 2015;
51. Keating A. Mesenchymal Stromal Cells: New Directions. Cell Stem Cell. 2012;10.
52. Kern S, Eichler H, Stoeve J, Klüter H, Bieback K. Comparative analysis of mesenchymal stem cells from bone marrow, umbilical cord blood, or adipose tissue. Stem Cells. 2006;24:1294–301.
53. Kim HK, Stephenson N, Garces A, Aya-ay J, & Bian H (2009) Effects of disruption of epiphyseal vasculature on the proximal femoral growth plate. J Bone Joint Surg Am 91(5):1149-1158.
54. Knowles HJ, et al. (2012) Chondroclasts are mature osteoclasts which are capable of cartilage matrix resorption. Virchows Archiv : an international journal of pathology 461(2):205-210.
55. Kock LM, Malda J, Dhert WJ, Ito K, & Gawlitta D (2014) Flow-perfusion interferes with chondrogenic and hypertrophic matrix production by mesenchymal stem cells. J Biomech 47(9):2122-2129.
56. Kronenberg HM. Developmental regulation of the growth plate. Nature. 2003;423:332–6.
57. Kuhn LT, et al. (2014) Developmental-like bone regeneration by human embryonic stem cell-derived mesenchymal cells. Tissue engineering. Part A 20(1-2):365-377.
58. Lenas P, Moos M, Luyten FP. Developmental engineering II: a new paradigm for the design and manufacturing of cell-based products. Part II: from genes to networks: tissue engineering from the viewpoint of systems biology and network science. Tissue engineering Part B, Reviews. Tissue engineering. Part B, Reviews; 2009;15:395–422.
59. Lenas P, Moos M, Luyten FP. Developmental Engineering: A New Paradigm for the Design and Manufacturing of Cell-Based Products. Part I: From Three-dimensional cell growth to Biomimetics of in vivo development. Tissue Engineering Part B: Reviews. Tissue Engineering Part B: Reviews; 2009;15:381–94.
60. Liebergall M, Schroeder J, Mosheiff R, Gazit Z, Yoram Z, Rasooly L, et al. Stem cell-based therapy for prevention of delayed fracture union: a randomized and prospective preliminary study. Mol Ther. 2013;21:1631–8.
61. Liebowitz SJ, Margolis SE. Path dependence, lock-in, and history. Journal of Law, Economics, and Organization [Internet]. Oxford Univ Press; 1995;11:205–26.
62. Long F (2012) Building strong bones: molecular regulation of the osteoblast lineage. Nature reviews. Molecular cell biology 13(1):27-38.
63. Lun S, Irvine SM, Johnson KD, Fisher NJ, Floden EW, Negron L, et al. A functional extracellular matrix biomaterial derived from ovine forestomach. Biomaterials. 2010;31:4517–29.
64. Mackie EJ, Ahmed YA, Tatarczuch L, Chen KS, & Mirams M (2008) Endochondral ossification: how cartilage is converted into bone in the developing skeleton. The international journal of biochemistry & cell biology 40(1):46-62.
65. Mackie EJ, Tatarczuch L, & Mirams M (2011) The skeleton: a multi-functional complex organ: the growth plate chondrocyte and endochondral ossification. The Journal of endocrinology 211(2):109-121.

66. Marcacci M, Kon E, Moukhachev V, Lavroukov A, Kutepov S, Quarto R, et al. Stem cells associated with macroporous bioceramics for long bone repair: 6- to 7-year outcome of a pilot clinical study. Tissue Eng. 2007;13:947–55.
67. Martin I, Muraglia A, Campanile G, Cancedda R, Quarto R. Fibroblast growth factor-2 supports ex vivo expansion and maintenance of osteogenic precursors from human bone marrow. Endocrinology. 1997;138:4456–62.
68. Martin I. Engineered Tissues as Customized Organ Germs. Tissue Engineering Part A. 2014;20.
69. Mumme M, Scotti C, Papadimitropoulos A, Todorov A, Hoffmann W, Bocelli-Tyndall C, et al. Interleukin-1β modulates endochondral ossification by human adult bone marrow stromal cells. Eur Cell Mater. 2012;24:224–36.
70. Murata D, Tokunaga S, Tamura T, Kawaguchi H, Miyoshi N, Fujiki M, et al. A preliminary study of osteochondral regeneration using a scaffold-free three-dimensional construct of porcine adipose tissue-derived mesenchymal stem cells. J Orthop Surg Res. 2015;10:35.
71. Nakao K, Morita R, Saji Y, Ishida K, Tomita Y, Ogawa M, et al. The development of a bioengineered organ germ method. Nat Methods. 2007;4:227–30.
72. Nakao N, Nakayama T, Yahata T, Muguruma Y, Saito S, Miyata Y, et al. Adipose Tissue-Derived Mesenchymal Stem Cells Facilitate Hematopoiesis in Vitro and in Vivo. The American Journal of Pathology. 2010;177:547554.
73. Ortega N, Behonick D, Stickens D, & Werb Z (2003) How proteases regulate bone morphogenesis. Annals of the New York Academy of Sciences 995:109-116.
74. Ortega N, Wang K, Ferrara N, Werb Z, & Vu TH (2010) Complementary interplay between matrix metalloproteinase-9, vascular endothelial growth factor and osteoclast function drives endochondral bone formation. Disease models & mechanisms 3(3-4):224-235.
75. Pittenger MF, et al. (1999) Multilineage potential of adult human mesenchymal stem cells. Science 284(5411):143-147.
76. Quarto R, Mastrogiacomo M, Cancedda R, Kutepov S, Mukhachev V, Lavroukov A, et al. Repair of Large Bone Defects with the Use of Autologous Bone Marrow Stromal Cells. New England Journal of Medicine. 2001;344:385–6.
77. Reichert JC, Gohlke J, Friis TE, Quent VM, & Hutmacher DW (2013) Mesodermal and neural crest derived ovine tibial and mandibular osteoblasts display distinct molecular differences. Gene 525(1):99-106.
78. Riminucci M, et al. (1998) Vis-a-vis cells and the priming of bone formation. Journal of bone and mineral research : the official journal of the American Society for Bone and Mineral Research 13(12):1852-1861.
79. Romanello M, et al. (2014) Osteoblastic cell secretome: a novel role for progranulin during risedronate treatment. Bone 58:81-91.
80. Sándor GK, Numminen J, Wolff J, Thesleff T, Miettinen A, Tuovinen VJ, et al. Adipose stem cells used to reconstruct 13 cases with cranio-maxillofacial hard-tissue defects. Stem Cells Transl Med. 2014;3:530–40.
81. Schwartz Z, Somers A, Mellonig JT, Carnes DL, Dean DD, Cochran DL, et al. Ability of commercial demineralized freeze-dried bone allograft to induce new bone formation is dependent on donor age but not gender. J Periodontol. 1998;69:470–8.
82. Scotti C, et al. (2010) Recapitulation of endochondral bone formation using human adult mesenchymal stem cells as a paradigm for developmental engineering.

Proceedings of the National Academy of Sciences of the United States of America 107(16):7251-7256.
83. Shao YY, Wang L, & Ballock RT (2006) Thyroid hormone and the growth plate. Reviews in endocrine & metabolic disorders 7(4):265-271.
84. Sharpe PT, Young CS. Test-tube teeth. Sci Am. 2005;293:34–41.
85. Sheehy EJ, Buckley CT, & Kelly DJ (2012) Oxygen tension regulates the osteogenic, chondrogenic and endochondral phenotype of bone marrow derived mesenchymal stem cells. Biochem Biophys Res Commun 417(1):305-310.
86. Sheehy EJ, et al. (2015) Tissue Engineering Whole Bones Through Endochondral Ossification: Regenerating the Distal Phalanx. BioResearch open access 4(1):229-241.
87. Sheehy EJ, Vinardell T, Buckley CT, & Kelly DJ (2013) Engineering osteochondral constructs through spatial regulation of endochondral ossification. Acta biomaterialia 9(3):5484-5492.
88. Sheehy EJ, Vinardell T, Toner ME, Buckley CT, Kelly DJ. Altering the architecture of tissue engineered hypertrophic cartilaginous grafts facilitates vascularisation and accelerates mineralisation. PLoS ONE. 2014;9:e90716.
89. Shiang R, et al. (1994) Mutations in the transmembrane domain of FGFR3 cause the most common genetic form of dwarfism, achondroplasia. Cell 78(2):335-342.
90. Siegel P, Massagué J. Cytostatic and apoptotic actions of TGF-β in homeostasis and cancer. Nature Reviews Cancer. 2003;3:807–20.
91. Silber JS, Anderson DG, Daffner SD, Brislin BT, Leland JM, Hilibrand AS, et al. Donor site morbidity after anterior iliac crest bone harvest for single-level anterior cervical discectomy and fusion. Spine. 2003;28:134–9.
92. Smith D, Cooper G, Mooney M, Marra K, Losee J. Bone Morphogenetic Protein 2 Therapy for Craniofacial Surgery. Journal of Craniofacial Surgery. 2008;
93. Solchaga LA, Penick KJ, & Welter JF (2011) Chondrogenic differentiation of bone marrow-derived mesenchymal stem cells: tips and tricks. Methods in molecular biology 698:253-278.
94. Steward AJ, Thorpe SD, Vinardell T, Buckley CT, Wagner DR, Kelly DJ. Cell-matrix interactions regulate mesenchymal stem cell response to hydrostatic pressure. Acta Biomater. 2012;8:2153–9.
95. Studer D, Millan C, Ozturk E, Maniura-Weber K, & Zenobi-Wong M (2012) Molecular and biophysical mechanisms regulating hypertrophic differentiation in chondrocytes and mesenchymal stem cells. European cells & materials 24:118-135; discussion 135.
96. Tavassoli M, Crosby WH. Transplantation of marrow to extramedullary sites. Science. 1968;161:54–6.
97. Tonnarelli B, Centola M, Barbero A, Zeller R, Martin I. Re-engineering development to instruct tissue regeneration. Curr Top Dev Biol. 2014;108:319–38.
98. van der Stok J, et al. (2014) Chondrogenically differentiated mesenchymal stromal cell pellets stimulate endochondral bone regeneration in critical-sized bone defects. European cells & materials 27:137-148; discussion 148.
99. van Donkelaar CC & Huiskes R (2007) The PTHrP-Ihh feedback loop in the embryonic growth plate allows PTHrP to control hypertrophy and Ihh to regulate proliferation. Biomechanics and modeling in mechanobiology 6(1-2):55-62.

100. Vilalta M, Dégano I, Bagó J, Gould D, Santos M, García-Arranz M, et al. Biodistribution, Long-term Survival, and Safety of Human Adipose Tissue-derived Mesenchymal Stem Cells Transplanted in Nude Mice by High Sensitivity Non-invasive Bioluminescence Imaging. Stem Cells and Development. 2008;
101. Vortkamp A, Pathi S, Peretti G, Caruso E, Zaleske D, Tabin C. Recapitulation of signals regulating embryonic bone formation during postnatal growth and in fracture repair. Mechanisms of Development. 1997;71.
102. Wainwright DJ. Use of an acellular allograft dermal matrix (AlloDerm) in the management of full-thickness burns. Burns. 1995;21:243–8.
103. Wang L, Shao YY, & Ballock RT (2007) Thyroid hormone interacts with the Wnt/beta-catenin signaling pathway in the terminal differentiation of growth plate chondrocytes. Journal of bone and mineral research : the official journal of the American Society for Bone and Mineral Research 22(12):1988-1995.
104. Warnke PH, et al. (2004) Growth and transplantation of a custom vascularised bone graft in a man. Lancet 364(9436):766-770.
105. Warnke PH, Springer IN, Wiltfang J, Acil Y, Eufinger H, Wehmöller M, et al. Growth and transplantation of a custom vascularised bone graft in a man. Lancet. 2004;364:766–70.
106. Weise M, et al. (2001) Effects of estrogen on growth plate senescence and epiphyseal fusion. Proceedings of the National Academy of Sciences of the United States of America 98(12):6871-6876.
107. Yadav MC, et al. (2011) Loss of skeletal mineralization by the simultaneous ablation of PHOSPHO1 and alkaline phosphatase function: a unified model of the mechanisms of initiation of skeletal calcification. Journal of bone and mineral research : the official journal of the American Society for Bone and Mineral Research 26(2):286-297.
108. Yang J, Yamato M, Shimizu T, Sekine H, Ohashi K, Kanzaki M, et al. Reconstruction of functional tissues with cell sheet engineering. Biomaterials. 2007;28:5033–43.
109. Yang L, Tsang KY, Tang HC, Chan D, & Cheah KS (2014) Hypertrophic chondrocytes can become osteoblasts and osteocytes in endochondral bone formation. Proceedings of the National Academy of Sciences of the United States of America 111(33):12097-12102.
110. Zuk PA, Zhu M, Ashjian P, De Ugarte DA, Huang JI, Mizuno H, et al. Human adipose tissue is a source of multipotent stem cells. Mol Biol Cell. 2002;13:4279–95.

CURRICULUM VITAE

Professional experiences

Date of birth	9 February 1980
Address	Steinentorstrasse 8, 4051 Basel-Stadt
Email	celestescotti@hotmail.com

Foreign languages	English (fluent; TOEFL IBT 109/120), French (basic), German (basic)
Current position	Associate Director – Translational medicine Expert Musculoskeletal Novartis Institutes for Biomedical Research

Institute	**Period**	**Position**
• Laboratory of Leukocyte Biology (Prof. R. Pardi), San Raffaele Scientific Institute, Milan	Sept. 2000	*Summer student*
• Department of Orthopaedics and Traumatology (Dr. G. Fraschini), San Raffaele Scientific Institute, Milan	2002-2005	*Intern student*
• Vita-Salute San Raffaele University, Milan	1999-2005	***M.D.*** *(Magna cum Laude)*
• Residency Program in Orthopaedics and Traumatology, University of Milan (5-year program) with the following rotations:	Autumn 2005-Autumn 2010	***Italian Board of Orthopaedic Surgery*** *(Magna cum Laude)*
• Department of Orthopaedics and Traumatology (Dr. G. Fraschini), San Raffaele Scientific Institute, Milan	Sept. 2005-Aug.2006	*Resident*
• Department of General Surgery (Prof. E. Trabucchi), L. Sacco Hospital, Milan	Sept. 2006-Feb. 2007	*Resident*
• Department of Orthopaedics and Traumatology (Dr. G. Fraschini), San Raffaele Scientific Institute, Milan	Mar. 2007-May 2008	*Resident*
• Tissue Engineering Laboratory, Basel University Hospital (Prof. Ivan Martin)	Jun. 2008-Ago. 2009	*Visiting Scientist*

• Department of Orthopaedics and Traumatology (Prof. G. Peretti), Istituto Clinico Sant'Ambrogio	Sept. 2009-Oct.2010	*Resident*
• Department of Trauma Surgery, Basel University Hospital (Prof. Marcel Jakob)	March 2011-August 2011	*Visiting Physician*
• Galeazzi Orthopaedic Institute, Milan (Shoulder, Knee and Sports Trauma)	Oct-2012 – Dec 2015	*Attending Orthopaedic Surgeon*

Awards and Honors

• **Jaques Duparc Award** for the best 10 posters presented at 7° EFORT Congres (European Federation of National Associations of Orthopaedics and Traumatology)	2005
• **Best Poster** at 8° National Congress of SICSEG (Società Italiana di Chirurgia della Spalla e del Gomito)	2006
• **Rossoni Award** for the best presentation by a young surgeon at the 46° National Congress of the Società Italiana di Chirurgia della Mano (SICM)	2008
• **Best scientific paper** presented at the 2° National Congress of Sigascot (Società Italiana del Ginocchio, Artroscopia, Sport, Cartilagine e Tecnologie Ortopediche)	2008
• **Best paper** award as Co-Author, at the 15° National Congress of Orthopaedics and Traumatology Residents. 19 March, 2010, Parma.	2010
• **European Arthroscopy Travelling Fellowship of ESSKA**	
• **Travel Grant Award for the 2012 10th annual ISSCR Meeting**	2011
• **Robert Mathys Student Award for the best oral presentation at the „XIII eCM Conference: Bone Fixation, Repair & Regeneration"**	2012
• **Travel Grant Award al TERMIS World Congress, Vienna, 5-8 september 2012**	2012
• **Basic Science Award at the 39th Annual Meeting of the European Group for Blood and Marrow Transplantation**	2012 2013
• **Best Poster at the Annual Meeting of the Swiss Stem Cell network**	2013
• **Bruno Speck Award by the Basel Stem Cell Network**	2013
• **Dirk Schaefer Wissenschaftspreis, Unispital Basel**	2013

- **ESSKA MITEK Sports Medicine Fellowship (1 month, Hopital Ambroise Pare', Paris)** 2015

- **Reviewer** for the following international, peer-reviewed journals: Journal of Orthopaedics and Traumatology (since 2008); Differentiation (since 2010); Journal of Visualized Experiments (since 2011); Tissue Engineering – A (since 2011); Clinical Orthopaedics and Related Research (since 2011); European Cells and Materials (since 2011); Citotherapy (since 2013); Acta Biomaterialia (since 2014); Osteoarthritis and Cartilage (since 2014), Biomaterials (since 2015)
- **Editorial Board** member: "Joints – Official Journal of Sigascot", "Frontiers. Tissue Engineering and Regenerative Medicine"
- **Associate Faculty Member of F1000**, section of Musculoskeletal Repair & regeneration (since 2011).
- **Reviewer of grant proposal** for the following Institutions: Health Research Board of Ireland; National Medical Research Council of Singapore; Netherlands Organisation for Scientific Research; Reumafonds (Dutch Arthritis Association).

Publications list

- Papers on peer-reviewed journal 41
- Book or Book Chapters 3

Full list of publications on peer-reviewed Journals

1. Peretti GM, Buragas M, **Scotti C**, Mangiavini L, Sosio C, Di Giancamillo A, Domeneghini C, Fraschini G. An in vitro tissue engineered model for osteochondral repair. *Sport Sciences for Health* 2006 1(4):153-157.
2. Ciampi P., **Scotti C**., Fraschini G. Extracorporeal shock wave treatment of humeral nonunion: a case report. *Sport Sciences for Health* 2007 2(1):42-45
3. Sosio C, Boschetti F, Bevilacqua C, Mangiavini L, **Scotti C**, Buragas M, Biressi S, Fraschini G, Gigante A, Peretti GM. Effect of blood on the morphological, biochemical and biomechanical properties of engineered cartilage. *Knee Surg Sports Traumatol Arthrosc* 2007 15(10):1251-7
4. **Scotti C**, Buragas MS, Mangiavini L, Sosio C, Di Giancamillo A, Domeneghini C, Fraschini G, Peretti GM. A tissue engineered osteochondral plug: an in vitro morphological evaluation. *Knee Surg Sports Traumatol Arthrosc* 2007 15(11):1363-9

5. Peretti GM, **Scotti C**, Mangiavini L, Pozzi A, Albisetti W, Fraschini G. La patologia ortopedica e traumatica del calciatore adolescente. *Archivio di Ortopedia e Reumatologia* 2007 118(3):7-9

6. Camnasio F, **Scotti C**, Peretti GM, Fontana F, Fraschini G. Prosthetic joint replacement for long bone metastases: analysis of 154 cases. *Arch Orthop Trauma Surg* 2008 128(8):787-793

7. Peretti GM, **Scotti C**, Pozzi A, Mangiavini L, Vitari F, Domeneghini C, Fraschini G. Bonding of meniscal tissue: a nude mouse repair model. *Sport Sciences for Health* 2008 3(3); 47-52

8. **Scotti C**, Camnasio F, Peretti GM, Fontana F, Fraschini G. Modular prostheses in the treatment of proximal humerus metastases: analysis of 40 cases. *J Orthop Traumatol* 2008 9(1):5-10

9. **Scotti C**, Camnasio F, Rizzo N, Fontana F, De Cobelli F, Peretti GM, Fraschini G. Mammary-type myofibroblastoma of politeal fossa: a case report. *Skeletal Radiology* 2008 37(6):549-53

10. **Scotti C**, Pozzi A, Mangiavini L, Vitari F, Boschetti F, Domeneghini C, Fraschini G, Peretti GM. Healing of meniscal tissue by cellular fibrin glue: an in vivo study. *Knee Surg Sports Traumatol Arthrosc* 2009 17(6):645-51

11. **Scotti C,** Wirz D, Wolf F, Schaefer DJ, Burgin V, Daniels AU, Valderrabano V, Candrian C, Jakob M, Martin I, Barbero A. Engineering human cell-based, functionally integrated osteochondral grafts by biological bonding of engineered cartilage tissues to bony scaffolds. *Biomaterials* 2010 31(8):2252-9

12. **Scotti C**, Tonnarelli B, Papadimitropoulos A, Scherberich A, Schaeren S, Schauerte A, Lopez-Rios J, Zeller R, Barbero A, and Martin I. Recapitulation of endochondral bone formation using human adult mesenchymal stem cells as a paradigm for developmental engineering. *Proc Natl Acad Sci USA* 2010 107(16):7251-7256 **This paper was highlighted by the Editor as the most relevant of the issue.**

13. **Scotti C**, Borri A, Fontana F, Camnasio F, Fraschini G. Solitary psoas muscle metastasis from renal cell carcinoma. *ANZ J Surg* - Jun;80(6):466-7

14. **Scotti C**, Mangiavini L, Boschetti F, Vitari F, Domeneghini C, Fraschini G, Peretti GM. Effect of in vitro culture on a chondrocyte-fibrin glue hydrogel for cartilage repair. *Knee Surg Sports Traumatol Arthrosc* 2010;18(10):1400-6

15. Fraschini G, Ciampi P, **Scotti C**, Ballis R, Peretti GM. Surgical treatment of chronic acromioclavicular dislocation: comparison between two surgical procedures for anatomic reconstruction. *Injury* 2010 Nov;41(11):1103-6

16. **Scotti C**, Marone EM, Brasca LE, Camnasio F, Peretti GM, Chiesa R, Del Maschio A, Fraschini G. Soft Pseudoaneurysm overlying an osteochondroma: a noteworthy complication. *J Orthop Traumatol* 2010 Dec;11(4):251-5

17. Sosio C, Boschetti F, Mangiavini L, **Scotti C**, Manzotti S, Buragas M, Biressi S, Fraschini G, Gigante A, Peretti GM. Blood exposure has a negative effect on engineered cartilage**.** *Knee Surg Sports Traumatol Arthrosc* – 2011 Jun;19(6):1035-42

18. Ciampi P; **Scotti C**; Gerevini S; De Cobelli F; Chiesa R; Fraschini G; Peretti GM. Surgical Treatment Of Thoracic Outlet Syndrome In Young Adults: Single Center Experience With Minimum 3-Year Follow Up. *Int Orthop – 2011 Aug;35(8):1179-86*

19. Gobbi A, Karnatzikos G, **Scotti C**, Mahajan V, Mazzucco L, Grigolo B. One-step Cartilage Repair with Bone Marrow Aspirate Concentrated Cells and Collagen Matrix in Full-thickness Knee Cartilage Lesions: Results at 2 year follow-up. *Cartilage – July 2011; vol. 2, 3: pp. 286-299*

20. Gioia G, **Scotti C**, Mandelli D, Sala G. Posterior spinal instrumentation: biomechanical study on the role of rods on hardware response to axial load. *Eur Spine J*. 2011 May;20 Suppl 1:S3-7

21. **Scotti C,** Nobile S, Peretti, GM. Biological materials for cartilage engineering. *J Orthopedics – Accepted*

22. **Scotti C**, Leumann A, Candrian C, Barbero A, Croci D, Schaefer DJ, Jakob M, Valderrabano V, Martin I. Autologous tissue-engineered osteochondral graft for talus osteochondral lesions: state of the art and future perspectives. *Techniques in Foot and Ankle Surgery* – 10(4):163-168.

23. **Scotti C**, Osmokrovic A, Wolf F, Miot S, Peretti GM, Barbero A, Martin I. Response of human engineered cartilage based on articular or nasal chondrocytes to il-1β and low oxygen. *Tissue Engineering A, 2011 Sept 8*

24. Jakob M, Saxer F, **Scotti C**, Schreiner S, Studer P, Scherberich A, Heberer M, Martin I Perspective On The Evolution Of Cell-Based Bone Tissue Engineering Strategies. *Eur Surg Res* **–** 2012 18(3-4):362-72

25. Mumme M, **Scotti C***, Papadimitropoulos A, Todorov A, Hoffmann W, Bocelli-Tyndall C, Jakob M, Wendt D, Martin I, Barbero. Interleukin-1beta modulates endochondral ossification by human adult bone marrow stromal cells. European Cells and Materials 24:224-36 (*** co-first author)**

26. Scotti C, Piccinini E, Takizawa H, Todorov A, Bourgine P, Papadimitropoulos A, Barbero A, Manz MG, Martin I. Engineering of a functional bone organ through endochondral ossification. Proc Natl Acad Sci U S A. 2013 Feb 11. **This paper was highlighted by the Editor among the most relevant of the issue.**

27. Centola M, Abbruzzese F, **Scotti C**, Barbero A, Vadalà G, Denaro V, Martin I Phd, Trombetta M, Rainer A, Marsano A. Scaffold-based delivery of a clinically-relevant anti-angiogenic drug promotes the formation of in vivo stable cartilage. Tissue Eng Part A. 2013 Apr 24. [Epub ahead of print] PubMed PMID: 23611597.

28. Deponti D, Di Giancamillo A, **Scotti C**, Peretti GM, Martin I. Animal models for meniscus repair and regeneration. J Tissue Eng Regen Med 2013 May 27 DOI: 10.1002/term.1760

29. **Scotti C**, Hirschmann MT, Antinolfi P, Martin I, Peretti GM. Meniscus repair and regeneration: review on current methods and research potential. Eur Cell Mater. 2013 Sep 23;26:150-70.

30. Ciampi P**., Scotti C**., Nonis A., Vitali M., Di Serio C., Peretti G.M., Fraschini G. The Benefit Of Synthetic Vs Biogical Patch Augmentation In The Repair Of Postero-Superior Massive Rotator Cuff Tears: A 3-Year Follow-Up Study. Am J Sports Med (In Press).

31. **Scotti C**. CORR Insights®: Mesenchymal Stem Cells in Synovial Fluid Increase After Meniscus Injury. Clin Orthop Relat Res. In press.

32. Pelttari K, Pippenger B, Mumme M, Feliciano S, **Scotti C**, Mainil-Varlet P, Procino A, von Rechenberg B, Schwamborn T, Jakob M, Cillo C, Barbero A, Martin I. Adult human neural crest-derived cells for articular cartilage repair. Sci Transl Med. 2014 Aug 27;6(251):251ra119.

33. Papadimitropoulos A, **Scotti C**, Bourgine P, Scherberich A, Martin I. Engineered Decellularized Matrices to instruct osteoprogenitor cells into bone regeneration processes. Bone. 2015 Jan;70:66-72

34. Bourgine P, **Scotti C**, Pigeot S, Tchang L, Todorov A, Martin I. Osteoinductivity of engineered cartilaginous templates devitalized by inducible apoptosis. Proc Natl Acad Sci U S A. 2014 Dec 9;111(49):17426-31

35. Barandun M, Iselin LD, Santini F, Pansini M, **Scotti C**, Baumhoer D, Bieri O, Studler U, Wirz D, Haug M, Jakob M, Schaefer DJ, Martin I, Barbero A. Generation and characterization of osteochondral grafts with human nasal chondrocytes. J Orthop Res. 2015 May 20.

36. Gobbi A, **Scotti C**, Lane JG, Peretti GM. Fresh osteochondral allografts in the knee: only a salvage procedure? Ann Transl Med. 2015 Jul;3(12):164.

37. **Scotti C**, Gobbi A, Karnatzikos G, Martin I, Shimomura K, Lane JG, Peretti GM, Nakamura N. Cartilage Repair in the Inflamed Joint: Considerations for Biological Augmentation Toward Tissue Regeneration. Tissue Eng Part B Rev. 2015 Dec 17.

38. Gobbi A, **Scotti C**, Karnatzikos G, Mudhigere A, Castro M, Peretti GM. One-step surgery with multipotent stem cells and Hyaluronan-based scaffold for the treatment of full-thickness chondral defects of the knee in patients older than 45 years. Knee Surg Sports Traumatol Arthrosc. 2016 Jan 14.

39. **Scotti C**, Tonnarelli B, Papadimitropoulos A, Piccinini E, Todorov A, Centola M, Barbero A, Martin I. Engineering small-scale and scaffold-based bone organs via endochondral ossification using adult progenitor cells. Meth Mol Biol. *Accepted*.

40. Fisher JN, Peretti GM, **Scotti C**. Stem cells for bone regeneration: from cell-based therapies to decellularized engineered extracellular matrices. Stem cells Int. *Accepted*

41. Ciampi P, Agnoletto M, **Scotti C**, Ballis R, Peretti GM, Fraschini G. THORACIC OUTLET SYNDROME IN THE OVERHEAD ATHLETE: A REPORT OF TWO CASES OF SUBCLAVIUS POSTICUS MUSCLE. Clin J Sport Med. *Accepted*

Books or Book Chapters

42. G.M. Peretti, **C. Scotti**. Nuovi e potenziali approcci terapeutici in ortopedia e traumatologia. In P. Gallinaro, G. Peretti, E. Rinaldi. *Manuale di Ortopedia e Traumatologia, 3° ed*., McGraw-Hill
43. **Scotti C.,** Peretti G.M. Biological materials for engineered cartilage. Theoretical and practical course for articular cartilage biology and regeneration: basic laboratory techniques. Pag. 49-57. Editors: Andrea Facchini, Giuseppe M. Peretti
44. Gobbi A, Scott C, Peretti GM. SCAFFOLDING AS TREATMENT FOR OSTEOCHONDRAL DEFECTS IN THE ANKLE. In "Arthroscopy, ESSKA", Springer. *In press.*

Basel-Stadt, 13.03.2016